THE MINISTRY OF NATIONAL
INFRASTRUCTURES
GEOLOGICAL SURVEY OF ISRAEL

PLIOCENE - PLEISTOCENE TECTONICS AND LANDSCAPE EVOLUTION IN THE GALILEE

Ari Matmon

Report GSI / 6 / 2001 Jerusalem, February 2001 Es/ 5 / 2001

THE MINISTRY OF NATIONAL
INFRASTRUCTURES
GEOLOGICAL SURVEY OF ISRAEL

PLIOCENE - PLEISTOCENE TECTONICS AND LANDSCAPE EVOLUTION IN THE GALILEE

Ari Matmon

Report GSI / 6 / 2001 Jerusalem, February 2001 Es/ 5 / 2001

Extended Summary

A morphotectonic study of the Galilee, northern Israel, reveals several stages of late Cenozoic tectonic activity that led to the development of the present landscape. A north-south extensional stress field that prevailed in northern Israel since the Miocene caused the formation of fault systems that were active in three phases and eventually formed the tectonic blocks that dominate the present-day topography of the Galilee. Arching of the Galilee in the Pliocene and Pleistocene formed the structural mountainous back-bone of Israel parallel to the Dead Sea Transform valley (DST). The main water divide between the Mediterranean and the DST is located along the axis of this structural arch. Fresh bedrock fault scarps found at various locations throughout the Galilee indicate episodic Holocene tectonic activity along normal faults was episodically intensive.

The lack of late Cenozoic sedimentary units or widespread volcanic in the Galilee prevented for many years the use of traditional geological methods to determine and to reconstruct the temporal framework of the late Cenozoic tectonic activity and landscape evolution. New approaches and methodologies were developed in this study to understand and interpret the geomorphic-tectonic relationships in the region by using morphometric analyses, studying and reconstructing ancient drainage systems, and dating exposed bedrock surfaces using cosmogenic radionuclides. These methods were applied along with more traditional research techniques such as radiometric dating of basalt clasts, XRF chemical analysis, and petrologic examination of thin sections.

By using a quantitative morphometric analysis it was possible for the first time to determine the relative ages of late Cenozoic block-bounding normal faults that form the

along with more traditional research techniques such as radiometric dating of basalt clasts, XRF chemical analysis, and petrologic examination of thin sections.

By using a quantitative morphometric analysis it was possible for the first time to determine the relative ages of late Cenozoic block-bounding normal faults that form the Galilee escarpments. The analysis considered only major topographic elements and utilized structural maps with 50 m contours based on the top of Judea Group datum. Therefore, only major tectonic and erosional phases were distinguished.

Two morphometric parameters are used to discriminate between tectonic phases: a) the ratio between the height of an escarpment and the total stratigraphic displacement (L); b) the normalized shape of the topographic profile of each escarpment relative to a reference slope profile of the escarpment of Mt. Tur'an dated at 4.23±0.23 Ma. The morphometric analysis indicates three groups of faults: (a) without topographic expression (L=0), (b) with L~0.5, indicating that topography related to the early stages of displacement was eroded and that recent topography is associated to a later phase of vertical displacement, and (c) with L>0.75, indicating that most of the vertical displacement is expressed by relief.

The erosion of relief formed by faulting, as indicated by the L-index value, was part of a regional denudation process that was active in the Oligocene and Miocene and in some places during the Pliocene. Although it discriminates between tectonic phases, the L-index is not a good enough indicator of the actual timing of the formation of escarpments associated with the normal faulting. Therefore, morphometric analysis of the slopes of the escarpments was preformed. This analysis shows that (a) generally, the topographic profiles of different parts of each individual escarpment have similar geometry; (b) in cases where there are systematic variations in profile shapes along escarpments, they are in accord with segmentation deduced from values of the L-index; (c) escarpments more concave or convex than the reference Tur'an escarpment are older or younger than 4 Ma, respectively, and (d) the Galilee escarpments did not form simultaneously. A few were already major morphologic features by the Early to Middle Pliocene and the rest are younger, having formed between 4-2 Ma.

The formation of the block structure in the Galilee cannot explain the regional configuration of the present drainage system. The development of the present main drainage divide in Israel in general, and in the Galilee in particular, is associated with a long wavelength flexing that formed a structural arch between the Mediterranean and the DST. During the Pleistocene, the arching was followed by the establishment of the main North-South water divide in the region and reversal of stream flow direction. A reconstruction of the Beit-Hakerem paleochannel, which drained large areas in the eastern Galilee to the Mediterranean, enabled the determination of age and amplitude of arching that occurred during the Quaternary. Dating of basalt clasts from ancient alluvial remnants, provides a maximum age limit of 1.8 Ma to the paleochannel. The Pleistocene tectonism arched the Galilee by 200 m over a wavelength of 40-60 km. A comparison between arched and unarched segments of the DST margins, indicates that fluvial and slope processes on the escarpment's edge cannot explain the location and shape of the main water divide. In the Galilee, tectonism is the only factor that controls the formation, location and shape of the main water divide.

Morphometric analysis and reconstruction of the drainage systems in the Beit-Hakerem and Bet-Ha'Emek valleys indicate that by the beginning of the Pleistocene the landscape in the Galilee was very similar to the present. Nevertheless, there is evidence for ongoing Quaternary tectonic activity in the region. One of the most striking features along some of the main tectonic escarpments in the Galilee is the fresh hard-rock fault-scarps. The timing of tectonic activity that formed one of these scarps was determined by measuring concentrations of cosmogenic isotopes.

The abundance of 36Cl, one of the cosmogenic isotopes and the most suitable for exposure dating of carbonate rocks, was measured in 41 limestone samples (and 4 duplicates) taken from and near the Nahef East fault scarp. Using production rates, production-at-depth relationships of 36Cl, and the geochemistry of the Nahef East scarp samples, a numerical model that enables the fit of a most likely earthquake (i.e. exposure) history was constructed. The numerical model indicates that the upper (vertical) meter of the scarp was exposed nearly 12,000 years ago, but the majority (6 m) of the scarp was exposed during a 3 kyr period in the middle Holocene. The rapid exposure of 6 meters of scarp indicates that large (M>6) earthquakes must have occurred during this time. The bottom 1.8 meters of the scarp were exposed as recently as 1500 kyr.

This is the most complete and detailed study to date, regarding in-situ cosmogenic 36Cl accumulation on a bedrock fault scarp; the availability of this method to others studying normal faults that form bedrock scarps, will vastly increase the amount of paleoseismic information. This research presents the first evidence for Holocene fault activity in the Beit Hakerem Valley in particular and in the Galilee in general. It also provides the first estimates of rates of landscape-forming processes, such as limestone erosion (~29 m/My) and fault scarp development. The project indicates that at least for the Nahef East fault scarp, the standard calculation of recurrence interval may not be valid because it appears that fault activity was limited to a short period of time. Comparing of the morphology of the dated Nahef fault scarp to other bedrock fault scarps in the Galilee, indicates that Holocene displacement along normal faults was widespread.

Geomorphological study of the Bet-Ha'Emek Valley, Upper Galilee, enables the detection of the different tectonic stages that took place in the region and a better understanding of the relation between long-term tectonic activity and surficial processes. Morphological, sedimentological, and structural data collected along the different reaches of the Bet-Ha'Emek and neighboring drainage systems indicate a number of tectonic phases during the regional landscape evolution. These data indicate that faulting was active from the Miocene and until the Late Pleistocene (or Holocene) and that the development of the landscape is mainly controlled by rates of faulting and regional uplift and less by surficial processes.

The pattern and evolution of the Bet-Ha'Emek drainage system implies that the relief of the Bet-Ha'Emek Valley and the development of the drainage system in it preceded the development of the Zurim Escarpment and the formation of the topographic and structural NW regional tilt of the Upper Galilee. The present relation between the Zurim Escarpment and the Bet-Ha'Emek drainage system suggests that no observable retreat occurred along the escarpment since its formation more than 4 Ma.

Incision of the Bet-Ha'Emek drainage system and adjacent streams into alluvial terraces signals the response of the drainage system to the regional-scale uplift and is not associated with displacement of the Bet-Ha'Emek fault system. The regional uplift is also expressed in the steep gradient of the Upper Galilee streams.

It is demonstrated in this research that morphologic and morphometric analysis are a good (and sometimes the only) way to study tectonic evolution in an erosional landscape. The use of cosmogenic isotopes as an indicator of exposure history and as a way to measure erosion rates is a powerful tool in the study of landscape development and tectonic evolution. The methods developed in this study can be applied in other areas of similar geologic and climatic conditions.

Three main phases of tectonic activity in the Galilee are determined from this study:

Normal faulting predating the eruption of the Cover Basalt Formation around 4 Ma. The morphology of the Zurim and Meron escarpments, which formed during this tectonic phase, is still preserved. This phase was dominated by strike-slip movement along NW and SW trending faults (Ron, 1978; Ron et al., 1984).

A second normal faulting phase postdating the eruption of the Cover Basalt Formation. The topographic expression of this phase builds most of the present morphotectonic features in the Galilee. The formation of these features took place between 4-2 Ma.

The arching of the Galilee and the formation of the present main water divide occurred during the Late Pliocene and Early Pleistocene.

It is unclear whether the first two stages were continuous or if there was a long period of relative tectonic quiescence between them. Although the arching phase perumably took place contemporaneous with both faulting phases, it established the present course of main water divide only in the Pleistocene.

The dated Nahef fault scarp and the morphology of many fresh looking bed-rock fault scarps that are developed in carbonate rocks throughout the Galilee, might indicate significant Holocene displacement in northern Israel.

Determination of escarpment age using morphologic analysis: An example from the Galilee, northern Israel

A. Matmon*
Institute of Earth Sciences, Hebrew University of Jerusalem, Jerusalem 91904, Israel, and *Geological Survey of Israel, 30 Malkhe Israel Street, Jerusalem 95501, Israel*

E. Zilberman
Geological Survey of Israel, 30 Malkhe Israel Street, Jerusalem 95501, Israel

Y. Enzel
Institute of Earth Sciences, Hebrew University of Jerusalem, Jerusalem 91904, Israel, and *Department of Geography, Hebrew University of Jerusalem, Jerusalem 91905, Israel*

ABSTRACT

We used topographic and structural data and very limited age control to perform quantitative morphometric analyses and to determine relative ages of escarpments bounded by late Cenozoic normal faults in the Galilee, Israel. The Galilee is an extensional zone composed of a series of uplifted and tilted blocks forming large escarpments built mainly of carbonate rocks. Two parameters used to discriminate tectonic stages are the ratio between the height of the escarpment and the total stratigraphic displacement (*L*) and the degree of concavity of escarpment slopes relative to a reference slope. The only dated reference slope is Mount Tur'an, ~300 m high and formed by the Tur'an fault system, which has a total stratigraphic displacement of 625 m. A basalt flow that delimits the age of the Tur'an escarpment is dated to 4.23 ± 0.23 Ma and displaced 300 m, which is identical to the present-day topographic expression of this escarpment. The *L* value for this escarpment is ~0.5. The Tur'an fault system was active prior to 4.23 Ma at slow uplift rates that enabled erosion to maintain the gentle slope over which the basalt flowed. Increased offset rates following the basalt extrusion led to the formation of the escarpment. The preservation of the basalt at the top of the escarpment indicates that erosional lowering of the upper surface of the Tur'an block has been minor since its formation.

The *L* values indicate two stages of uplift; an early stage during which offset rates were probably low enough that they did not form topography, and a later stage that formed topography, which is preserved. The timing of the change in displacement rates from a slow continuous stage to a fast, topography-forming stage was determined by comparing the shape of the dated slope of Tur'an to that of other slopes. We conclude the following: (1) generally, the topographic profiles of different parts of each individual escarpment have similar shapes indicating similar ages; (2) escarpments having slopes that are more concave or convex than the reference Tur'an escarpment are older or younger than 4 Ma, respectively; and (3) the Galilee escarpments did not form simultaneously. A few escarpments were already major morphologic features by the early to middle Pliocene, whereas the rest formed during the late Pliocene.

Morphometric analysis is a useful method for studying the geologic history of a landscape controlled by normal fault uplift and characterized by the absence of sediment deposition and where carbonate dissolution is the main erosional process. This and similar approaches can be used to discriminate tectonic stages and understand the relationship between tectonic activity and surface processes in other extensional regions.

Keywords: Israel, normal faulting, slopes, morphometry, topography.

INTRODUCTION

Understanding the temporal framework of ongoing active faulting in erosional terrains is difficult due to the absence of datable sediments or volcanic rocks. In such terrains, tectonic and landscape evolution studies cannot rely on precise time indicators and only the relief and its relation to geologic structure offer insight into stages of landscape evolution and tectonic activity.

The Galilee, northern Israel (Fig. 1), is an erosional terrain (i.e., very little clastic deposition) where landscape evolution has been controlled mainly by Neogene to Quaternary tectonic activity (Freund, 1970; Ron et al., 1984; Matmon et al., 1999a). Neogene and Quaternary sediments and volcanic rocks accumulated only at the margins of the Galilee (Schulman, 1962; Kafri and Ecker, 1964; Glikson, 1965; Issar and Kafri, 1972; Mor et al., 1987; Heimann, 1990; Shaliv, 1991; Sivan, 1996). Most of its mountainous area was subjected to erosion during the Neogene and Quaternary and, therefore, the youngest exposed rocks in this area are of Eocene age. The general absence of upper Tertiary rocks means that over most of the Galilee, there are very few stratigraphic markers or datable geologic features available to reconstruct the post-Eocene tectonic development of the region. For this reason, the temporal development of the morphology of the Galilee is incompletely understood. Similar difficulties face researchers in areas undergoing extensional tectonics around the Mediterranean as well as other carbonate terrains in the world.

This study was aimed at providing time constraints on the age of the main escarpments in the Galilee and understanding the relationship between tectonics and erosional processes in this region using morphological analysis.

*E-mail: amatmon@zoo.uvm.edu.

GSA Bulletin; December 2000; v. 112; no. 12; p. 1864–1876; 13 figures; 1 table; Data Repository item 2000113.

vey of Canada, Geology of Canada, v. 4, p. 419–434 (Geological Society of America, Geology of North America, v. G-2).
CORDLINK, 1999, A window on Cordilleran geology: http//132.156.108.208/Cordlink1/English/Module_Document/fromhome.cfm, date accessed June 22, 1999.
Davis, N.F.G., and Mathews, W.H., 1944, Four phases of glaciation with illustrations from southwestern British Columbia: Journal of Geology, v. 52, p. 403–413.
Dredge, L.A., and Cowan, W.R., 1989, Quaternary geology of the southwestern Canadian shield, *in* Fulton, R.J., ed., Quaternary geology of Canada and Greenland, Quaternary geology of the Canadian shield: Geological Survey of Canada, Geology of Canada, v. 1, p. 239–248 (Geological Society of America, Geology of North America, v. K-1).
Duffell, S., 1959, Whitesail Lake map area, British Columbia: Geological Survey of Canada Memoir 299, 19 p.
Duffet, L.L., and Owsiacki, G., 1995, Mineral occurrence (MINFILE) map of the Smithers (093L) area: Victoria, British Columbia, British Columbia Geological Survey, scale 1:250 000.
Easterbrook, D.J., 1992, Advance and retreat of the Cordilleran ice sheets in Washington, U.S.A.: Géographie Physique et Quaternaire, v. 46, p. 51–68.
Eyles, N., and Clague, J.J., 1991, Glaciolacustrine sedimentation during advance and retreat of the Cordilleran Ice Sheet in central British Columbia: Géographie Physique et Quaternaire, v. 45, p. 317–331.
Fairbanks, R.G., 1989, A 17,000 year glacio-eustatic sea level record: Influence of glacial melting rates on the Younger Dryas event and deep-ocean circulation: Nature, v. 342, p. 637–642.
Fulton, R.J., 1991, A conceptual model for growth and decay of the Cordilleran Ice Sheet: Géographie Physique et Quaternaire, v. 45, p. 281–286.
Fulton, R.J., 1995, Surficial materials of Canada: Geological Survey of Canada Map 1880A, scale 1:5 000 000.
Fulton, R.J., and Smith, G.W., 1978, Late Pleistocene stratigraphy of south-central British Columbia: Canadian Journal of Earth Sciences, v. 6, p. 971–980.
Gabrielse, H., Monger, J.W.H., Wheeler, J.O., and Yorath, C.J., 1992, Morphogeological belts, tectonic assemblages and terranes: Part A, *in* Gabrielse, H., and Yorath, C.J., eds., Geology of the Cordilleran orogen in Canada, Tectonic framework: Geological Survey of Canada, Geology of Canada, v. 4, p. 15–28 (Geological Society of America, Geology of North America, v. G-2).
Gravel, J.L., and Sibbick, S.J., 1991, Geochemical dispersion in complex glacial drift at the Mount Milligan copper-gold porphyry deposit (93N/1E, 93O/4W), Exploration in British Columbia 1990: Victoria, British Columbia, British Columbia Geological Survey, p. 117–134.
Hall, N.M., Valdes, P.L., and Dong, B., 1996, The maintenance of the last great ice sheets: A UGAMP GCM study: Journal of Climate, v. 9, p. 1004–1019.
Hicock, S.R., and Armstrong, J.E., 1985, Vashon Drift: Definition of the formation in the Georgia Depression, southwest British Columbia: Canadian Journal of Earth Sciences, v. 22, p. 748–757.
Hicock, S.R., and Fuller, E.A., 1995, Lobal interactions, rheologic superposition, and implication for a Pleistocene ice stream on the continental shelf of British Columbia: Geomorphology, v. 14, p. 167–184.
Holland, S.S., 1976, Landforms of British Columbia, a physiographic outline: British Columbia Department of Mines and Petroleum Resources Bulletin 48, 138 p.
Huntley, D.H., Stumpf, A.J., Levson, V.M., and Broster, B.E., 1996a, Babine Porphyry Belt Project: Quaternary geology and regional till geochemistry sampling in the Old Fort (93 M/01) and Fulton Lake (93 L/16) map areas, British Columbia, *in* Grant, B., and Newell, J.M., eds., Geological fieldwork 1995: British Columbia Geological Survey Paper 1996–1, p. 45–53.
Huntley, D.H., Levson, V.M., and Weary, G.F., 1996b, Surficial geology and Quaternary history of the Old Fort Mountain area (NTS 93 M/01): British Columbia Ministry Geological Survey Branch Open-File 1996–9, scale 1:50 000.
Jackson, L.E., Phillips, F.M., Shimamura, K., and Little, E.C., 1997, Cosmogenic ^{36}Cl dating of the Foothills erratics train, Alberta, Canada: Geology, v. 25, p. 195–198.
Josenhans, H.W., Fedje, D.W., Conway, K.W., and Barrie, J.V., 1995, Post glacial sea levels on the Western Canadian continental shelf: Evidence for rapid change, extensive exposure, and early human habitation: Marine Geology, v. 125, p. 73–94.
Kerr, F.A., 1934, Glaciation in northern British Columbia: Royal Society of Canada Transactions, ser. 3, v. 28, p. 17–31.
Levson, V.M., and Giles, T.R., 1997, Quaternary geology and till geochemistry studies in the Nechako and Fraser plateaus, central British Columbia, *in* Diakow, L.J., and Newell, J.M., eds., Interior Plateau geoscience project: Summary of geological, geochemical and geophysical studies: British Columbia Geological Survey Paper 1997–2, p. 121–145.
Levson, V.M., and Rutter, N.W., 1996, Evidence of Cordilleran late Wisconsinan glaciers in the 'ice-free corridor': Quaternary International, v. 32, p. 31–51.
Levson, V.M., Mate, D., and Stuart, A.J., 1999, Quaternary geology and drift prospecting studies in the north central Nechako Plateau (93 F and K), Geological fieldwork 1998: British Columbia Geological Survey Paper 1999–1, p. 15–23.
Luternauer, J.L., and Murray, J.W., 1983, Late Quaternary morphologic development and sedimentation, central British Columbia continental shelf: Geological Survey of Canada Paper 83–21, 31 p.
MacIntyre, D.G., Webster, I.C.L., and Bellefontaine, K., 1996, Geology of the Fulton Lake map sheet (93L/16): British Columbia Geological Survey Open File 1996–29, scale 1:50 000.
MacIntyre, D.G., Webster, I.C.L., and Dejardins, P., 1998, Bedrock geology of the Old Fort Mountain map area (NTS 93M/01), north-central British Columbia: British Columbia Geological Survey Open File 1997–10, scale 1:50 000.
Mann, D.H., and Hamilton, T.D., 1995, Late Pleistocene and Holocene paleoenvironments of the north Pacific coast: Quaternary Science Reviews, v. 14, p. 449–471.
Mathews, W.H., 1980, Retreat of the last ice sheets in northeastern British Columbia and adjacent Alberta: Geological Survey of Canada Bulletin 331, 22 p.
McMillan, R.H., 1995, Mineral occurrence (MINFILE) map of the Hazelton (093M) area: British Columbia Geological Survey, scale 1:250 000.
Patterson, C.J., 1998, Laurentide glacial landscapes: The role of ice streams: Geology, v. 26, 643–646.
Plouffe, A., 1991, Preliminary study of the Quaternary geology of the northern interior of British Columbia, *in* Current research, Part A: Geological Survey of Canada Paper 91A–1A, p. 7–13.
Plouffe, A., 1992, Quaternary stratigraphy and history of central British Columbia, *in* Current research, Part A: Geological Survey of Canada Paper 92–1A, p. 189–193.
Plouffe, A., 1995, Geochemistry, lithology, mineralogy and visible gold grain content of till in the Manson River and Fort Fraser map areas, central British Columbia (NTS 93K and N): Geological Survey of Canada Open-File 3194, 119 p.
Plouffe, A., 1997a, Ice flow and late glacial lakes of the Fraser Glaciation, central British Columbia, *in* Current research 1997-A: Geological Survey of Canada Paper, p. 133–143.
Plouffe, A., 1997b, Géologie glaciaire et étudie du contenu de mercure dans le till, partie centrale de la Colombie-Britannique [Ph.D. dissert.]: Montréal, Université de Montréal, 238 p.
Plouffe, A., 1999, New data on till geochemistry in the northern sector of the Nechako river map area, British Columbia, *in* Current research 1999-A: Geological Survey of Canada Paper, p. 169–178.
Porter, S.C., and Swanson, T.W., 1998, Radiocarbon age constraints on rates of advance and retreat of the Puget Lobe of the Cordilleran Ice Sheet during the last glaciation: Quaternary Research, v. 50, p. 205–213.
Rutter, N.W., 1977, Multiple glaciation in the area of Williston Lake, British Columbia: Geological Survey of Canada Bulletin 273, 31 p.
Ryder, J.M., and Maynard, D., 1991, The Cordilleran Ice Sheet in northern British Columbia: Géographie Physique et Quaternaire, v. 45, p. 355–363.
Ryder, J.M., Fulton, R.J., and Clague, J.J., 1991, The Cordilleran Ice Sheet and the glacial geomorphology of southern and central British Columbia: Géographie Physique et Quaternaire, v. 45, p. 365–377.
Schiarizza, P., 1998, Sitlika rocks of the Kutcho Assemblage and their tectonic relationship to the Cache Creek and Takla groups near Takla Lake, *in* Struik L.C., and MacIntyre D.G., eds., New geological constraints on Mesozoic to Tertiary metallogenesis and on mineral exploration in central British Columbia: Nechako NATMAP Project: Vancouver, British Columbia, Geological Association of Canada Cordilleran Section Short Course, p. 133–156.
Schiarizza, P., and MacIntyre, D.G., 1999, Geology of the Babine Lake–Takla Lake area, central British Columbia (93 K/11, 12, 13, 14; 93 N/3, 4, 5, 6), *in* Geological fieldwork 1998: British Columbia Geological Survey Paper 1999–1, p. 33–68.
Shaw, J., 1994, A qualitative view of sub-ice-sheet landscape evolution: Progress in Physical Geography, v. 18, p. 159–184.
Shoemaker, E.M., 1991, On the formation of large subglacial lakes: Canadian Journal of Earth Sciences, v. 28, p. 1975–1981.
Stumpf, A.J., Huntley, D.H., Levson, V.M., and O'Brien, E.K., 1996, Surficial geology and Quaternary stratigraphy of the Fulton Lake Area (NTS 93 L/16): British Columbia Geological Survey Branch Open-File 1996–10, scale 1:50 000.
Stumpf, A.J., Broster, B.E., and Levson, V.M., 1997, Evaluating the use of till geochemistry to define buried mineral targets: A case study from Bell mine (93 L/16, M1), west-central British Columbia, *in* Grant, B., and Newell, J.M., eds., Geological fieldwork 1996: British Columbia Geological Survey Paper 1997–1, p. 439–456.
Tipper, H.W., 1971a, Glacial geomorphology and Pleistocene history of central British Columbia: Geological Survey of Canada Bulletin 196, 89 p.
Tipper, H.W., 1971b, Multiple glaciation in central British Columbia: Canadian Journal of Earth Sciences, v. 8, p. 743–752.
Tipper, H.W., 1994, Preliminary interpretation of glacial and geomorphic features of Smithers map area (93L), British Columbia: Geological Survey of Canada Open File 2837, 7 p., scale 1: 250 000.
West, C.A., 1997, Glacial flow patterns and till geochemistry in the eastern Manson River map area (NTS 93K), central British Columbia [Master's thesis]: Ottawa, Ontario, Carleton University, 244 p.

MANUSCRIPT RECEIVED BY THE SOCIETY JULY 19, 1999
REVISED MANUSCRIPT RECEIVED FEBRUARY 7, 2000
MANUSCRIPT ACCEPTED FEBRUARY 9, 2000

Printed in the USA

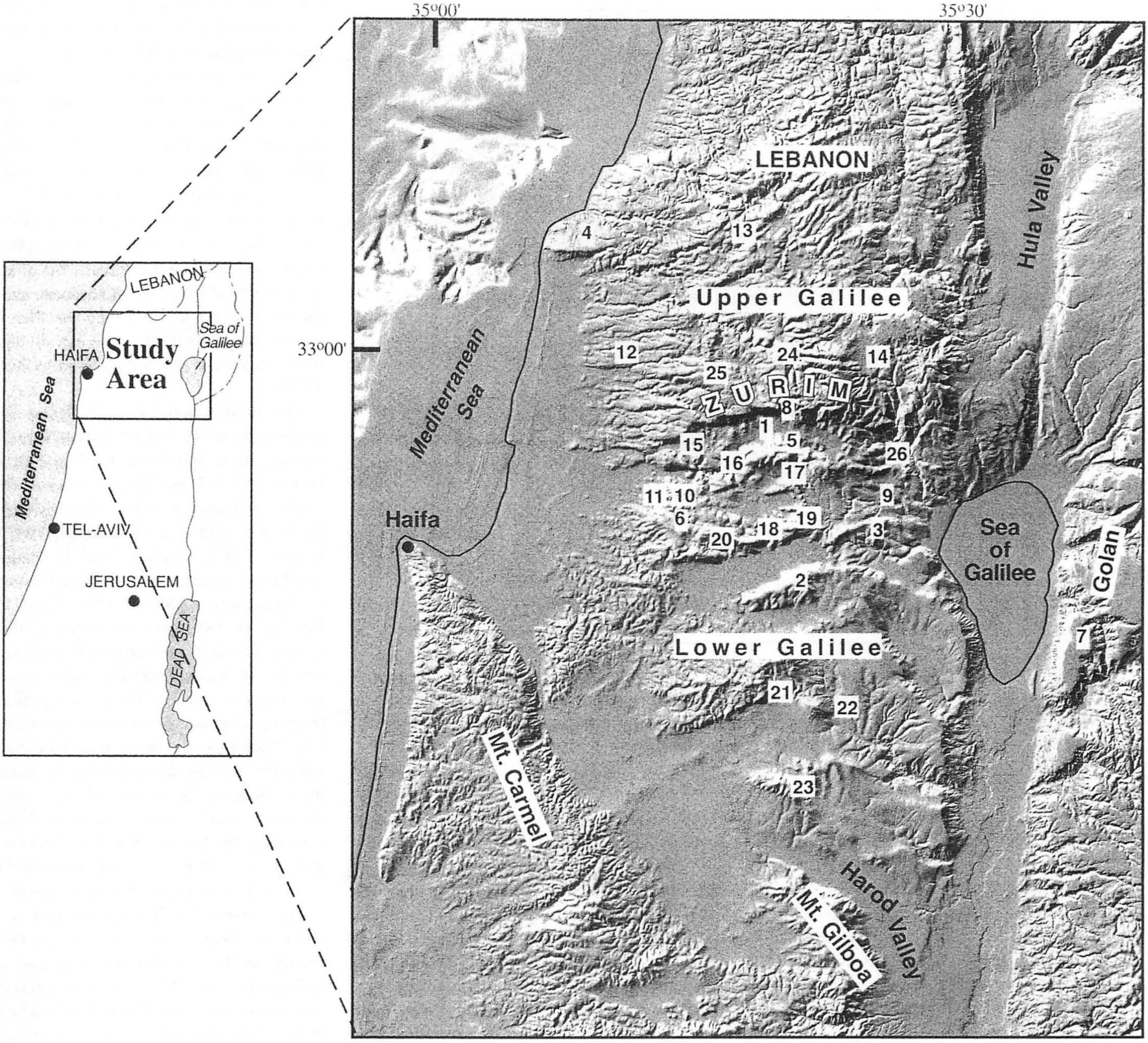

Figure 1. Location map. Shaded relief map by Hall (1993). 1—Nahef, 2—Mount Tur'an, 3—Mount Mimlah, 4—Rosh-Haniqra, 5—Mount Kamon, 6—Qoranit, 7—Ha'on, 8—Mount Sahzor, 9—Nahal Zalmon, 10—Nahal Segev, 11—Kabul, 12—Bet-Ha'emek, 13—Mount Zonem, 14—Mount Meiron, 15—Mount Gilon, 16—Mount Esh'har, 17—Mount Hilazon, 18—Mount Sha'abi, 19—Hararit, 20—Mount Azmon, 21—Nazerat, 22—Mount Tabor, 23—Givat Hamore, 24—Peqi'in, 25—Kisra, 26—Mount Livnim.

The method presented here is based on structural, topographic, and morphologic data and involves (1) the ratio between the height of escarpments and the total stratigraphic displacement that formed them, and (2) an analysis of the shape of the escarpments. These two parameters, together with the available age control, are applied to determine the relative age of tectonically formed escarpments in the Galilee.

PREVIOUS STUDIES

Morphologic features in general, and the evolution of the shape of slopes in particular, have been used as tools to study tectonic activity. Classic landscape evolution models based on morphologic analysis were integrated with tectonic interpretations by early researchers (e.g., Gilbert, 1877; Davis, 1899; King, 1957; Simons, 1962). Later studies (e.g., Hack, 1960) added insight into the relationship between topography and tectonic activity. In recent years, the use of morphology to interpret tectonic activity has increased. Bull and McFadden (1977) and Bull (1977) used geomorphic features to describe the relationship between tectonics and geomorphologic processes. Adams (1984) pointed to the secondary influence of lithology on the development of escarpments in the mountain

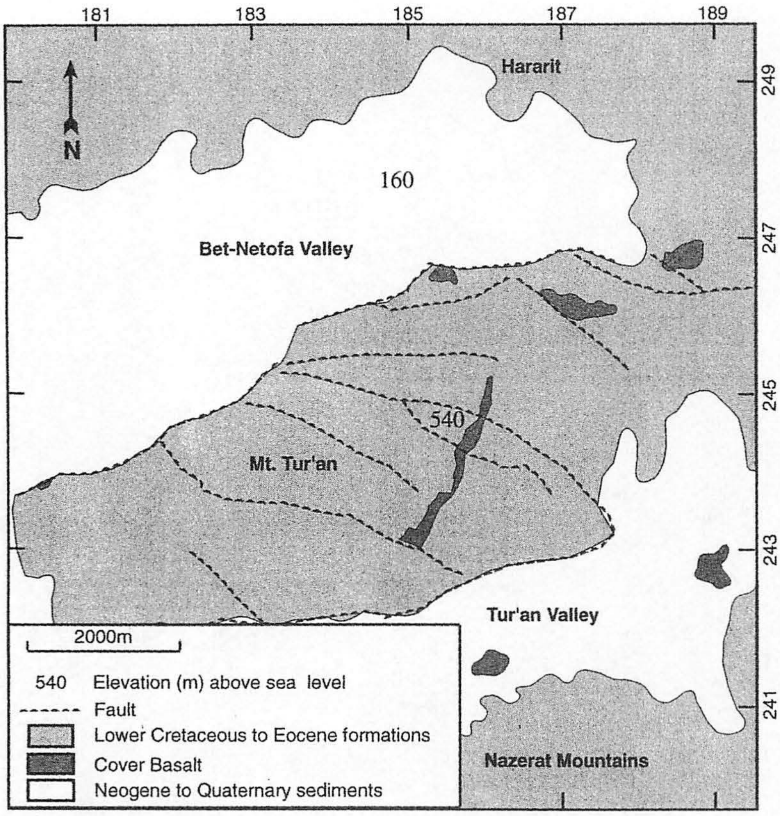

Figure 2. Geologic map of Mount Tur'an. The Cover Basalt flowed over a gentle topography that preceded normal faulting and formation of the Tur'an block. Outcrops of the Cover Basalt are found at several locations on top and around the base of Mount Tur'an. The geology is after Vroman (1958) and Michelson (1970).

front of the Southern Alps of New Zealand. Hare and Gardner (1984) analyzed uplifted surfaces to determine the relative timing of tectonic activity in Costa Rica. Mayer (1986) proposed several morphologic indices along mountain fronts and escarpments that can be used as tectonic indicators, and Keller (1986) discussed the use of surface erosion processes as tools for tectonic investigation. Wells et al. (1988) and Menges (1988) applied morphometric analyses to infer variations in tectonic activity using mountain-front morphology, riverbed gradients, and ridge shapes. Menges (1988) concluded that lithology plays only a secondary role in the development of tectonically formed slopes in the Rio Grande rift in New Mexico.

Only a few studies have examined the relationship between tectonics and morphology in the Galilee (Picard, 1943; Yair, 1962; Freund, 1970; Nir, 1970; Bar and Harash, 1983; Ron et al., 1984; Kafri, 1997; Matmon et al., 1999a). Nir (1970) distinguished morphologic surfaces in the Galilee and attributed them to a recent uplift. Bar and Harash (1983) compared slope morphology of different tectonic escarpments in northern Israel and categorized them into several groups according to their shapes. Ron et al. (1984) distinguished between a pre-Pliocene tectonic phase that does not contribute to the present landscape, and a Pleistocene tectonic phase that controls the present landscape. Kafri (1997) did comprehensive work on the Miocene drainage systems in the Lower Galilee and related the changes in their routes to the development of the base level in the east (the Dead Sea transform valley) and in the south (Yizre'el Valley).

GEOGRAPHIC AND GEOLOGIC SETTING

The Galilee, northern Israel, is divided along the Zurim escarpment into the Lower and Upper Galilee (Fig. 1). The Lower Galilee consists of a series of east-west–trending ridges bounded by normal faults (Freund, 1970) and separated by elongated valleys. The Upper Galilee is the largest, highest, and northernmost uplifted block. It is internally faulted and dissected by deep valleys. The Galilee is characterized by a Mediterranean climate, i.e., dry summers and mild rainy winters, and the annual precipitation is 600–800 mm.

Two major fault systems are identified in the Galilee: (1) strike-slip faults oriented northwest-southeast and northeast-southwest (Freund, 1970; Ron et al., 1984). Most of these faults have no topographic expression and were probably active before 4 Ma (Ron et al., 1984). (2) East-west–oriented normal faults that form most of the morphotectonic features in the Galilee. A broad structural arch, bounded between the Mediterranean and the Dead Sea Rift, formed during the Pleistocene and caused the establishment of the main regional water divide (Matmon et al., 1999a).

The mountainous area of the Galilee is composed mainly of Cenomanian and Turonian limestone and dolomite (Picard and Golani, 1965). A Lower Cretaceous sequence of marls, sandstone, and limestone is exposed at the base of several escarpments (Eliezri, 1965; Golani, 1957). Senonian and Eocene chalk and limestone are exposed along the margins of the mountains (Shlein, 1961; Kafri, 1972). Because of the carbonate lithology, dissolution is the dominant erosional process. Deposition of clastic material in the basins is minor, because most of the eroded material is transported in solution through the karst system. Therefore, the development of slopes is not influenced by deposition in the basins. In the Galilee, the basins contain clay soils that do not exceed several meters in thickness. Generally, the basins are not well drained and there is no evidence of a deposition and reexcavation history of the drainage system.

The present-day drainage network is composed of short channels (<30 km) that are limited in their erosion potential and rarely undergo any flow. The formation of this drainage system was controlled by the development of the Dead Sea Rift Valley as a morphologic feature that cut the Mediterranean watershed from its eastern drainage area ca. 8 Ma (Shaliv, 1991), the development of the east-west Basin and Range structure in the Lower Galilee, and the late Pliocene and Pleistocene arching of the Galilee (Picard, 1943; Matmon et al., 1999a).

Mount Tur'an—The Only Well-Dated Escarpment

The tectonic and erosional history of Mount Tur'an is the key to understanding the morphometric parameters used in this study and the implications of the morphometric analysis on the late Cenozoic tectonic history of the

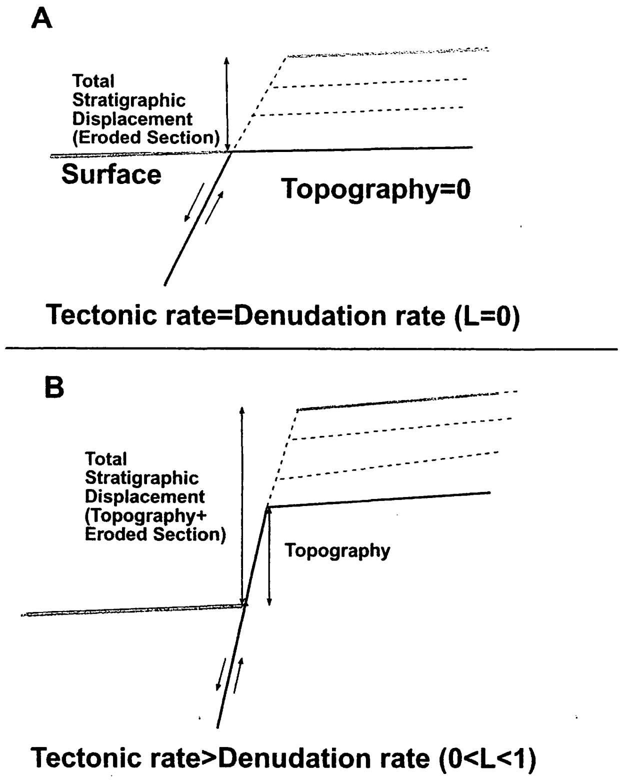

Figure 3. The *L*-index concept. (A) Vertical displacement takes place but topography does not form; the ratio between topography and vertical displacement is zero. This situation occurs when the rate of vertical displacement does not exceed the rate of denudation. (B) Vertical uplift rate is greater than the rate of denudation and topography forms; the ratio between topography and vertical displacement ranges between 0 and 1.

Galilee. The Tur'an block is located in the Lower Galilee (2 in Fig. 1). The total stratigraphic displacement along the Tur'an fault system is 625 m (Freund, 1970). The escarpment is 300 m high. A basalt flow of the Cover Basalt Formation (Schulman, 1962), 4.23 ± 0.23 Ma (Heimann et al., 1996), is displaced by 300 m (Fig. 2; Golani, 1957). Outcrops of this volcanic formation are located at the base of the Tur'an block and on top of it (Fig. 2). Field relations in Mount Tur'an as well as in other exposures of the Cover Basalt in the Galilee indicate that the basalt spilled over a gentle landscape and that its thickness in the mountainous part of the Galilee did not exceed several tens of meters (Heimann, 1990; Shaliv, 1991; Heimann et al., 1996).

METHODOLOGY

To describe the morphology of the Galilee escarpments we use two parameters: the *L* value, the ratio between the height of the escarpment and the total stratigraphic displacement, which provides information regarding displacement stages, and the relationship between tectonic and erosion rates and the degree of concavity of undated tectonic slopes. These slopes are then compared to the concavity of the slope of Mount Tur'an, which provides the time constraint on the age of topography.

The *L* Value—Definition, Data Sources, and Errors

The *L* value is defined as the ratio between the relief (h) of an escarpment (i.e., the topographic difference between the base and the top of the escarpment) and the total vertical stratigraphic displacement (s) (Fig. 3). *L* values can range between 0 and 1. Low *L* values indicate that most of the topographic expression of the vertical tectonic activity has been erased by a combination of erosion of the uplifted block and deposition of material on the down-faulted block. Alternatively, such values characterize faults with low displacement rates that did not exceed denudation rates, and therefore had very little or no topographic expression. High *L* values indicate that most of the vertical uplift is expressed as relief, indicating that the rate of vertical uplift along the fault exceeded denudation rates. Intermediate *L* values indicate that a portion of the total uplift was eroded. However, the *L* value does not give any indication of the timing of erosion, i.e., whether it occurred after total stratigraphic displacement was achieved or some time during uplift.

Topographic data were obtained from digital terrain modeling of Israel (Hall, 1993). Stratigraphic data were compiled from structural maps of the Galilee, which are based on the datum of the top of the Judea Group (Saltzman, 1964; Eliezri, 1965; Glikson, 1965; Bein, 1967; Kafri, 1972; Levy, 1983; Cohen, 1988). Because the structural contour interval on these maps is 50 m and we consider only major escarpments (scale of hundreds of meters), the analysis accounts for large tectonic blocks and regional erosion. These two data sets were combined with a geographical information system (GIS) procedure to calculate *L* values at several points along each escarpment in the study area. The results are separated into three groups indicating low (0–0.25), intermediate (0.25–0.75), and high (≥0.75) values. Values higher than 1 were obtained in a few cases along low-relief escarpments (<100 m). These values result from inaccuracy in the determination of the structural elevation. Therefore, low-relief escarpments were not analyzed further. *L* values between 1 and 1.1 are considered in the high group values. *L* values above 1.1 were rejected.

A standard error function is used to calculate errors in *L* (ΔL):

$$\Delta L = \frac{\Delta h}{s} + \frac{h \cdot \Delta s}{s^2} \qquad (1)$$

where s is the total stratigraphic displacement and h is the elevation difference between the top and the base of the escarpment. We assume that the error (ΔL) arises from contour-line interpolation in topographic and structural maps and depends on the contour interval of the maps. Therefore, $\Delta h = 10$ and $\Delta s = 50$. The value of ΔL increases with decreasing total amount of displacement and decreases with decreasing relief. Therefore, the lowest ΔL values are in cases of large stratigraphic displacement and low *L* values. Generally, along escarpments with a total displacement of more than 200 m, ΔL causes small changes in *L* values (Data Repository Table DR1[1]). Most of

[1]GSA Data Repository item 2000113, estimation of ΔL, is available on the Web at http://www.geosociety.org/pubs/ft2000.htm. Requests may also be sent to Documents Secretary, GSA, P.O. Box 9140, Boulder, CO 80301; e-mail: editing@geosociety.org.

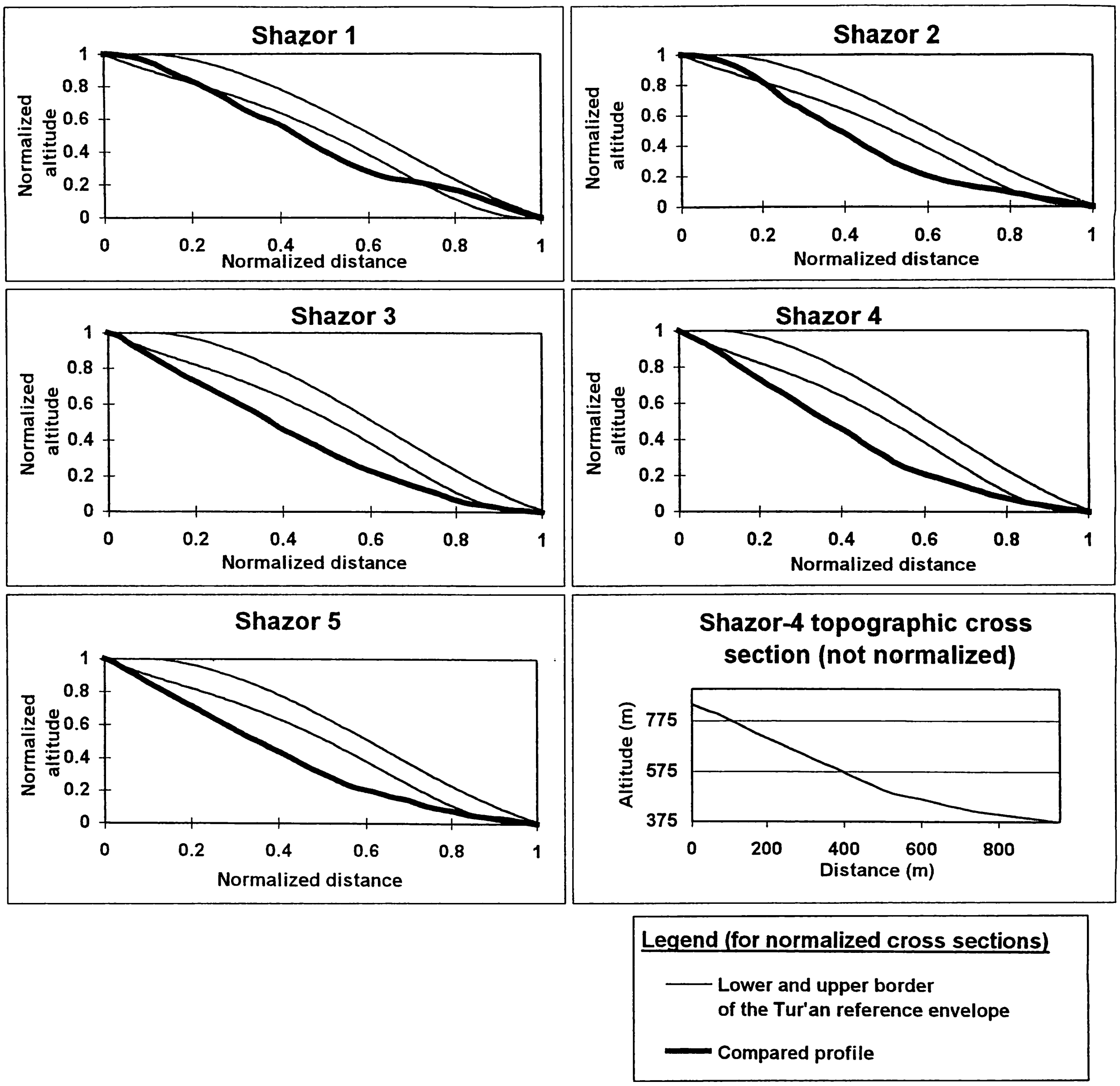

Figure 4. Comparison between constructed profiles along the undated Shazor escarpment and the Tur'an reference envelope. The Shazor profiles are significantly more concave than the Tur'an reference envelope, and therefore the Shazor escarpment is older than the Tur'an block.

the analyzed escarpments include displacements of >200 m so the tectonic implication deduced from their corresponding *L* values does not change.

Shape of Escarpments—Construction, Comparison, and Reference Shape

Topographic profiles were constructed on each escarpment along lines perpendicular to the strike of the fault that formed the escarpment. The profiles were constructed along interfluves to avoid the influence of channel erosion. All profiles were normalized so that maximum and minimum heights equaled 1 and 0, respectively, and the length of the profile ranged from 0 to 1 (Fig. 4). This normalization enabled comparison of the shapes of the different profiles regardless of their actual length or height. In the Galilee, normalization of the topographic profiles does not obscure morphologic information because the different escarpments are generally of the same size (300–500 m high), and the upper part of the escarpments erodes slowly and is relatively stable (as is shown later for Mount Tur'an). The comparison of different tectonic slopes is restricted to those that are composed of hard carbonate rocks (limestone and/or dolomite) of the Cenomanian and Turonian Judea Group, and not affected by axial streams at their base.

To establish the reference slope we used the Mount Tur'an topography. Of 15 topographic cross sections of the Tur'an block that were constructed (Figs. 5 and 6), 14 exhibited good similarity (Fig. 6). These slope profiles were normalized and used to calculate a reference envelope (Fig. 7), which allows for natural variation of the slope's shape due to factors such as lithology, escarpment aspect, relation of dip direction to the aspect, and random variation of shape. In places where the escarp-

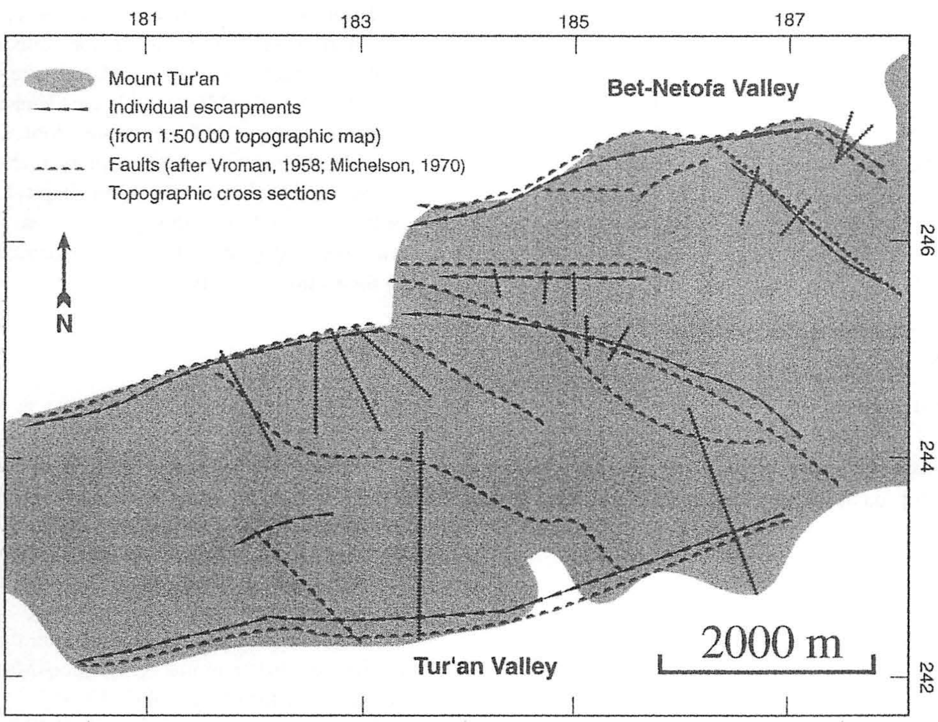

Figure 5. Locations of the topographic cross sections on the Tur'an block. The topographic escarpments generally coincide with the normal faults that cross the block. This agreement is evidence for the morphology of the block being controlled by the distribution and activity of the faults, and not by lithology.

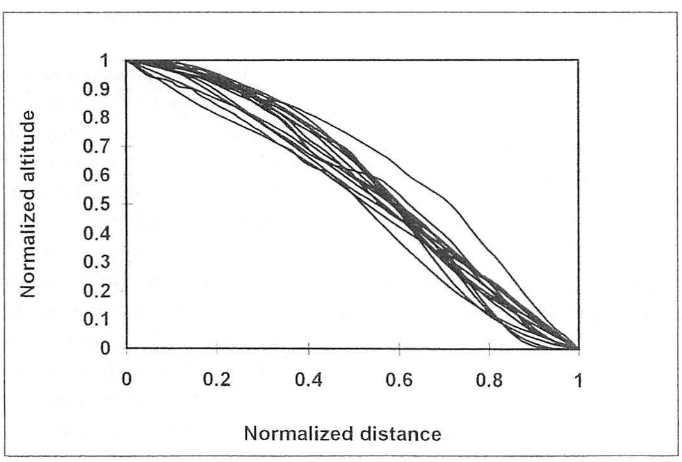

Figure 6. The Tur'an reference profiles with plots of 15 topographic profiles across the various escarpments of the Tur'an block. The profiles include all sides of the uplifted block in order to accommodate natural variations in the shapes of the profiles that result from minor variations in lithology, proximity to drainage channels, and face aspect. Of the profiles, 14 are similar and were used to determine the Tur'an reference envelope (Fig. 7). All profiles were normalized to enable comparison with profiles of different heights and lengths.

ment is constructed of a single fault, the profiles include the entire escarpment; in places where the escarpment is composed of several parallel faults, the cross sections include individual faults and the specific escarpments formed by them (Fig. 5). All the constructed escarpment profiles in the Galilee were compared to the Tur'an reference envelope. The basic assumption was that profiles that are more concave, fall within, or are more convex than the Tur'an reference envelope indicate older, same age, and younger escarpments, respectively.

Methodological Assumptions

The present morphometric analysis for landscape evolution is based on several assumptions explained in the following.

The recent topography of the Galilee has been shaped by late Miocene–Pliocene extensional deformation of a low-relief Oligocene–Miocene erosional surface (Garfunkel, 1988). Throughout its history, the entire area has undergone similar climatic conditions, climatic variations, and variations in base level. It is composed of similar lithologies, soil cover, and vegetation. Therefore, variations in the shape of the slope are time dependent.

With respect to slope shape, it is assumed that with time, the development of fault-controlled slopes is generally from convex to concave (e.g., Davis, 1899; Simons, 1962; King, 1957; Ahnert, 1966, 1973a, 1973b). As long as the rate of uplift is higher than the rate of erosion, the tectonic slope maintains its convex shape. When the rate of tectonic uplift declines, the slope gradually becomes concave (Wallace, 1987). Therefore, in a morphotectonic setting that is controlled mainly by time, the degree of concavity is directly related to the age of the escarpment and to the length of time of relative slow uplift rates or tectonic quiescence (Mayer, 1986). The Nahef escarpment (1 in Fig. 1) is a good example of this assumption. It has been developing since the middle or late Pleistocene until recently (Gran et al., 1999). The shape of the tectonic slope of the Nahef escarpment, which has a well-preserved fault scarp at its base, is convex (Fig. 8). The concave shapes of older nearby escarpments that lack fresh fault scarps (e.g., Shazor, Fig. 4) indicate that tectonic slopes in the Galilee evolve from a convex to a concave shape.

We also assume that erosion rates are relatively low on top of the topographic elements that constitute a local drainage divide and rise high above their surroundings. Horsts and tilted blocks are an example of such topographic

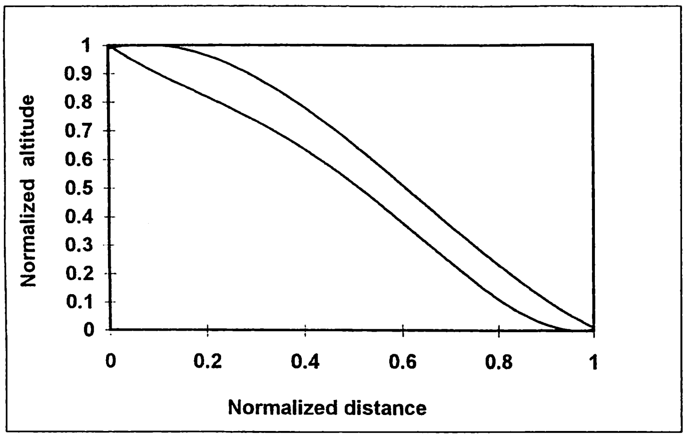

Figure 7. The Tur'an reference envelope was determined by digitizing the lower and upper boundaries of the space defined by the topographic profiles (excluding the Tur'an-8 profile).

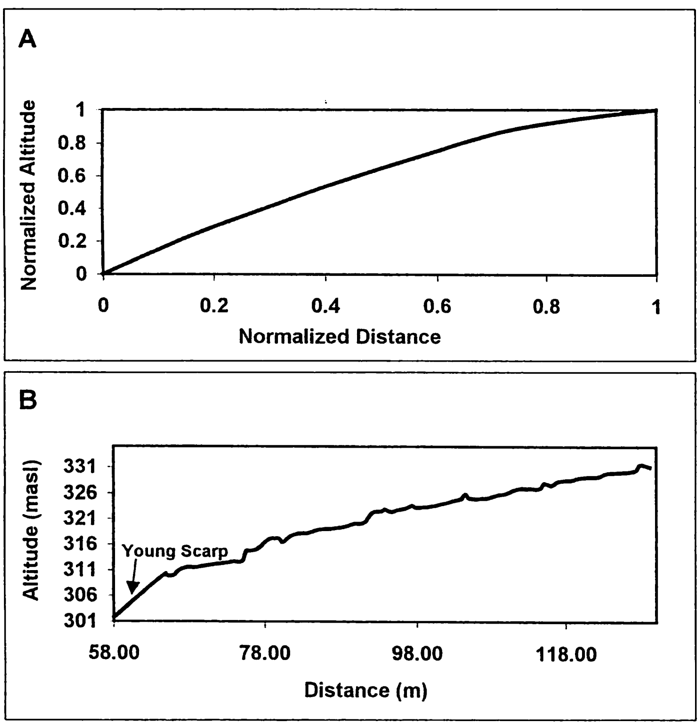

Figure 8. Topographic cross section of the Nahef escarpment. (A) A normalized profile using digital terrain model data. (B) A detailed topographic profile of the Nahef escarpment using global positioning system measurements.

elements. In other rock types, lowering these drainage divides requires temporal scales much longer than several million years (Bierman and Turner, 1995; Bierman et al., 1995; Matmon et al., 1999b). In carbonate terrain, denudation by carbonate dissolution is estimated to be 30–40 m/m.y. in regions where precipitation is 600–800 mm/yr (e.g., Jennings, 1971; Atkinson and Smith, 1978; Trudgill, 1985; Dreybrodt, 1988; Bloom, 1991). This range of denudation rates agrees with the rate of denudation of 29 m/m.y. calculated from measured concentrations of ^{36}Cl in limestone along the Zurim escarpment (Gran et al., 1999). Denudation rates calculated by Yaalon (1959) and Gerson (1974) based on Corbel's equation range between 10 and 20 m/m.y., and Ritter et al. (1995) provided a denudation rate of 20 m/m.y. for the eastern Mediterranean region. Begin and Zilberman (1997) estimated a mean denudation rate of 20 m/m.y. since the Miocene. These denudation rates and the ages of the morphotectonic structures based on the profile comparison exclude the possibility that first the entire displacement of the tectonic blocks took place and only then was their topography lowered by denudation to their current position.

RESULTS

L Values

The *L* values were calculated along most of the normal faults expressed by escarpments throughout the Galilee (Table DR2; see footnote 1). This selection leaves out most of the Galilee faults because they have no topographic expression (*L* value = 0) (Fig. 9), indicating that they were not active after the formation of the regional Oligocene–Miocene erosional surface (Garfunkel, 1988).

L values range between 0.18 and 1.13 (Fig. 10). Low *L* values, which indicate a long period of slow activity, generally characterize some of the large escarpments, such as that of Rosh-Haniqra (4 in Fig. 1). These escarpments contain morphologic elements such as hanging valleys and fresh bedrock fault scarps that indicate Quaternary offset. The *L* values (n = 61) show a bimodal distribution indicating two groups of faults: the first group at 0.4–0.5 and the second group at 0.8 and higher (Fig. 11).

Slope Comparison

The escarpments that were compared with the Tur'an reference envelope are shown in Figure 1. They are divided into three groups: (1) those having more concave profiles, (2) those within the reference envelope, and (3) those that are more convex than the Tur'an reference envelope (Table 1; Fig. 12).

Most of the Galilee escarpments have slope profiles that are within the Tur'an reference envelope. The Zurim escarpment (which includes Mounts Haluz, Lavon, and Shazor, Fig. 1) and Meiron escarpment (14 in Fig. 1) are the bounding escarpments of the Upper Galilee and present profiles, which are more concave than the Tur'an reference envelope. Other escarpments, such as the Esh'har (16 in Fig. 1), Rosh-Haniqra (4 in Fig. 1), the southern part of the Peqi'in fault, and western Gilboa escarpments have concave profiles that are significantly different from the Tur'an reference envelope. The eastern part of the Mount

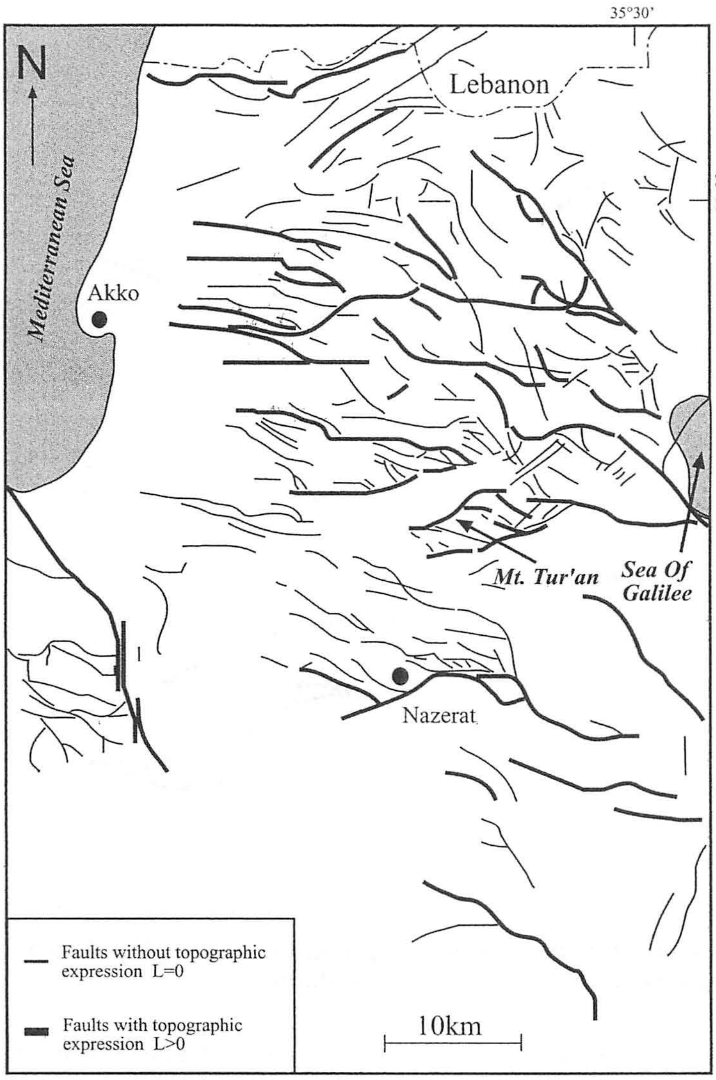

Figure 9. Fault map of the Galilee. The faults indicated with a thick line have topographic expression. Most of the faults in the Galilee have no topographic expression, indicating a lack of activity after the Oligocene to Miocene denudation period.

TABLE 1. RESULTS OF SLOPE PROFILE COMPARISON

Name of escarpment (location in Fig. 1)	Result of comparison with Tur'an reference envelope
West Mount Zonem (13), Tuval (western part of the Zurim escarpment), Kisra (25), Peqi'in (24), Mount Gilon (15), Mount Kamon (5), Qoranit (6), Mount Sha'abi (18), Mount Azmon (20), Nazerat (21), Givat Hamoreh (23), Mount Tabor (22), eastern Gilboa	Within the Tur'an reference envelope
Mount Haluz, Mount Lavon and Mount Shazor (which are part of the Zurim escarpment), Esh'har (16), Rosh-Haniqra (4), Meiron (14), southern part of the Peqi'in fault and western Gilboa escarpments	More concave than the Tur'an reference envelope
East Mount Zonem (13)	More convex than the Tur'an reference envelope

Zonem (13 in Fig. 1) escarpment has a convex profile, which significantly differs from the Tur'an reference envelope.

A comparison between profiles indicates that generally, all profiles on each individual block-bounding fault are similar (Fig. 4). In some cases, there are systematic variations in the slope profiles along fault lines that can be correlated to segmentation deduced from *L* values (e.g., the Mount Zonem [13 in Fig. 1] and Gilon [15 in Fig. 1] escarpments).

Testing Slope Comparisons

We were able to test the validity of the results of the slope comparison procedure at two sites.

1. The western part of the Mimlah escarpment (3 in Fig. 1) is composed of Cenomanian–Turonian limestone and dolomite (Saltzman, 1964) capped by basalt of the Cover Basalt Formation. The same basalt is exposed at the base of the escarpment (on the downfaulted block), indicating vertical displacement after ca. 4 Ma. The height of the escarpment and the amount of displacement of the Cover Basalt are ~100 m. Seven slope profiles constructed along the Mimlah escarpment were compared with the Tur'an reference envelope (Fig. 13A). Six of the profiles fit within the Tur'an reference envelope and the Mimlah–4 profile was slightly more convex. Thus, aside from this exception, the Mimlah escarpment profiles fit into the Tur'an reference envelope, which is the expected behavior of escarpments of the same age (ca. 4 Ma) and similar lithology.

2. The Gilboa escarpment (Fig. 1) rises 300–400 m above the Harod Valley. It displaces a ca. 6 Ma basalt flow by ~350 m (Shaliv, 1991). The good preservation of the basalt on the top of the uplifted block suggests that the escarpment formed a short time after the basalt flowed, securing it from rapid erosion. Therefore, the Gilboa escarpment is probably older or similar in age to the Tur'an escarpment, but definitely not younger. The Gilboa escarpment exhibits slope profiles significantly more concave than the Tur'an reference envelope (Fig. 13B), indicating that it is older than the Tur'an escarpment. This agrees with the conclusion of Shaliv et al. (1991) regarding the age of the Gilboa escarpment. These two case studies are the only other available slopes with independent information on the timing of their formation in the Galilee. They demonstrate that the methodology outlined earlier correctly predicts their age relative to the age of the Tur'an escarpment.

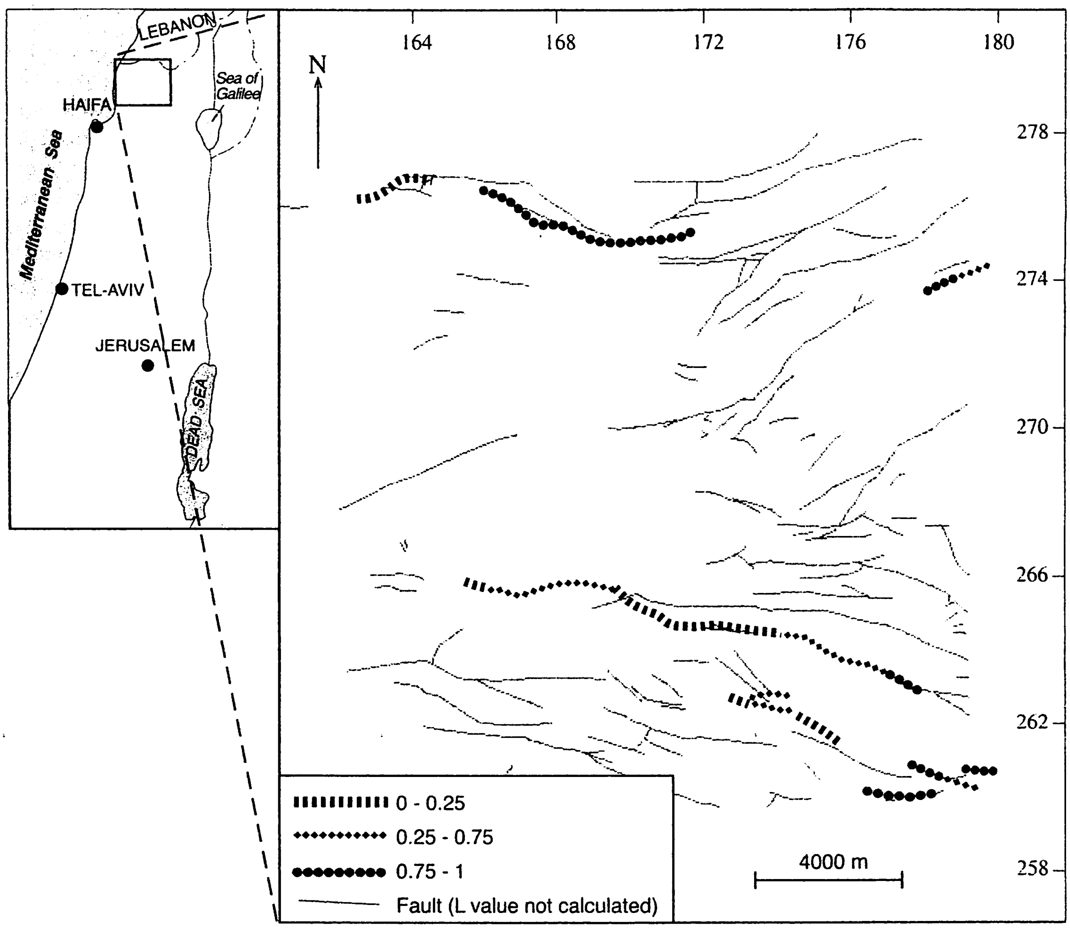

Figure 10. Example of *L* indices calculated along escarpments in the northwestern part of the Galilee. Most of the faults do not form topography and their *L* value is zero. Numbers along figure margin are Israel grid coordinates.

DISCUSSION

Effect of Lithology

Lithology affects the rate at which slopes develop. Slopes of similar age that are composed of different stratigraphic units within the Judea Group, as in the case of Mount Tur'an, have similar slope profiles (Fig. 6), indicating that lithologic variations within the Judea Group are not great enough to have a significant influence on the rate of slope development. Therefore, slopes composed of similar lithology but having different profiles are probably of different ages, as in the Shazor escarpment (Fig. 13C). Conversely, slopes composed of stratigraphic formations not of the Judea Group have different slope profiles even if they are of similar age. For example, the tectonic escarpment of Ha'on (7 in Fig. 1) displaces the Cover Basalt, thus its age is similar to or younger than the Tur'an escarpment. Nevertheless, the Ha'on slope, which is composed of Neogene continental sediments and volcanic rocks, has a profile that is significantly more concave than the Tur'an reference envelope (Fig. 13D). These examples indicate that the influence of lithologic variation depends on the degree of similarity of the rock units composing the escarpment. The differences in properties between similar rock types, such as the hard limestone and dolomite of the Judea Group, do not have much influence on the rate at which slopes develop. The differences between limestone and/or dolomite and chalk or continental sediments cause a significant variation in the rate of slope development. Therefore, tectonic slopes that are not built of a Judea Group sequence (such as the escarpments in the eastern Lower Galilee) were not compared with the Tur'an reference envelope.

Importance of Incision

Stream incision along the base of tectonic escarpments can have a significant influence on slope development. In such cases, which can be observed at the Mount Kamon and Qoranit escarpments (5 and 6 in Fig. 1), slope evolution depends on fluvial processes as well as time. Fluvial activity accelerates the development of the slope by carrying material away from it and causes it to be more concave than an identical slope that is not influenced by fluvial activity at its base. The summit of Mount Kamon (5 in Fig. 1) is situated at the southeast corner of the Kamon ridge and rises above both the southern and eastern escarpments. Even though the stratigraphy and the age of the southern and eastern slopes below the summit are identical (Golani, 1957), the eastern escarpment is mostly concave whereas the southern is convex (Fig. 13E). This reflects the incision of Nahal Zalmon (9 in Fig. 1) along the eastern escarpment. Similarly, Nahal Segev (10 in Fig. 1) is incised along the base of the Qoranit escarpment (6 in Fig. 1). In some places, it is incised directly along the fault line. In other places, it meanders away from the escarpment into the down-faulted block. Even though the stratigraphy and age along the escarpment remain constant (Kafri, 1965), the slope profile of the segment incised by Nahal Segev differs from that of the seg-

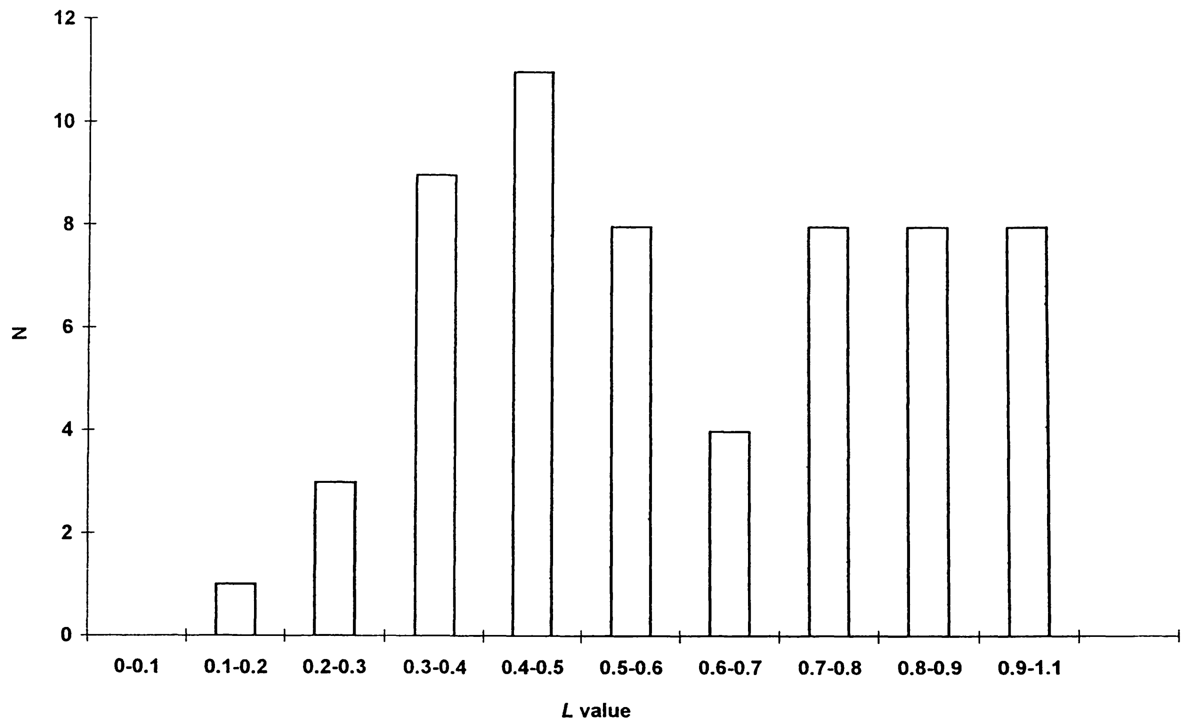

Figure 11. Occurrence (N) of *L* value as a function of *L* value. The distribution of *L* values indicates that the normal faults of the Galilee are divided into two groups that differ in the length of time they were active under truncation conditions and the time that topography was formed.

ment where the river does not abut the escarpment (Fig. 13F). In both cases, it is evident that the presence of incising axial streams leads to the development of more concave slopes. Therefore, slope profiles of the escarpments that are incised at their base by axial streams were not compared to the Tur'an reference envelope.

Implication of the History of Mount Tur'an on the Tectonics of the Galilee

The *L* value of Mount Tur'an is ~0.5. The difference of more than 300 m between the total vertical displacement and the vertical displacement of the Cover Basalt, which is identical to the relief of Mount Tur'an, indicates that about half of the motion took place prior to the basalt flow dated as 4.23 Ma. The Cover Basalt spilled over a gentle landscape that did not express the prebasalt displacement. A postbasalt stage of displacement deformed the basalt flow and formed the present relief of Mount Tur'an.

The field evidence from Mount Tur'an indicates that the normal faults bounding the Tur'an block were active in two temporal stages: an early stage that is not expressed by topography and a younger stage that formed substantial topography. These stages were separated by the extrusion of the Cover Basalt. It is not clear whether the early stage that occurred prior to 4.23 Ma formed relief of ~300 m, which was eroded before the Cover Basalt spilled, or whether it did not form relief because rates of uplift did not exceed rates of denudation at that time. The latter alternative is supported by the regional change of stress fields between the Miocene and the Pliocene (Ron et al., 1984).

During the earlier period of tectonic activity, most of the motion along the faults in the Galilee was lateral, with a small vertical component (Ron et al., 1984); thus, its topographic expression was easily eroded. However, in some cases *L* values indicate large amounts of vertical displacement during this phase. The large vertical displacement may reflect the long period during which the faults were active. The latter period of activity was characterized mainly by normal displacement that formed topography faster than erosion processes could obliterate it. This period of tectonic activity was shorter than the first, and might have been accompanied by minor lateral movement. The change in the character of the motion was also accompanied by, although not necessarily related to, the collapse of the large drainage network that was active in the region, the formation of the present drainage network, and the dramatic decline of erosional potential of the drainage system (Matmon et al., 1999a).

Shortly after the Cover Basalt event, tectonic rates must have increased. Otherwise, the Cover Basalt would have been eroded away, as were the 300 m of former vertical displacement. The basalt was preserved because it was uplifted, and situated on the local water divide where erosion rates decreased. The stability of the upper surface of Mount Tur'an, which is manifested by the preservation of the Cover Basalt Formation on the top of the uplifted block (Figs. 2), the development of thick calcrete coatings around the basalt outcrop, and the preservation of the Pliocene stream morphology in which the basalt flowed, indicates that elevated morphotectonic features were not subjected to intensive erosion during Pliocene–Pleistocene time. Therefore, in such a time interval, ranges that are at least 200 m higher than their surroundings are not substantially lowered by erosion.

The tectonic and erosional history of Mount Tur'an serves as an example of the development of other escarpments in the Galilee because it is reasonable to assume that the tectonic development of other blocks in the region is similar. The eroded portions of the uplifted sequences along the Galilee escarpments were stripped away during a time of slow uplift rates or during a long

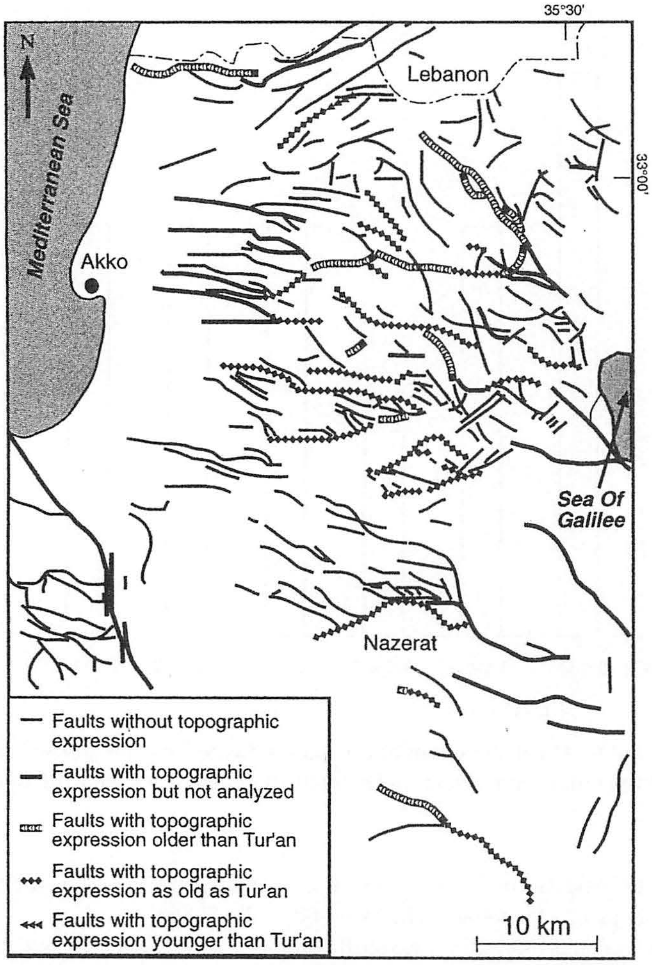

Figure 12. Fault map of the Galilee dividing the relief-forming faults into three age groups relative to the age of the Tur'an block. The relative age is determined by comparing the degree of concavity among the slopes of the different escarpments.

period of tectonic quiescence. Topographic expression was formed when tectonic uplift exceeded the rates of erosional processes. At that point, alluvial activity on top of the escarpments decreased, as they became local water divides. This implies that the *L* value reflects the tectonic history of the vertical displacement along a fault.

Accurate *L* value calculations are made possible by the widespread occurrence of Mesozoic marine sediments that maintain their thickness throughout the Galilee. This enables comparisons between the amount of tectonic displacement and its morphologic expression. The time of topography formation, which is not given by the *L* value, is determined by a comparison of slope profiles. A comparison of the degree of concavity between the Tur'an block and other escarpments provides the necessary time constraint for the transfer between the first and second stage of uplift because the age of the morphologic expression of the Tur'an block is defined by the age of a basalt flow of the Cover Basalt Formation.

CONCLUSIONS

Calculation of the *L* value along tectonic slopes in the Galilee leads to several principal conclusions: *L* values vary systematically along specific fault lines. This variation indicates the division of the faults into segments, which have different tectonic histories. Some escarpments, such as that of Rosh-Haniqra (4 in Fig. 1), developed along fault systems that had been active from the onset of extensional deformation in the Galilee in the Miocene (Freund, 1970; Ron et al., 1984) until the late Pleistocene. The long duration of activity is indicated both by the low *L* values and by morphologic elements such as fresh bedrock fault scarps, indicating late Pleistocene and Holocene activity (Gran et al., 1999).

Most of the escarpments in the Galilee have intermediate *L* values (0.4–0.5), similar to that of Mount Tur'an. These values indicate that most of the faults in the Galilee were active during the Miocene and early Pliocene at rates compatible to denudation and did not form topography at least until the middle to late Pliocene. The similarity of these escarpment slope profiles to the Tur'an reference envelope suggests that topography was formed after 4 Ma. Tectonic activity along these faults was again significantly reduced after forming the recent topography during the early Pleistocene (Matmon et al., 1999a).

The bimodal distribution of the *L* values (L = 0.4–0.5 and *L* = 0.8–1) indicates two groups of faults: one characterized by two periods of vertical displacement that were separated by the development of low-relief landscape, and a second characterized by one period of vertical displacement that formed the recent topography. A comparison of slope profiles shows that the two groups differ in the time they formed topography as well as in the length of time that they were active without forming topography.

Combining the *L* value calculation and the slope shape analysis for the Galilee escarpments leads to several conclusions:

1. The main escarpments in the Lower Galilee have slope profiles similar to the Tur'an escarpment and therefore are of similar age, ca. 4 Ma. The main and bounding escarpments of the Upper Galilee (the Zurim and Meiron escarpments) are more concave than the Tur'an reference envelope and therefore are older than the Tur'an escarpment. The Zurim and Meiron escarpments developed earlier than those in the Lower Galilee and were morphologic features at the time that the Cover Basalt flowed over a relatively flat Galilee. This conclusion agrees with the existence of a thick Neogene sequence in the eastern Lower Galilee (Shaliv, 1991) and the absence of any Neogene or Pleistocene sediments in the Upper Galilee.

2. The escarpments have a wide range of *L* index values. This indicates that there is no correlation between the length of time that a fault was active at slow uplift rates and subjected to continuous truncation, and the time of increased tectonic activity and formation of substantial topography.

3. Most of the faults in the Galilee were not active after the formation of the main erosion surface and are not expressed by topography.

4. Morphometric analysis of tectonic slopes in an erosional landscape is a valid method for understanding the tectonics of a region where there is no accumulation of sediments.

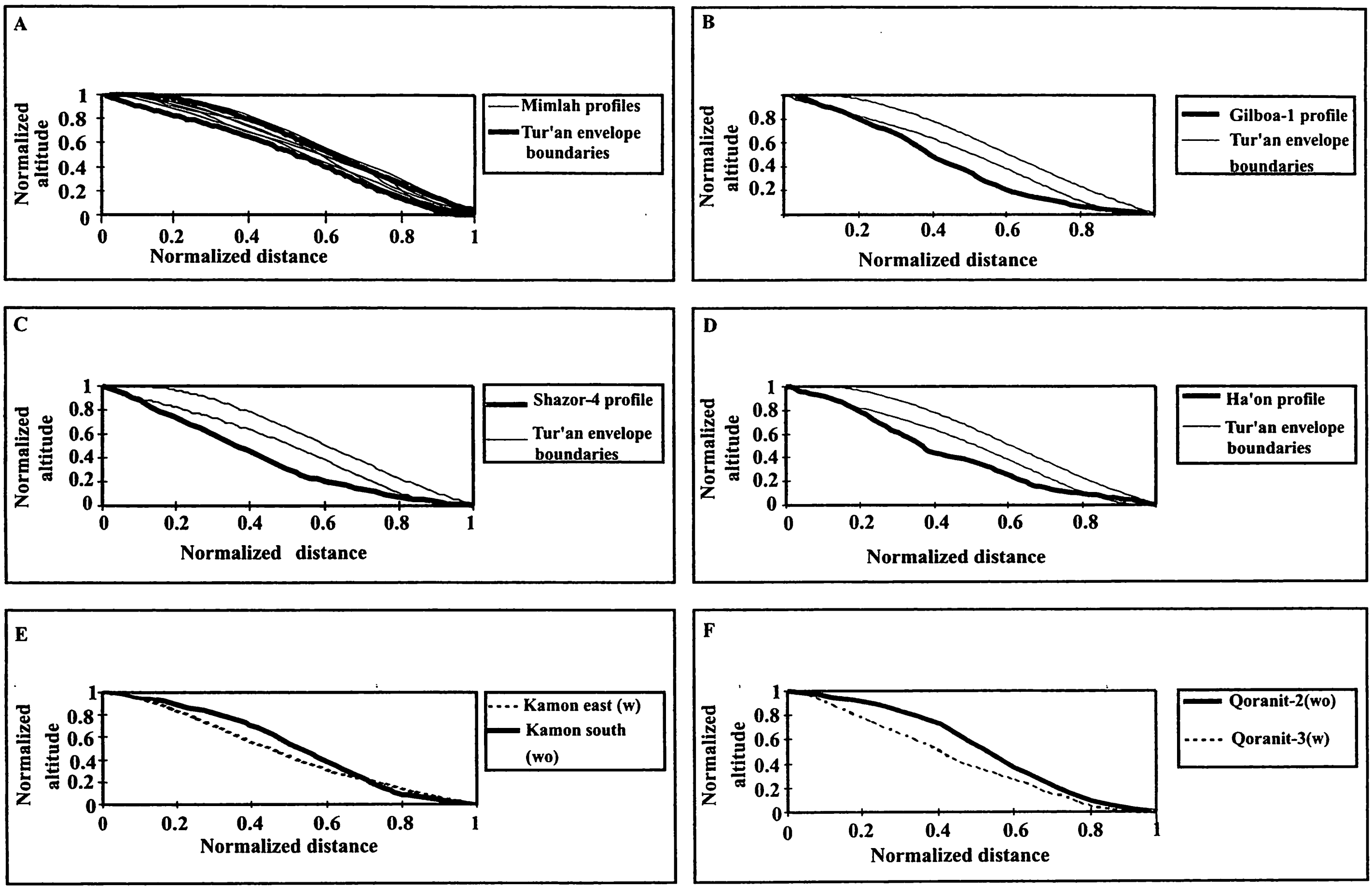

Figure 13. (A) Comparison between the Tur'an reference envelope and the Mimlah profiles. (B) Comparison between the Tur'an reference envelope and the Gilboa profile. (C) Comparison between the Tur'an reference envelope and the Shazor–4 profile. (D) Comparison between the Tur'an reference envelope and the Ha'on escarpment profile. (E) Comparison between the slope of the southern escarpment of the Kamon block and the slope of the eastern escarpment of the Kamon block where Nahal Zalmon is incised at the base. Dashed line—eastern escarpment with incising stream; solid line—southern escarpment without incising stream. (F) Comparison between two parts of the Qoranit escarpment, demonstrating the influence of stream incision at the base of the escarpment on the shape of the slope. Dashed line—Qoranit–3 profile with incising stream; solid line—Qoranit–2 profile without incising stream.

ACKNOWLEDGMENTS

We thank A. Ben-Nun and E. Vienrot from the GIS (geographical information system) division (Hebrew University) and Y. Sagi for helping in the compilation of structural data. The manuscript has benefited a great deal from excellent reviews by P. Bierman, L. Mayer, and an anonymous reader. This study was supported by the Atomic Energy Commission (Israel), the Geological Survey of Israel, and the Earth Sciences Administration, Israel.

REFERENCES CITED

Adams, J., 1984, Large-scale geomorphology of the Southern Alps, New Zealand, *in* Morisawa, M., and Hack, J.T., eds., Tectonic geomorphology: Boston, Unwin Hyman, p. 105–128.

Ahnert, F., 1966, Zur rolleder elekronische rechenmaschine und des mathematischen modells in der geomorphologie: Geographische Zeitschrift, v. 54, p. 118–133.

Ahnert, F., 1973a, COSLOPE2—A comprehensive model program for simulating slope profile development: Geocomputers Bulletin, v. 6, p. 99–122.

Ahnert, F., 1973b, A comparison of theoretical slope models with slopes in the field, *in* Schumm, S.A., and Mosley, M.P., eds., Slope morphology: Stroudsburg, Pennsylvania, Dowden, Hutchinson and Ross, Inc, p. 128–141.

Atkinson, T.C., and Smith, D.I., 1978, The erosion of limestones, *in* Ford, T.D., and Cullingford C.H.D., eds., The science of speleology: p. 151–177.

Bar, Y., and Harash, A., 1983, The analysis of young tectonic activity: The use of geomorphologic elements: Earth Sciences Administration, State of Israel, Research no. 83–200–179, Final report, 10 p. (in Hebrew).

Begin, Z.B., and Zilberman, E., 1997, Main stages and rates of relief development in Israel: Geological Survey of Israel Report GSI/24/97, 63 p.

Bein, A., 1967, The hydrogeology of Cenomanian and Turonian formations in the east-central Galilee [Master's thesis]: Jerusalem, Hebrew University, 66 p. (in Hebrew).

Bierman, P., and Turner, J., 1995, ^{10}Be and ^{26}Al evidence for exceptionally low rates of Australian bedrock erosion and the likely existence of pre-Pleistocene landscapes: Quaternary Research, v. 44, p. 378–382.

Bierman, P., Gillespie, A., Caffe, M., and Elmore, D., 1995, Estimating erosion rates and exposure ages with ^{36}Cl produced by neutron activation: Geochimica et Cosmochimica Acta, v. 58, p. 3779–3798.

Bloom, A.L., 1991, Geomorphology: A systematic analysis of late Cenozoic landforms (second edition): Englewood Cliffs, New Jersey, Prentice-Hall, 532 p.

Bull, W.B., 1977, Tectonic geomorphology of the Mojave Desert: Menlo Park, California, U.S. Geological Survey, Office of Earthquakes, Volcanoes and Engineering, Contract report 14–08–001-G-394, 188 p.

Bull, W.B., and McFadden, L.D., 1977, Tectonic geomorphology north and south of the Garlock fault, California, *in* Doehring D.O., ed., Geomorphology in arid regions: Proceedings, Eighth Annual Geomorphology Symposium: Binghamton, State University of New York, p. 115–138.

Cohen, Z., 1988, Hydrocarbon potential of Israel, highlights of basin analysis: Oil Exploration in Israel Ltd., Exploration Department, 79 p.

Davis, W.M., 1899, The geographical cycle: Journal of Geography, v. 14, p. 481–504.

Dreybrodt, W., 1988, Processes in karst systems: Physics, chemistry and geology: Berlin, Springer-Verlag, 288 p.

Eliezri, I.Z., 1965, The geology of the Beit-Jann region (Galilee, Israel): Israel Journal of Earth Sciences, v. 14, p. 51–66.

Freund, R., 1970, The Geometry of faulting in Galilee: Israel Journal of Earth Sciences, v. 19, p. 117–140.

Garfunkel, Z., 1988, The pre-Quaternary geology of Israel, *in* Yom-Tov, Y., and Tchernov, E., eds., The zoogeography of Israel: The Hague, Netherlands, W. Junk, p. 7–34.
Gerson, R., 1974, Karst processes in the eastern Upper Galilee, northern Israel: Journal of Hydrology, v. 21, p. 31–152.
Gilbert, G.K., 1877, Report on the geology of the Henry Mountains, *in* U.S. Geographical and Geological Survey of the Rocky Mountain region: Washington, D.C., U.S. Government Printing Office, 160 p.
Glikson, Y.A., 1965, Geology of the Southern Naftali mountains (northeastern Galilee, Israel): Israel Journal of Earth Sciences, v. 15, p. 135–154.
Golani, U., 1957, The geology of the Meghar region [Master's thesis]: Jerusalem, Hebrew University, 54 p. (in Hebrew).
Gran, S.E., Matmon, A., Bierman, P.R., Enzel, Y., and Caffee, M., 1999, Calculating fault displacement rates, in situ cosmogenic chlorine–36 concentrations of a limestone normal fault scarp, northern Israel: Geological Society of America Abstracts with Programs, v. 30, no. 7, p. A142–143.
Hack, J.T., 1960, Interpretation of erosional topography in humid temperate regions: American Journal of Science, v. 258-A, p. 80–97.
Hall, J., 1993, The GSI digital terrain model (DTM) project completed: Geological Survey of Israel Current Research, v. 8, p. 47–50.
Hare, P.W., and Gardner, T.W., 1984, Geomorphic indicators of vertical neotectonism along converging plate margins, Nicoya Peninsula, Costa Rica, *in* Morisawa, M., and Hack, J.T., eds., Tectonic geomorphology: Boston, Unwin Hyman, p. 75–104.
Heimann, A., 1990, The development of the Dead Sea Transform and its margins in northern Israel during the Pliocene and Pleistocene: Geological Survey of Israel Report GSI/28/90, 83 p. (in Hebrew, English summary).
Heimann, A., Steinitz, G., Mor, D., and Shaliv, G., 1996, The geochronology of the Cover Basalt: Revised K-Ar and new $^{40}Ar/^{39}Ar$ results: Geological Survey of Israel Report GSI/6/96, 35 p.
Issar, A., and Kafri, U., 1972, Neogene and Pleistocene geology of the Western Galilee Coastal Plain: Geological Survey of Israel Bulletin, v. 53, 14 p.
Jennings, J.N., 1971, Karst: Cambridge, Massachusetts, and London, England, Massachusetts Institute of Technology Press, 252 p.
Kafri, U., 1965, The geology of the Segev area (western Galilee, Israel): Israel Journal of Earth Sciences, v. 14, p. 67–75.
Kafri, U., 1972, The geological map of Israel, Nahariyya: Geological Survey of Israel, Ministry of Development, sheet 1-IV, scale 1:50 000.
Kafri, U., 1997, Neogene to Quaternary drainage systems and their relationship to young tectonics: Lower Galilee, Israel: Geological Survey of Israel Report GSI/1/97, 50 p.
Kafri, U., and Ecker, A., 1964, Neogene and Quarternary subsurface geology and hydrology of the Zvulun Plain: Geological Survey of Israel Bulletin, v. 37, 13 p.
Keller, E.A., 1986, Investigation of active tectonics: Use of surficial processes, *in* Wallace, R.E., ed., Active tectonics: Washington, D.C., National Academy Press, p. 136–147.
King, L.C., 1957, The uniformitarian nature of hillslopes: Edinburgh Geological Society Transactions, v. 17, p. 81–104.
Levy, Y., 1983, The geological map of Israel, Shefar'am: Geological Survey of Israel, Ministry of Development, sheet 3-II, scale 1:50 000.
Matmon, A., Enzel, Y., Zilberman, E., and Heimann, A., 1999a, Late Pliocene and Pleistocene reversal of drainage systems in northern Israel: Tectonic implications: Geomorphology, v. 28, p. 43–59.
Matmon, A., Bierman, P., Caffee, M., and Enzel, Y, 1999b, How fast do rift escarpments retreat?: Geological Society of America Abstracts with Programs, v. 31, no. 7, p. A-445.
Mayer, L., 1986, Tectonic geomorphology of escarpments and mountain fronts, *in* Wallace, R.E., ed., Active tectonics: Washington, D.C., National Academy Press, p. 125–135.
Menges, C.M., 1988, The tectonic geomorphology of mountain front landforms in the northern Rio Grande Rift near Taos, New Mexico [Ph.D. dissert.]: Albuquerque, University of New Mexico, 346 p.
Michelson, H., 1970, Geological map of Western and Central Galilee, compilation map: Tel-Aviv, Israel, TAHAL, scale 1:50 000.
Mor, D., Levitte, D., Steinitz, G., and Lang, B., 1987, The volcanic history of the Ramat Dalton (Upper Galilee) according to K-Ar dating: Israel Geological Society Annual Meeting Abstracts, p. 93.
Nir, D., 1970, Geomorphology of Israel: Jerusalem, Israel, Aqademon, 404 p.
Picard, L., 1943, Structure and evolution of Palestine with comparative notes on neighboring countries: Hebrew University, Jerusalem, Geological Department Bulletin, v. 4, 134 p.
Picard, L., and Golani, U., 1965, The geological map of Israel, northern sheet: Jerusalem, Israel Geological Survey, scale 1:250 000.
Ritter, D.F., Kochel, R.C., and Miller, J.R., 1995, Process geomorphology (third edition): Dubuque, Iowa, W.C. Brown, 546 p.
Ron, H., Freund, R., Garfunkel, Z., and Nur, A., 1984, Block rotation by strike slip faulting: Structural and paleomagnetic evidence: Journal of Geophysical Research, v. 89, p. 6256–6270.
Saltzman, U., 1964, The geology of the Tabha-Huquq-Migdal area [Master's thesis]: Jerusalem, Hebrew University, 55 p. (in Hebrew).
Schulman, N., 1962, The geology of the Central Jordan valley [Ph.D. dissert.]: Jerusalem, Hebrew University, 103 p. (in Hebrew).
Shaliv, G., 1991, Stages in the tectonic and volcanic history of the Neogene Basin in the Lower Galilee and the valleys: Geological Survey of Israel Report GSI/11/91, 101 p.
Shaliv, G., Mimran, Y., and Hazor, Y., 1991, The sedimentary and structural history of the Bet-Shean area and its regional implications: Israel Journal of Earth Sciences, v. 40, p. 161–179.
Shlein, N., 1961, The geology of the Alma region [Master's thesis]: Jerusalem, Hebrew University, 46 p. (in Hebrew).
Simons, M., 1962, The morphological analysis of landforms; a new review on the work of Walter Penck (1888–1923): Institute of British Geographers Transactions, v. 31, p. 1–14.
Sivan, D., 1996, Paleogeography of the Galilee coastal plain during the Quaternary: Geological Survey of Israel Report GSI/18/96, 228 p. (in Hebrew).
Trudgill, S., 1985, Limestone geomorphology: London, New York, Longman, 196 p.
Vroman, A., 1958, The geological map of Israel, series 1, Galilee: Geological Survey of Israel, sheet 1, scale 1: 50 000.
Wallace, R.E., 1987, Grouping and migration of surface faulting and variations in slip rates on faults in the Great Basin province: Seismological Society of America Bulletin, v. 77, p. 868–876.
Wells, S.G., Bullard, T.F., Menges, C.M., Drake, P.G., Karas, P.A., Kelson, K.I., Ritter, J.B., and Wesling, J.R., 1988, Regional variations in tectonic geomorphology along a segmented convergent plate boundary, Pacific coast of Costa Rica: Geomorphology, v. 1, p. 239–265.
Yaalon, D.H., 1959, Dynamics of limestone solution and its application in the interpretation of geological processes: Research Council of Israel Bulletin, v. 8G, p. 217–218.
Yair, A., 1962, The morphology of Nahal Dishon [Master's thesis]: Jerusalem, Hebrew University, 196 p. (in Hebrew).

Manuscript Received by the Society July 29, 1999
Revised Manuscript Received March 17, 2000
Manuscript Accepted April 14, 2000

Printed in the USA

ELSEVIER

Geomorphology 28 (1999) 43–59

GEOMORPHOLOGY

Late Pliocene and Pleistocene reversal of drainage systems in northern Israel: tectonic implications

A. Matmon [a,b,*], Y. Enzel [a,c], E. Zilberman [b], A. Heimann [b]

[a] *Department of Geology, Institute of Earth Sciences, Hebrew University of Jerusalem, Jerusalem 91904, Israel*
[b] *Geological Survey of Israel, 30 Malkhe Yisrael Street, Jerusalem 95501, Israel*
[c] *Department of Geography, Hebrew University of Jerusalem, Jerusalem 91905, Israel*

Received 1 April 1998; received in revised form 20 August 1998; accepted 8 September 1998

Abstract

The arching of the Galilee, northern Israel, is associated with sediment loading in the Dead Sea Transform and Rift. During the Pleistocene, the arching caused the formation of the main North–South water divide in the region and the reversal of stream flow direction. A reconstruction of a main paleochannel which drained large areas in the eastern Galilee to the Mediterranean enabled the determination of age and amplitude of the arching. This reconstruction is based on topographic analysis of thirteen sites containing fluvial remnants in the Beit-Hakerem Valley. We demonstrate that the widespread normal faulting cannot explain the present-day drainage pattern. Dating of basalt clasts from ancient alluvial remnants along the Beit-Hakerem Valley provides a maximum age limit of 1.8 Ma to the paleochannel. The Pleistocene tectonism arched the Galilee by 200 m over a wavelength of 40–60 km. A comparison between arched and unarched segments of the rift's margins indicates that fluvial and slope processes on the rift escarpment cannot explain the location and shape of the main water divide. In the Galilee, tectonism is the only factor that controls the formation, location and shape of the main water divide. © 1999 Elsevier Science B.V. All rights reserved.

Keywords: northern Israel; drainage system; arching; rift-margin; Pleistocene

1. Introduction

Active tectonism influence alluvial rivers through changes in valley floor slope (Schumm, 1977, 1986) by either subsidence or uplift and by direct faulting on all temporal scales (e.g., Wallace, 1967; Stevens, 1974). The change in slope causes changes in stream pattern and aggradation and/or incision of the stream. When stream incision occurs more slowly than uplift, a disruption of the drainage pattern will follow (Sparling, 1967; Twidale, 1971; Ollier, 1981; Harvey and Wells, 1987; Burbank et al., 1996; Gupta, 1997). The effect of direct displacement (vertical or lateral) by faulting can be very dramatic, immediately affecting the fluvial system (e.g., Keller, 1986; Rockwell et al., 1988; Spitz and Schumm, 1997). Slower, perhaps aseismic deformation is more difficult to detect. However, long-term activity will result in the accumulation of both recognizable tectonic structures and deformation of the fluvial system (e.g.,

* Corresponding author. Fax: +972-2-5380688; E-mail: matmon@techunix.technion.ac.il

PII: S0169-555X(98)00097-X

Gerson et al., 1984; Markewich, 1984; Ouchi, 1985; Merritts and Vincent, 1989; Chorowicz and Fabre, 1997; Spitz and Schumm, 1997).

In Israel, fluvial systems have been largely modified by recent tectonics (e.g., Bentor and Vroman, 1951; Garfunkel and Horovitz, 1966; Freund et al., 1968; Kafri and Heimann, 1994; Ginat et al., 1998) and the drainage pattern has adjusted to the development of different morphotectonic features. The present topography in Israel includes two main drainage basins separated by a N–S oriented drainage divide (Fig. 1a). This divide follows the mountainous backbone that is subparallel to the Dead Sea Transform and Rift (DSTR) valley. The western drainage basin drains into the Mediterranean while the eastern one drains into the DSTR valley. The distance between the water divide and the DSTR valley varies from 2–3 km in northern Israel to tens of kilometers in the south. Prior to the formation of the DSTR valley, the region drained only towards the west into the Mediterranean (e.g., Garfunkel, 1981; Garfunkel and Ben-Avraham, 1996; Kafri, 1997). Previous studies discussed the idea of drainage reversal in northern Israel (e.g., Golani, 1957; Kafri and Heimann, 1994; Kafri, 1997), but the timing and the connection between fluvial changes and Quaternary tectonics are not clear. The area is located at the margins of the DSTR; thus drainage development was affected both by the large-scale tectonics and by local inner Galilee faulting (Fig. 1b).

In this study, we reconstruct the drainage system development in northern Israel west of the DSTR valley, and explain this development in relation to tectonic activity that took place in the region during the Quaternary. We reconstruct a pre-Quaternary main drainage channel and its adjustments during tectonic activity by using morphology, sedimentology and age-dating. We then determine the total deformation of the Galilee that accumulated over the Pleistocene. Based on this reconstruction, we evaluate the influence of tectonic activity on the drainage system and propose a model to explain the modification of the drainage pattern in the area. Since the DSTR valley has been continuously active since the Miocene and there is basic knowledge concerning the variations in this activity (type of motion, rates, segmentation, etc.,) the relationship between rift development and modification of adjacent drainage systems can be well understood and the proposed model can be applicable to margins of other rift and transform valleys.

2. Study area

The Galilee can be subdivided into four main parts (Fig. 1b): Upper Galilee, Lower Galilee, DSTR valley in the east and the coastal plain in the west. The western and eastern parts of the Galilee are not described. The Lower Galilee consists of a series of east–west oriented tectonic blocks bounded by normal faults (Freund, 1970) and separated from each other by elongated valleys. The average altitude of the ridge crests is 500 m a.s.l. The Upper Galilee is located north of the Beit-Hakerem Valley, the northernmost, East-West Valley of the Lower Galilee. In the Upper Galilee the highest summit reaches 1200 m a.s.l.

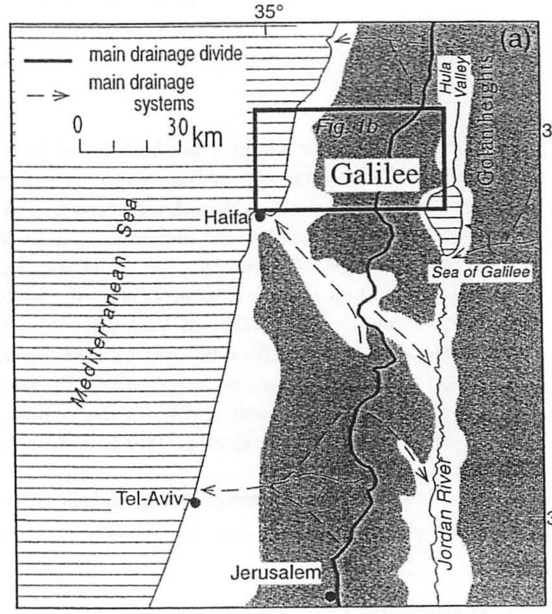

Fig. 1. (a) Location map. The distance of the main water divide from the DSRT varies between 20 to 30 km except in the northernmost part of the Galilee where it is on the rim of the rift. Study area presented in (b) is outlined. (b) Generalized map of the Galilee. DSTR = Dead Sea Transform and Rift; C.B. = cover basalt, a volcanic formation of Pliocene age covering large areas in the eastern Galilee and the Golan Heights. (c) A detailed map of the study area. C.B. = cover basalt.

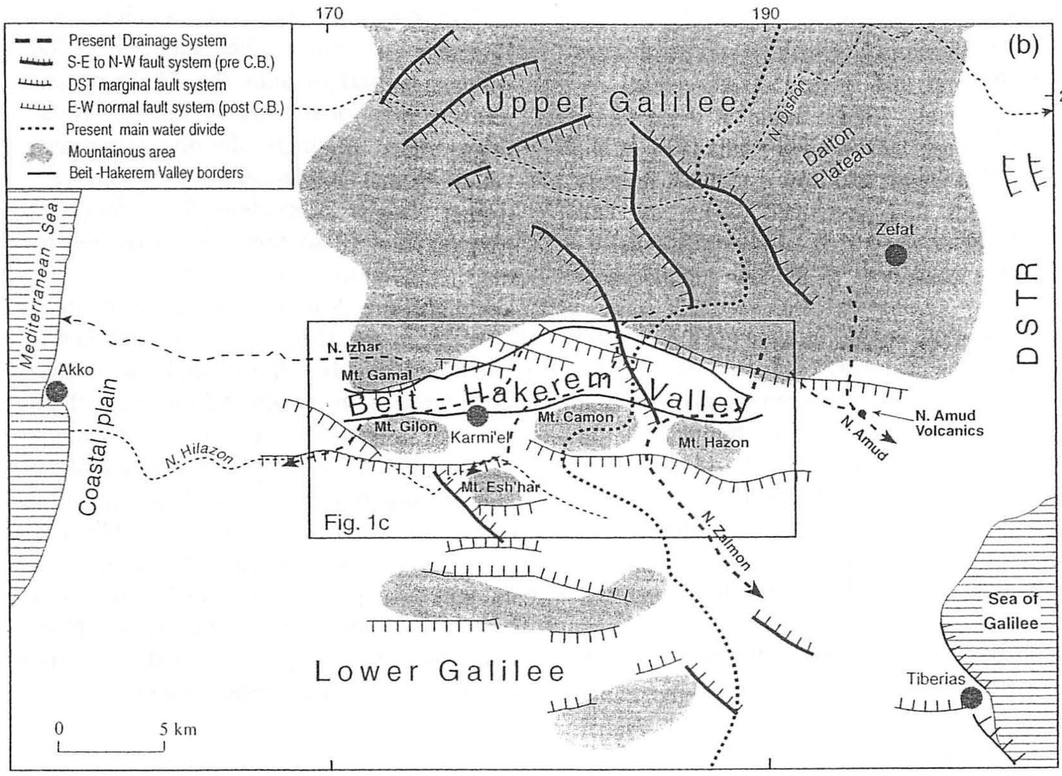

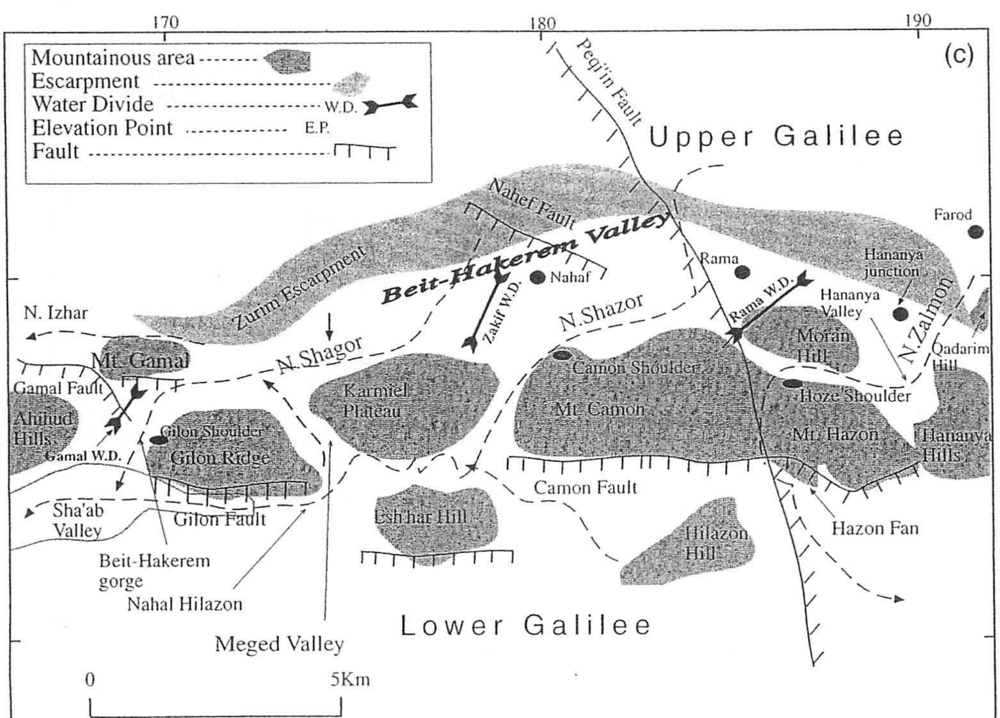

Fig. 1 (continued).

The Upper and Lower Galilee are crossed by two systems of faults trending North-West and North-East which have sinistral and dextral displacements respectively (Ron et al., 1984). Some of these faults curve to become east–west normal faults (Ron et al., 1984). In both the Upper and Lower Galilee, there is evidence for folds that developed during the late Mesozoic (Flexer et al., 1970), although this deformation does not contribute to the current morphology of the area.

The Beit-Hakerem Valley divides the Lower and Upper Galilee (Fig. 1c). This valley, presently located at 200–350 m a.s.l., is about 20 km long and up to 2 km wide. To the north, it is bounded by the tectonic Zurim Escarpment (Fig. 1c) which rises up to 700 m above the valley floor. This escarpment consists of a series of *en-echlon* arranged normal faults. The southern side of the valley is composed of four blocks (Hazon in the east, Camon and Esh'har in the center and Gilon in the west) which rise up to 350 m above the valley floor (Fig. 1c).

At present, the valley is drained by three transverse streams: Nahal Zalmon in the east, Nahal Shazor in the center and Nahal Shagor in the west (Fig. 1c). All the streams have their headwaters in the Upper Galilee and flow southward to the Beit-Hakerem Valley. Each flow several kilometers westward in the valley, then curve south and cross the southern ridges that border the valley. South of these ridges these streams drain either into the DSTR valley (Nahal Zalmon) or into the Mediterranean (Nahal Shagor and Nahal Shazor) through Nahal Hilazon (Fig. 1c). Surprisingly, the divides between the streams within the Beit-Hakerem Valley are very low and rise only up to 50 m above the stream beds (Fig. 2). In contrast, the southern ridges crossed by the streams reach 350 m above the valley.

The Beit-Hakerem Valley is crossed by three NW–SE trending faults (Fig. 2): The eastern one is the Peqi'in fault (Fig. 1c); the central one (Nahef fault) and the western one (Ahihud fault) (Fig. 2) are the eastern tails of two of the Zurim Escarpment segments. The stratigraphic sequence exposed along the margins of the Beit-Hakerem Valley includes Lower Cretaceous sandstones and marls (Kurnob Group), the Upper Cretaceous limestone and Dolomite (Judea Group) and some small outcrops of Senonian chert and chalk (Mt. Scopus Group). Most of the Beit-Hakerem Valley is covered by Pleistocene to Holocene silty clay deposits and vertisols.

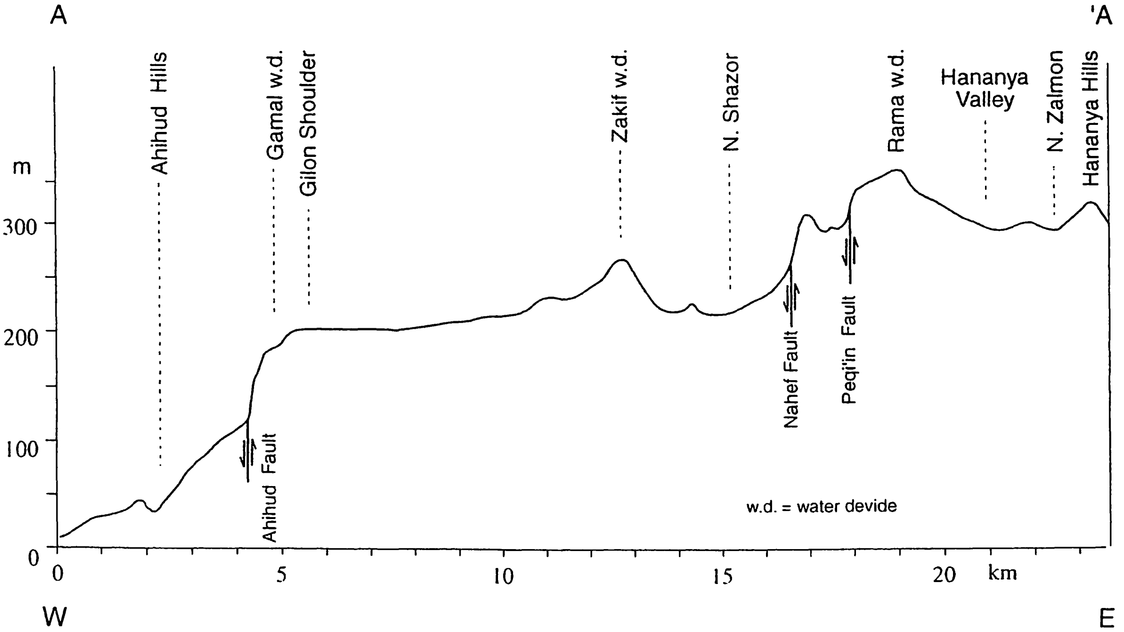

Fig. 2. Topographic cross section of Beit-Hakerem Valley.

Since the climate of the area is semi-humid Mediterranean (annual mean precipitation is 700–900 mm/year), and carbonate rocks are the main lithology, intensive karstification has obliterated much evidence of past fluvial systems.

3. Methods

Topographical, geological and structural maps were analyzed to detect remnants of ancient drainage systems such as wide saddles, shoulders and flat hill tops. Within each tectonic block, as defined by structural maps, the mentioned topographical features were marked to determine whether they are grouped into specific altitudes. Drainage systems that present a misfit between their large dimensions and their small catchments were marked. Field work was based on the analyses of the maps. The sites which appear to be remnants of ancient streams were surveyed for direct evidence of fluvial deposits. The survey was accompanied by archeologists as it included a search for human artifacts. At sites where these deposits were identified, we concentrated our efforts on exotic gravels that have no source in the present-day drainage basin. Exotic basalt gravel was dated by K–Ar and chemically analyzed by XRF. The results of the dating and the chemical analysis were compared to the ages and chemical compositions of basalts from different volcanic fields in the Galilee. This comparison enabled us to trace the gravel units to their source and form the temporal framework of the ancient fluvial systems. The use of basalt pebbles to reconstruct an ancient drainage system has been used in earlier studies (McKee and McKee, 1972). Based on these data the Plio-Pleistocene Beit-Hakerem fluvial system was reconstructed and its relation to tectonic activity was established.

4. Results and discussion

Topographic features indicative of ancient drainage systems were identified mainly along the southern margins of the Beit-Hakerem Valley. These features are grouped into specific altitudes in each tectonic block. On the eastern block these features are concentrated at the altitude of 310 ± 10 m a.s.l. (except for the Rama saddle site which is at an altitude of 350 m a.s.l.). On the central block they are concentrated in two groups: one at 350 ± 20 m a.s.l. and the other at 225 ± 25 m a.s.l. On the western block the topographic features are concentrated at an altitude of 220 ± 20 m a.s.l. At the western part of the study area, three valleys show a large misfit between their large dimensions and their present-day small catchments. These three valleys begin at a wide saddle and have a low gradient and straight longitudinal profile that are not typical of the headwaters of other streams in the region. Another striking feature, located south of the central part of the Beit-Hakerem Valley, is the highly developed incised meander system into the hard limestones of the Judea Group of Nahal Hilazon.

Ancient remnants of fluvial gravels were found along the Beit-Hakerem Valley and its southern margins at 13 sites (Table 1 and Fig. 3). These sites are located on the topographic features identified during the map analysis. The sites are neither part of an active drainage system nor obviously related to fluvial terraces of the present day streams. No human artifacts were identified at these sites and the distribution of the basalt clasts is not typical of human sites (I. Shaked, 1997, personal communication). Remnants were found only at sites that resulted from

Table 1
Description of gravel sites

Site no. and name	Altitude (m a.s.l.)	Lithology
(1) Hananya Hills	320	B, Q, L, BC
(2) Quadarim Hill	300	B
(3) Hananya junction	300	B, RL, C, IOSS, BC, YC
(4) Rama water divide	350	BC, B, Q
(5) Rama water divide	300	BC, B, OL
(6) Moran Hill	320	C, B, Q, IOSS
(7) Hoze Shoulder	320	B, C, IOSS, BC, Q
(8) Hazon Fan	190	B
(9) Mt. Camon Shoulder	370–340	B
(10) Nahef	260	B, RL, BC, YSS
(11) Meged Valley	220	B, C, SS, BC, Q
(12) Gilon Shoulder	240	B, IOSS, BC, Q
(13) Ahihud Hills	40–100	B, RL, C, IOSS, BC

B = basalt, Q = quartzolite, L = limestone, BC = bituminous chalk, RL = red limestone, C = chert, IOSS = iron-oxidized sandstone, YC = yellow chalk, YSS = yellow sandstone, OL = oolite limestone, SS = sandstone. See Fig. 3 for location of sites.

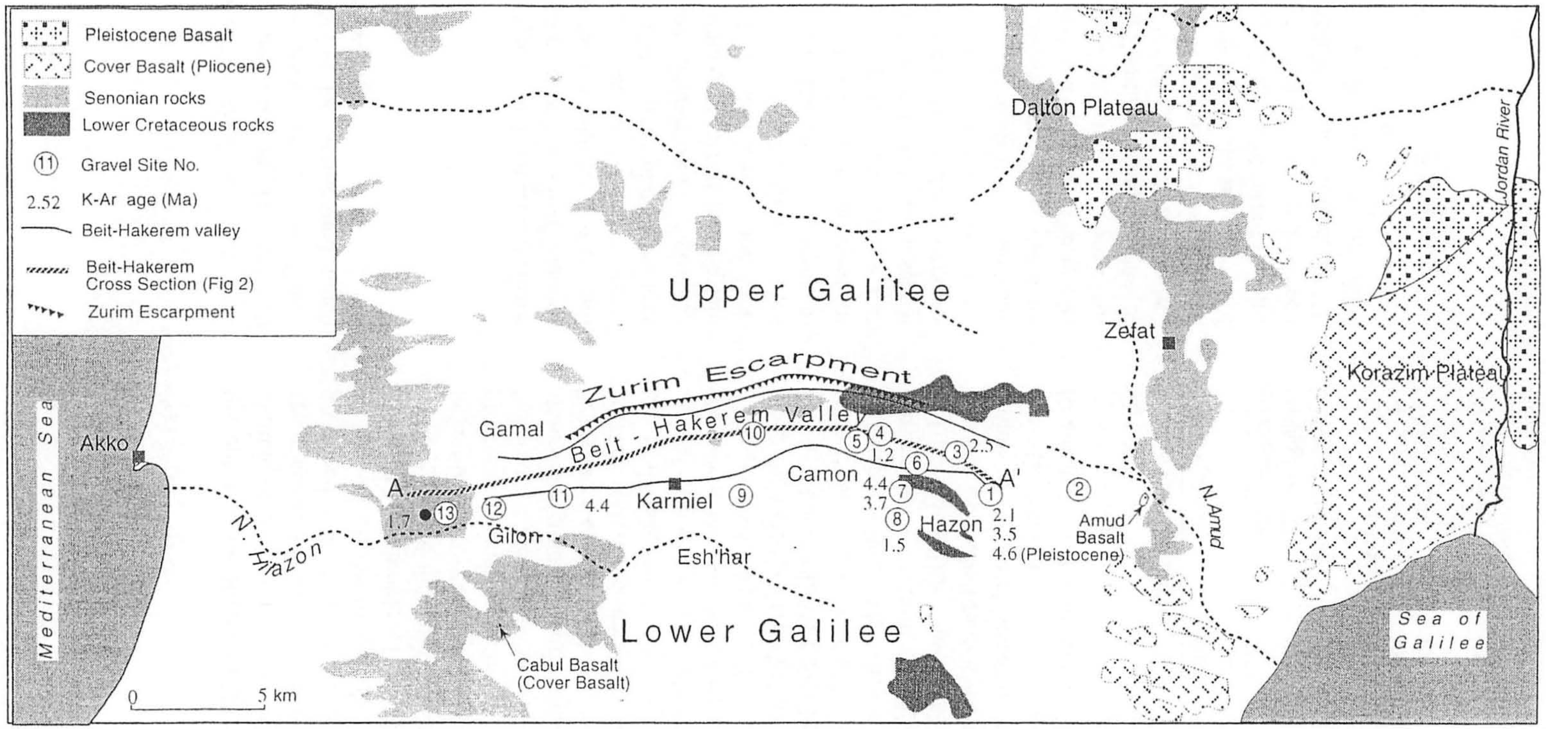

Fig. 3. Location of gravel sites in the Beit-Hakerem Valley. Ages are given by K–Ar dating and in-situ location of possible sources of the gravel. Rocks of ages other than those indicated appear in the figure as white area. Geology after: Golani (1957), Flexer et al. (1970), Mor et al. (1987), Shaliv (1991), Heimann and Ron (1993).

the topographic analysis. The remnants include gravel of different lithologies: limestone (Cenomanian and Turonian), chalk and bituminous chalk (Senonian), sandstone (Lower Cretaceous) and basalt (Middle Pliocene and Lower Pleistocene) (Table 1). The gravel clasts generally do not exceed 10 cm in diameter. The area has been cultivated for hundreds of years and therefore, the structure of the gravelly deposits has been destroyed; ploughing exposed the alluvial sediments as scattered clasts above the clay soils that accumulated in these sites. In a few sites where surface runoff incised the clay soils, the clasts are exposed in definite beds.

Limestone and chalk formations are exposed in the present drainage basins and thus, related gravels do not bear any relevant paleogeographical information. In contrast, exotic gravels of basalt, sandstone and bituminous chalk help to put constraints on the fluvial evolution of the Beit-Hakerem Valley.

4.1. Basalt gravel

Dating of basalt pebbles from 13 sites along the Beit-Hakerem Valley and its margins yielded ages ranging between 4.42 ± 0.41–1.16 ± 0.12 Ma (Table 2). Except for two sites, all ages are between 4.42–1.7

Table 2
K–Ar dating of basalt pebbles

Location	Coordinate (Israel grid)	Sample no.	Measurement no.	% K	% ^{40}Ar (rad)	^{40}Ar (rad CC STP/g × 10^7)	Age (Ma)	Error (Ma)	Mean age (Ma)
Ahihud Hills, site 13	16795/25620	AMD-2	9503	1.1	5.1	0.815	1.9	0.12	1.72 ± 0.38
			9584		5.7	0.724	1.69	0.1	
			9681		6.3	0.677	1.58	0.09	
Meged Valley, site 11	17450/25700	AMD-3	9498	0.92	44.6	1.613	4.5	0.1	4.41 ± 0.34
			9585		48.1	1.557	4.35	0.12	
			9674		52.3	1.569	4.38	0.1	
Hoze Shoulder, site 7	18620/25780	AMD-5	9504	0.74	28.2	1.328	4.61	0.14	4.42 ± 0.41
			9603		33.1	1.196	4.15	0.09	
			9657		38.8	1.297	4.5	0.1	
Hoze Shoulder, site 7	18620/25780	AMD-6	9497	0.83	13.0	1.249	3.87	0.12	3.66 ± 0.22
			9605		15.4	1.117	3.46	0.16	
			9659		17.6	1.183	3.66	0.13	
Hananya Hills, site 1	18970/25720	AMD-7	9518	0.63	25.3	1.131	4.61	0.14	4.55 ± 0.34
			9613		27.5	1.102	4.49	0.13	
			9668		27.0	1.045	4.26	0.13	
Hananya Junction, site 3	18800/25915	AMD-8	9502	0.76	13.5	0.825	2.79	0.1	2.54 ± 0.30
			9607		48.0	0.65	2.2	0.05	
			9677		50.6	0.758	2.57	0.09	
Hananya Hills, site 1	19000/25700	AMD-11	9517	1.36	47.8	1.185	2.24	0.06	2.14 ± 0.10
			9621		50.2	1.126	2.13	0.05	
			9650		49.6	1.085	2.05	0.05	
Hananya Hills, site 1	19000/25700	AMD-12	8784	0.81	32.4	0.893	3.53	0.16	3.49 ± 0.16
			9505		31.6	1.164	3.69	0.08	
			9614		51.2	1.056	3.35	0.07	
			9647		43.5	1.07	3.4	0.12	
Hazon Fan, site 8	18550/25605	AMD-13	8786	0.62	4.6	0.898	1.7	0.13	1.53 ± 0.30
			9519		3.7	0.447	1.85	0.17	
			9616		2.8	0.294	1.22	0.17	
			9652		3.3	0.33	1.37	0.13	
Rama Saddle, site 4	18550/25950	AMD-14	8785	1.14	19.4	0.434	1.38	0.08	1.23 ± 0.14
			9520		29.2	0.528	1.19	0.05	
			9623		32.7	0.474	1.07	0.05	
			9661		41.3	0.57	1.29	0.06	

Ma, indicating a source at the volcanic fields of the Dalton Plateau, Nahal Amud, and Korazim Plateau as well as other volcanic fields in the Lower Galilee (Fig. 3, Table 3). The two youngest ages of approximately 1–1.4 Ma were not used in the paleodrainage reconstruction and the tectonic implications, since we do not have precise information on their possible source.

At present, all these volcanic fields are drained eastward to the DSTR valley and cannot contribute to the alluvial material that the recent drainage systems transport to the Mediterranean Sea. The basalt gravel that yielded ages between 3.5 and 4.5 Ma is related to the Cover Basalt formation of Middle Pliocene age which covers large areas in the eastern Galilee and the Golan Heights. The age range of the Cover Basalt formation is between 3.5 and 5.5 Ma (Heimann et al., 1996). Since there is no way of distinguishing among the different fields of the Cover Basalt, we can only conclude that the basalt pebbles were derived from the volcanic fields in the Eastern Lower Galilee (Fig. 3). The basalt gravel that yielded ages between 1.7 and 2.5 Ma corresponds to the late Pliocene and early Pleistocene volcanic fields of Nahal Amud and the Dalton Plateau (Fig. 3). The age range of the late Pliocene and early Pleistocene Basalt formations is between 1.7 and 2.5 Ma (Mor et al., 1987; Kafri and Heimann, 1994). The chemical analyses of basalt pebbles that yield ages between 1.7 and 2.5 Ma demonstrate that basalt pebbles of identical age from the Dalton Plateau and Nahal Amud can be distinguished by their different concentration of chemical elements, mainly that of Sr (Y. Wienshtein, personal communication, 1996; Table 4).

Basalt pebbles from the Rama Saddle and the Hazon fan (sites 4 and 8 in Fig. 3) yielded ages of about 1–1.4 Ma. Volcanic fields of such age are known only from the Golan Heights and the northern part of the Korazim Plateau (Heimann and Ron, 1993). Basalt pebbles in the Rama Saddle and Hazon fan may have been derived from (a) basalt flows in the Galilee that have yet to be identified and (b) a fluvial connection between the Golan and the Galilee that crossed the Korazim Plateau and transported basalt pebbles. These two possibilities have yet to be investigated and do not contradict the conclusions of this study.

Since the basalt clasts of different ages were identified as remnants of the same drainage system, then the age of its most recent active period is given by the youngest basalt clasts, in this case 1.7 Ma.

Table 3
Location of basalt gravel from the Beit-Hakerem Valley and possible sources

Site no. and name	Mean age	Possible source of gravel
(1) Hananya hills	2.14 ± 0.10	PBLG and/or KP
	3.49 ± 0.16	DPPB and/or
	4.55 ± 0.34	NAPB
(2) Quadarim hills	XRF data	DPPB
(3) Hananya junction	2.54 ± 0.30	DPPB and/or NAPB
(4) Rama water divide	1.23 ± 0.14	Unknown Source
(5) Minor saddle adjacent to the main Rama Saddle	not analyzed	
(6) Moran Hills	not analyzed	
(7) Hoze shoulder	4.42 ± 0.41	PBLG and/or KP
	3.66 ± 0.22	PBLG and/or KP
(8) Hazon fan	1.53 ± 0.30	DPPB and/or NAPB
(9) Lower slopes of Mt. Camon	not analyzed	
(10) Bottom of Beit-Hakerem Valley, near Nahef	not analyzed	
(11) Meged Valley	4.41 ± 0.34	PBLG and/or KP
(12) Gilon shoulder	not analyzed	
(13) Ahihud hills	1.72 ± 0.38	DPPB and/or NAPB

PBLG = Pliocene basalt lower Galilee, KPCB = Korazim Plateau cover basalt, DPPB = Dalton Plateau Pleistocene basalt, NAPB = Nahal Amud Pleistocene basalt.

Table 4
Chemical analysis of basalt gravel from the Beit-Hakerem Valley

Sc	V	Cr	Co	Ni	Cu	Zn	Ga	Rb	Sr	Y	Zr	Nb	Ba	Pb	Th	U	Sampling location	Sample name	Possible source	Site no.
18	213	164	39	140	36	129	21.4	31	1743	28	332	98	769	7	7.6	1.8	Amud volcanic field	WY-420[a]		
NA	211	186	42	154	20	137	23.2	15	1498	28	340	95	618	4.1	4.6	1.2	Alma Plateau	WY-309[b]		
NA	202	187	40	165	28	134	23	17	1476	27	348	92	720	4.3	3.8	0.9	Dalton Plateau	WY-387[c]		
19	216	207	39	164	32	138	22.6	16	1466	27	353	96	747	4.7	5	0.9	Qadarim	AMC-1	DPPB	2
24	241	58	34	47	28	126	25.8	17	787	29	283	68	329	5.1	4	0.6	Rama Saddle	AMC-2a	PBLG	4
23	219	271	47	114	36	108	21	11	636	25	163	31	246	2.2	2.8	0.2	Rama Saddle	AMC-2b	PBLG	4
20	230	371	57	306	47	124	19.2	18	1021	21	240	63	821	3.4	3.5	0.9	Hazon Fán	AMC-3	PBLG	8

[a]Typical XRF analysis of Nahal Amud Basalt.
[b]Typical XRF analysis of Alma Plateau Basalt (Alma Plateau and Dalton Plateau are parts of the same volcanic fields separated by normal faults).
[c]Typical XRF analysis of Dalton Plateau Basalt. All concentrations are in ppm.
NA = not analyzed, DPPB = Dalton Plateau Pleistocene basalt, PBLG = Pliocene basalt Lower Galilee.

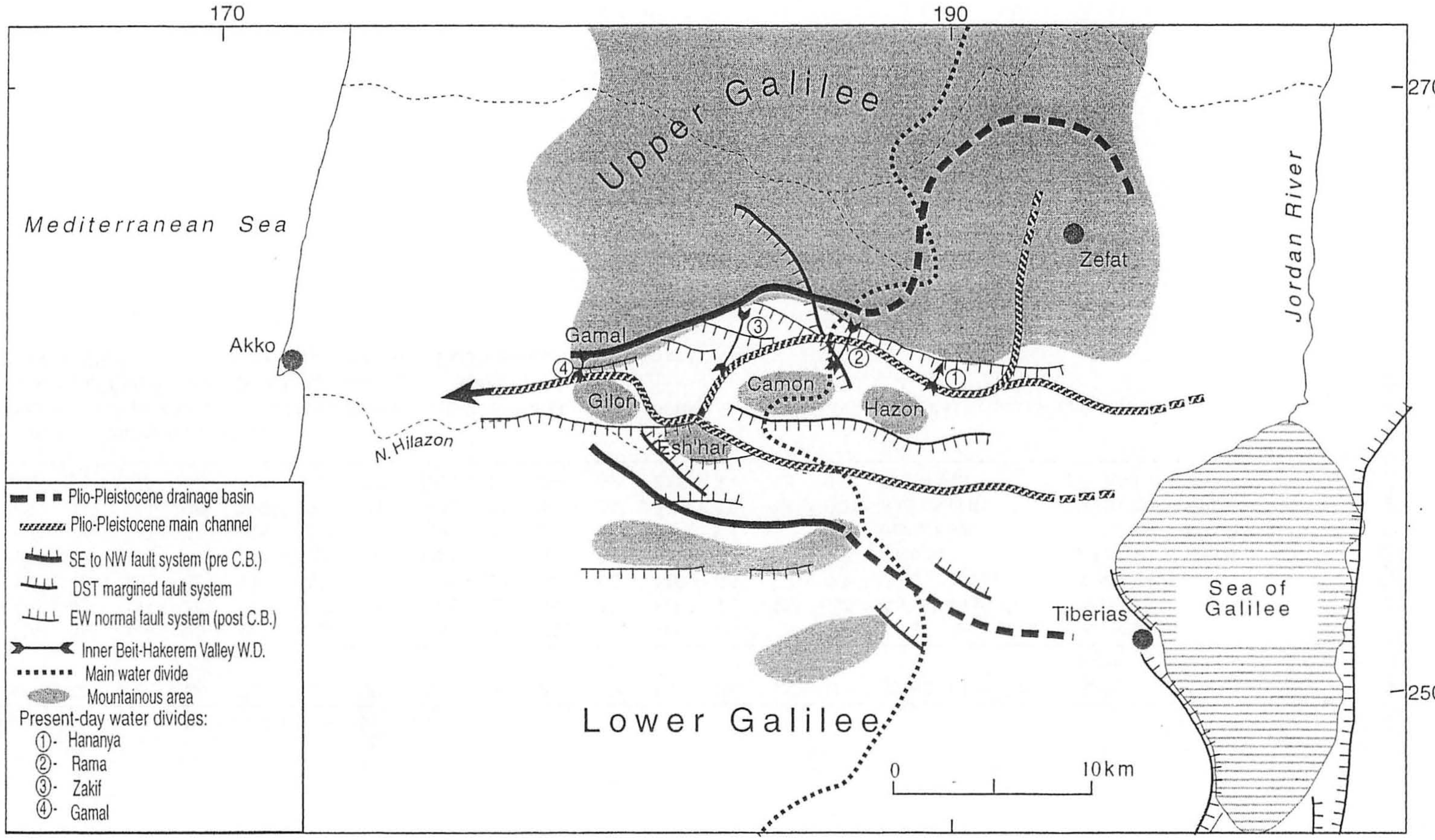

Fig. 4. Reconstruction of the Pleistocene drainage system in the Beit-Hakerem Valley. The drainage system boundaries are marked with a dashed line in the areas where they are uncertain.

This age indicates that at the beginning of the Pleistocene, most of the eastern part of the Galilee drained westward through a fluvial system that followed the Beit-Hakerem Valley (Fig. 4). This fluvial system is in contrast to the present-day main drainage divide between the Mediterranean and the DSTR valley, and the present fluvial systems that cross the Beit-Hakerem Valley from north to south (Fig. 1c). Basalt clasts that were found in the active drainage system (in Nahal Zalmon) were dated to 1.8 and 3.8 Ma. These clasts are located in the active system due to reworking of the gravel from earlier alluvial deposits.

4.2. Bituminous chalk gravel

This gravel originated from Senonian rocks of the Mt. Scopus Group, which are exposed along the Zefat Mountain (Fig. 3). Outcrops of these rocks in the western flank of the Galilee cannot be the source of the chalk gravel, since they are situated downstream from the gravel sites in the Beit-Hakerem Valley, as indicated by the sources of the basalt pebbles. The Zefat Mountain that at present drains eastward into the DSTR valley was part of the catchment area of the Beit-Hakerem Valley (Fig. 4). This conclusion supports the paleogeography reconstruction based on the basalt pebbles.

4.3. Sandstone gravel

This gravel originated from Lower Cretaceous rocks. Of all the Lower Cretaceous outcrops in the area, only two sites located at the lower half of the Zurim Escarpment (Fig. 3) expose sandstone (which is at the bottom of the Lower Cretaceous sequence (Eliezri, 1959). These two sites are the only nearby possible sources of the sandstone gravel. The existence of sandstone gravel indicates that during the early Pleistocene the lower part of the Lower Cretaceous sequence was already exposed and the eastern and higher part of the Zurim Escarpment was almost in its present form. Although there is evidence of recent (late Pleistocene or even Holocene) tectonic activity, presented as bedrock fault scarps ranging in height between 2 to 12 m at the base of the escarpment, this activity did not contribute much to the total topography of the escarpment and did not affect the active drainage system.

5. Pleistocene deformation within the Beit-Hakerem valley

Normal faulting that took place in the Galilee during the Pliocene and Pleistocene formed the main morphotectonic features that control the topography of the Galilee (Freund, 1970; Ron et al., 1984). The reconstruction of the Late Pliocene and Pleistocene Beit-Hakerem drainage system enables us to identify some of the tectonic events that took place in the area. Normal tectonic displacement can be observed at different parts of the Beit-Hakerem Valley. Although the normal activity formed the main morphotectonic features, it did not dramatically influence the main drainage system and the location of the main drainage divide cannot be explained by this normal displacement.

5.1. The eastern part

In the eastern part of the valley, four levels of river beds can be recognized. The wide Rama Saddle (sites 4, 5 of Fig. 3) is a remnant of the oldest and highest level and represents the fluvial system that flowed directly westward to the Mediterranean through the Beit-Hakerem Valley. The continuation of this fluvial channel is represented by sites 9 and 10 (Fig. 3). The second level is marked by a series of morphological features including: wide saddles, shoulders and flat hill tops (sites 1, 2, 3, 6, 7, Fig. 3) at an altitude of 320 m a.s.l. These features were part of a drainage system that also flowed westward to the Mediterranean along the southern side of the Camon ridge. These two levels are capped by gravel that contains 1.8 Ma old basalt pebbles. Assuming that a first order channel (flowing northward into the Beit-Hakerem Valley) was already cut along the Peqi'in Fault between Mt. Camon and Mt. Hoze (Fig. 1c), it can be concluded that only minor displacement on the Peqi'in fault (about 30 m) and a local tilt to the south (1–2%) were required to divert the ancient channel to the south of Mt. Camon. As a result of this diversion, the oldest channel at the level of the Rama Saddle was abandoned.

The third level is part of a fluvial system that drained the eastern part of the Beit-Hakerem Valley towards the DSTR valley. This level is represented by site 8 (Fig. 3) on the Hazon fan, developed at the base of the Hazon ridge. The fourth level, which is the recent active drainage system, is incised 10 to 20 m into the third level and drains the eastern part of the Beit-Hakerem Valley to the DSTR valley. This incision is assumed to be a response of the drainage system to the latest activity of the Camon fault.

The change from the paleolandscape controlled by a single large west flowing fluvial system (regardless of whether it flowed north or south of the Camon-Hazon ridge) to two drainage systems that flow east and west of a main water divide, did not occur as a response to the faulting events mentioned. Normal displacement along the Peqi'in Fault caused a change in the westwardly flowing route but did not cause the reverse in the flow direction. Ongoing activity along the Camon-Hazon fault is expressed by the incision of the recent drainage system into the third alluvial level.

5.2. *The central part*

In the central part of the Beit-Hakerem Valley, both Pleistocene drainage systems (as described above) followed the same route. We assume they flowed through the recent meandering reach of Nahal Hilazon. The meanders in this reach are incised about 150 m into the limestone bedrock. The significance of incised meanders into bedrock as markers of tectonic uplift has been discussed by different researchers (e.g., Gardner, 1975). The downcutting of the Pleistocene channel and the formation of the incised meanders took place as a result of the uplift of the block over which the river flowed. Uplift was slow enough to be accompanied by incision of the drainage system. Prior to this uplift, the stream had a meandering pattern and flowed on a relatively flat landscape. This block was uplifted along the normal fault at its southern side (Levi, 1983) and was tilted about 10° to the north. Since there are no alluvial terraces on the slopes of Nahal Hilazon nor breaks in the slope's angle, the rates and stages of uplift and incision are not known.

The uplift of this block along its southern fault caused the erosion of the entire Mt. Scopus Group cover from the southern side of the block. Remnants of the Mt. Scopus Group are preserved only along the base of the Zurim Escarpment at the northern and lower edge of the block, in the Beit-Hakerem Valley. These remnants appear as isolated chalky hills in the middle of the valley. At present, this area is located at the headwaters of the small drainage system and it is not affected by fluvial processes. Therefore, these isolated chalky hills are assumed to represent an ancient part of the Pleistocene landscape that was influenced by the fluvial system active in the Beit-Hakerem Valley.

From the western edge of the meandering section, the Pleistocene drainage system continued westward through the Meged Valley (Fig. 1c). The Meged Valley is incised into the Gilon Ridge and it joins the western side of the Beit-Hakerem Valley. Its length is about 2 km and it is about a half a kilometer wide. The Meged Valley is bounded on the south by a very wide and shallow topographic saddle that separates it from the deeply incised Nahal Hilazon meanders.

The assumption that the Meged Valley was part of the Pleistocene drainage system is based on the various pebbles found in the valley (site 11, Fig. 3) and the fact that the geometry of the Meged Valley indicates that it was a part of a large drainage system (Kafri, 1997). The Meged Valley presents a low gradient and straight longitudinal profile that could indicate a middle or lower section of a stream, but is not typical of the headwaters of a stream.

As in the eastern part of the Beit-Hakerem Valley, the normal fault activity that took place in the central part was followed by local adjustments in the drainage system. But it was not responsible for the major regional modification of the Pleistocene drainage system.

5.3. *The western part*

After emerging from the Meged Valley, the Pleistocene drainage system flowed westward in the Beit-Hakerem Valley. At the western edge of the Beit-Hakerem Valley there are three drainage outlets to the coastal plain: Nahal Izhar, Ahihud hills and the Beit-Hakerem gorge. Nahal Izhar (Fig. 1c) is the most elevated and northernmost one, and is assumed to have been part of a larger drainage system due to a large misfit between its geometry and present drainage basin (Kafri, 1997). Site 12 (Fig. 3), located at an altitude of 240 m a.s.l. was part of this drainage system. The second outlet is located in the Ahihud hills (site 13, Fig. 3). In comparison with the Nahal Izhar outlet, a large amount of basalt clasts was found in various places along the Ahihud hills. This large amount of clasts indicates that the Ahihud hills were an active drainage outlet for a long time after the Nahal Izhar outlet was abandoned. The third and lowest outlet is the Beit-Hakerem gorge, which is the present valley outlet. Due to difference in altitude between the Beit-Hakerem Valley and the coastal plain, this active fluvial outlet is incised 150 m below its flat shoulders.

The southward shifting of the ancient drainage outlets of the Beit-Hakerem Valley seems to be controlled by two parallel normal faults: the Gamal Fault in the north and the Gilon Fault in the south (Fig. 1c). Drainage diversion from the Izhar stream to the Ahihud hills took place as a response to late Pliocene–early Pleistocene activity on the Gamal Fault. Later activity on the Gilon Fault caused the development of the Sha'ab Valley (Fig. 1c), the abandonment of the Meged Valley and the westward flow of Nahal Hilazon, followed by the incision of the Beit-Hakerem gorge and the abandonment of the Ahihud hills (Fig. 1c) outlet. Again, as described in the eastern and central parts of the valley, normal fault activity affected the stream locally, but did not cause a major change in the drainage pattern of the area.

6. Styles of deformation

The behavior of the recent drainage system in the Beit-Hakerem Valley results from the Plio-Pleistocene tectonic activity in the Galilee in general, and along specific faults in particular. We have shown earlier that the tectonic activity along the inner Galilee faults had local effects on the drainage systems. Different faulting events were followed by changes in the routing of streams or by deep incision. In spite of this activity no dramatic change in the drainage pattern of the area occurred and a single drainage system that flowed from east to west towards the Mediterranean persisted. If so, what caused the major modification in the large scale drainage system? It is obvious that the formation of the DSTR valley was a necessary stage in the development of the recent drainage system, but by itself this process was not enough. We suggest that tilting of a large area towards the developing base level is required to cause the capture of a drainage basin and the reverse of flow direction (Fig. 5). In places where this tilting did not occur, the main water divide is located on top of the western rim of the DSTR valley. For example, in the northernmost part of the DSTR valley (west of the Hula Valley; Fig. 1a), the western margins of the rift do not exhibit any tilt towards the DSTR base level and the main water divide is located at the top

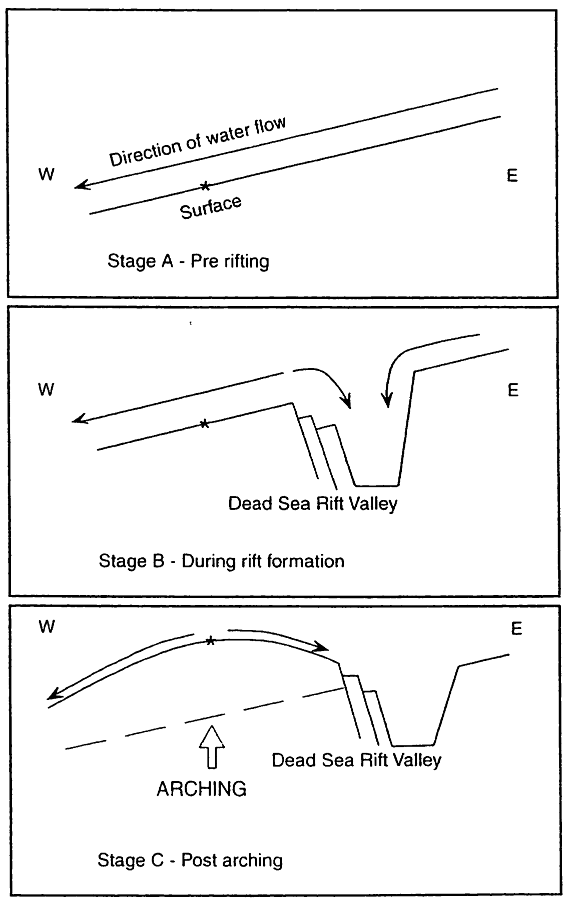

Fig. 5. Schematic diagram showing the relation between the rift's formation and the development of drainage basins in adjacent areas. A substantial drainage basin can develop only if the rifting is accompanied by the tilting of the adjacent area towards the rift valley. This tilting is achieved by arching the rift's margins.

of the rift's western rim. Thus, the entire area west of the rift drains into the Mediterranean (Fig. 1a). Even though the Hula Valley (Fig. 1b) reached its present topographic configuration about 2 Ma (Heimann, 1990), there is no westward retreat of the water divide, indicating that fluvial and slope processes by themselves, without tectonism, cannot explain the retreat of the water divide westward away from the shoulders of the DSTR valley. Therefore, a stage of regional tilting towards the rift is necessary to reverse the flow direction and to drain a large area towards the DSTR valley.

To demonstrate the deformation affecting the Plio-Pleistocene drainage surface in the Beit-Hakerem area, the height of the gravel sites are projected on a vertical east–west plain (Fig. 6). The Pleistocene drainage surface is represented by the best fit line through the different gravel sites. The sites form a wide arch and their deviation from the line is largest in the center, decreasing towards the east and west. It is difficult to quantify the contribution of inner-Galilee faulting relative to the regional folding to the total altitude of each gravel site. We suggest that the shape of the line represents the effect of regional tectonics, whereas the deviation of the sites from the line represents local faulting offsets.

From this projection, the total deformation of the Pleistocene fluvial surfaces can be estimated. The relationship between this line and the different gravel sites indicates two tectonic styles: (a) A wide arch extends from the coastal plain to the DSTR valley. Wdowinski and Zilberman (1996) show that the axis of the arch corresponded to the main drainage divide of Israel and is subparallel to the DSTR valley. The wavelength of the arch is 40–60 km and its ampli-

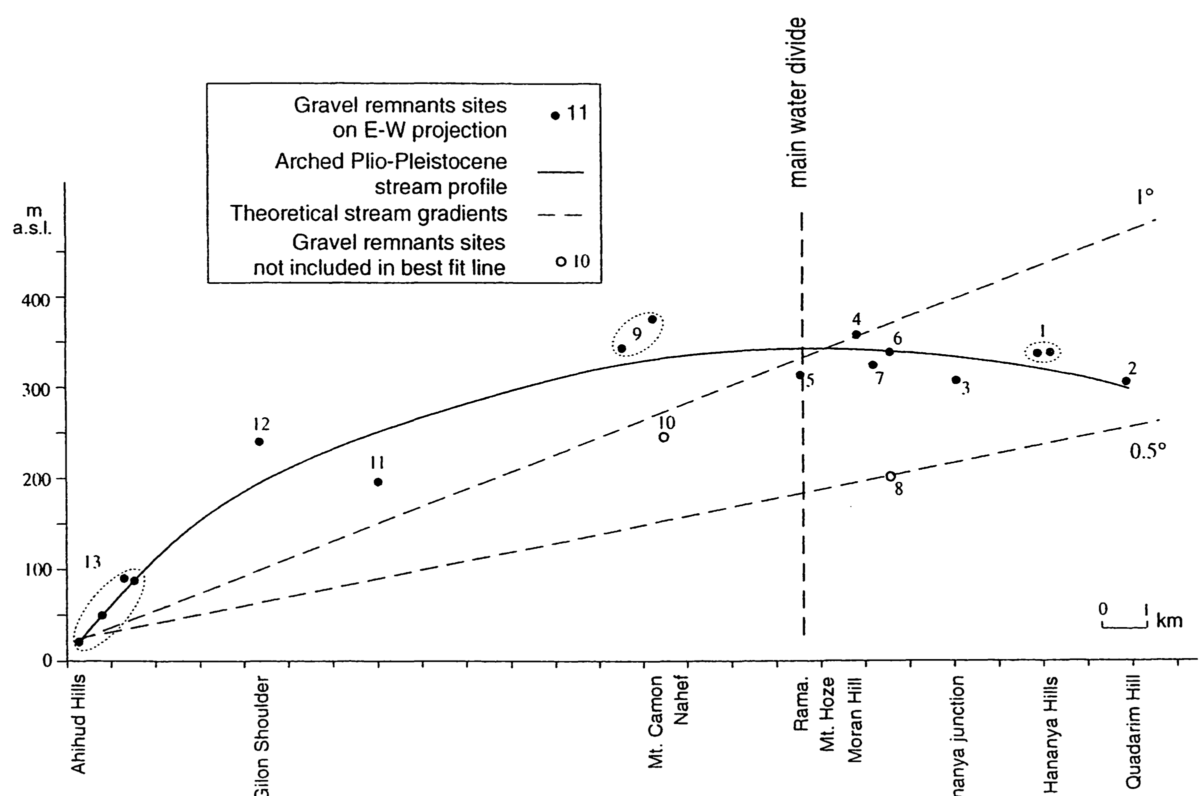

Fig. 6. Projection of gravel sites elevations in the Beit-Hakerem Valley and its margins on an east–west vertical plain. It can be seen that the western part is strongly arched. The main water divide crosses the valley at Rama. Sites 8 and 10 were not included in the construction of the deformed profile since they represent reworked material.

tude is 200–300 m. This arching is most likely an isostatic response of the rift's shoulder to the deepening and filling of the Dead Sea Transform Valley (Wdowinski and Zilberman, 1996). (b) Normal faulting causes a large elevation range of gravel sites that are close to each other (on the east–west projection) but are located on different blocks. Such faulting is suggested in the central part of the Beit-Hakerem Valley by the large scatter of sites around the surface line (Fig. 6).

The arching tilted the eastern Galilee eastward and established a regional N–S trending drainage divide. This tilting promoted drainage reversal in eastwardly tilted channels (Fig. 5) as described by the aforementioned evolution of Nahal Zalmon. The arching of the western margins of the DSTR valley has been mentioned and discussed by previous authors. Picard (1943) argued that the arching in the southern part of Israel occurred during the Pliocene while Bentor and Vroman (1951, 1961) estimated an arching of about 400 m for that region. They thought that it occurred during the early Pleistocene. Ball and Ball (1953) proposed that the arching began during the Eocene. None mentioned a relation between the arching and the development of the DSTR Valley. By measuring the deformation of different sedimentary units that were deposited horizontally, Salamon (1987) showed that 40% (200–400 m in southern Israel) of the total arching occurred between the Toronian and the Eocene and the rest from the Miocene to the Pliocene. Ten Brink et al. (1990) pointed out the relationship between the rift axis isostatic compensation and the topography at the rift's margins. Wdowinski and Zilberman (1996) constructed more than 60 topographic and structural cross-sections perpendicular to the rift's axis and proposed a mechanism that relates the development of the DSTR valley to the topography of its margins. This type of arching has been observed in other rifts as well (e.g., East African Rift, Rosendahl, 1987; Ebinger et al., 1989). This wide folding that occurred along major parts of the western margins of the DSTR valley, is responsible for the establishment of the North–South trending mountainous backbone of Israel and, therefore, was the main factor controlling the establishment of the subsequent drainage network pattern. According to the results of this study, approximately 200 m of arching in the Galilee occurred during the Pleistocene. It is younger than the arching reported for southern Israel, where it was related to the Miocene and Pliocene periods (Picard, 1943; Salamon, 1987).

7. Conclusions

From the reconstruction of a Pleistocene drainage system in northern Israel, we were able to point to the tectonic systems that were active at that time and tie the tectonic activity to the development of the drainage system in the Beit-Hakerem Valley in particular, and to the entire landscape of northern Israel in general. A Plio-Pleistocene fluvial system crossed the present-day drainage divide of Israel in the Beit-Hakerem Valley. This system used to drain most of the Galilee into the Mediterranean. Its maximum age is determined by the youngest basalt clasts that originated at the Dalton and Amud volcanic fields and is dated to 1.8 Ma. The topography during that period was quite similar to the present-day topography. Faulting and the development of the block systems in the Galilee that began in the Miocene (Ron et al., 1984) continued during the Pleistocene and were followed by local adjustments of the drainage system. This normal fault activity did not cause the reverse in flow direction and did not form the main drainage divide which was formed by the arching of the western margins of the DSTR valley as a response to its deepening and filling. The arching caused the tilt and changed the flow direction in the eastern flowing channels. In places where the arching did not occur, the main water divide is located at the rim of the rift, and slope and fluvial processes are not able to cause the migration of the divide further west, away from the rift's shoulder.

Acknowledgements

We thank B.Z. Begin and P. Bierman for the collegial reviews of early drafts of this manuscript, Z. Garfunkel and H. Ron for fruitful discussions, and Y. Wienshtein for his help with XRF analysis of the samples. We are grateful to H. Weiler, License Division of the IAEC, for funding major parts of this project. Our thanks to P.G. Silva and an anonymous reviewer for very constructive comments that significantly improved this paper.

References

Ball, M.H., Ball, D., 1953. Oil prospects of Israel. Bull. Am. Ass. Petr. Geol. 37, 1–113.

Bentor, Y.K., Vroman, A.J., 1951. Map of the Negev. Sheet 18: Avedat, scale 1:100000, Isr. Army SCI., 98 pp. (maps and figures).

Bentor, Y.K., Vroman, A.J., 1961. Map of the Negev. Sheet 16: Mt. Sedom, scale 1:100000, Isr. Army SCI., 98 pp. (maps and figures).

Burbank, W.D., Leland, J., Fielding, E., Anderson, R.S., Brozovic, N., Reid, M.R., Duncan, C., 1996. Bedrock incision, rock uplift and threshold hillslopes in the northwestern Himalayas. Nature 379, 505–510.

Chorowicz, J., Fabre, J., 1997. Organization of drainage networks from space imagery in the Taneztouft Plateau (Western Sahara): implications for the recent intracratonic deformation. Geomorphology 21 (2), 139–151.

Ebinger, C.J., Battle, T.D., Forsyth, D.W., Bowin, C.O., 1989. Effective elastic plate thickness beneath the East African and Afar Plateaus and dynamic compensation of the uplift. J. Geophys. Res. 94, 2883–2901.

Eliezri, I.Z., 1959. The geology of the Beit-Jann region (Galilee, Israel). MS thesis, Institute of Earth Sciences, Hebrew Univ., Jerusalem, Israel (in Hebrew).

Flexer, A., Freund, R., Reiss, Z., Buchbinder, B., 1970. Santonian paleostructure of the Galilee. Isr. J. Earth Sci. 19, 14–146.

Freund, R., 1970. The geometry of faulting in Galilee. Isr. J. Earth Sci. 19, 117–140.

Freund, R., Zak, I., Garfunkel, Z., 1968. Age and rate of seismic movement along the Dead Sea Transform. Nature 220, 253–255.

Gardner, T.W., 1975. The history of part of the Colorado River and its tributaries, an experimental study. Four Corners Geol. Soc. Guidebook. 8th Field Conference (Canyonlands), pp. 87–95.

Garfunkel, Z., 1981. Internal structure of the Dead Sea leaky transform (rift) in relation to plate kinematics. Tectonophysics 80, 81–108.

Garfunkel, Z., Ben-Avraham, Z., 1996. The structure of the Dead Sea basin. Tectonophysics 266, 155–176.

Garfunkel, Z., Horovitz, A., 1966. The upper tertiary and quaternary morphology of the Negev. Isr. J. Earth Sci. 15, 101–117.

Gerson, R., Grossman, S., Bowman, D., 1984. Stages in the creation of a large rift valley—geomorphic evolution along the Southern Dead Sea rift. In: Morisawa, M., Hack, J.T., (Eds.), Tectonic Geomorphology. Proceedings of the 15th annual Binghamton Geomorphology Symposium, September 1984, pp. 53–73.

Ginat, H., Enzel, Y., Avni, Y., 1998. Translocated Plio-Pleistocene drainage systems along the Arava fault of the Dead Sea transform. Tectonophysics 284 (1–2), 151–160.

Golani, U., 1957. The geology of the Meghar region. MS thesis, Hebrew Univ., Jerusalem, Israel (in Hebrew).

Gupta, S., 1997. Himalayan drainage patterns and the origin of fluvial megafans in the Ganges foreland basin. Geology 25 (1), 11–14.

Harvey, A.M., Wells, S.G., 1987. Response of Quaternary fluvial systems to differential epeiorogenic uplift: Aguas and Feos river systems, southern Spain. Geology 15, 689–693.

Heimann, A., 1990. The development of the Dead Sea Transform and its margins in northern Israel during the Pliocene and Pleistocene. PhD thesis, Hebrew Univ., Jerusalem, Isr. Geo. Surv. Rep. GSI/28/90, pp. 1–83 (in Hebrew, with English summary).

Heimann, A., Ron, H., 1993. Geometric changes of plate boundaries along part of the northern Dead Sea transform: geochronologic and paleomagnetic evidence. Tectonics 12 (2), 477–491.

Heimann, A., Steinitz, G., Mor, D., Shaliv, G., 1996. The geochronology of the Cover Basalt: revised K–Ar and new $^{40}Ar/^{39}Ar$ results. GSI report, GSI/6/96.

Kafri, U., 1997. Neogene to Quaternary drainage systems and their relationship to young tectonics: lower Galilee, Israel. GSI Report, GSI/1/97.

Kafri, U., Heimann, A., 1994. Reversal of the palaeodrainage system in the sea of Galilee area as an indicator of the formation timing of the Dead Sea rift valley base level in northern Israel. Palaeogeography, Palaeoclimatology, Palaeoecology 109, 101–109.

Keller, E.A., 1986, Investigation of active tectonics: use of surficial processes. In: Wallace, R.E. (Ed.), Active Tectonics. Washington, DC National Academy Press, pp. 136–147.

Levi, Y., 1983. Shefar'am geological map. Geological Survey of Israel.

Markewich, H.M., 1984. Geomorphic evidence for Pliocene–Pleistocene uplift in the area of the Cape-Fear Arch, North Carolina. In: Morisawa, M., Hack, J.T., (Eds.), Tectonic Geomorphology. Proceedings of the 15th Annual Binghamton Geomorphology Symposium, September 1984, pp. 279–297.

McKee, E.D., McKee, E.H., 1972. Pliocene uplift of the Grand Canyon Region—time of drainage adjustment. Bull. Geo. Soc. Am. 83, 1923–1932.

Merritts, D., Vincent, K.R., 1989. Geomorphic response of coastal streams to low, intermediate, and high rates of uplift, Mendocino triple junction region, northern California. Geol. Soc. of Am. Bull. 101, 1373–1388.

Mor, D., Levitte, D., Steinitz, G., Lang, B., 1987. The volcanic history of the Ramat Dalton (Upper Galilee) according to K–Ar dating. Israel Geological Society, Annual meeting, p. 93 (abstract).

Ollier, C.C., 1981. Tectonics and Landforms. Longmans, New York, 324 pp.

Ouchi, S., 1985. Response of alluvial rivers to slow active tectonic movement. Geol. Soc. of Am. Bull. 96, 504–515.

Picard, L., 1943. Structure and evolution of Palestine with comparative notes on neighboring countries. Hebrew Univ. Jerusalem, Geol. Dept. Bull. 4 (2–4), 134.

Rockwell, T.K., Keller, E.A., Dembroff, G.R., 1988. Quaternary rate of folding of the Ventura Avenue Anticline, western Transverse Ranges, Southern California. Geol. Soc. Am. Bull. 100, 850–858.

Ron, H., Freund, R., Garfunkel, Z., Nur, A., 1984. Block rotation by strike slip faulting: structural and paleomagnetic evidence. J. Geophys. Res. 89, 6256–6270.

Rosendahl, B.R., 1987. Architecture of continental rift with special reference to East Africa. Annu. Rev. Earth Planet. Sci. 15, 445–503.

Salamon, A., 1987. The monoclines in the northern Negev: a model of tilted blocks and shortening. MS thesis, Hebrew Univ., Jerusalem, 101 pp. (in Hebrew, with English abstract).

Schumm, S.A., 1977. The Fluvial System. Wiley, New York, 338 pp.

Schumm, S.A., 1986. Alluvial river response to active tectonics. In: Active Tectonics: Studies in Geophysics. National Academy Press, Washington DC.

Shaliv, G., 1991. Stages in the tectonic and volcanic history of the Neogene Basin in the Lower Galilee and the valleys. GSI Report, GSI/11/91.

Sparling, D.R., 1967. Anomalous drainage pattern and crustal tilting in Ottawa County, Ohio. Ohio J. Sci. 67, 378–381.

Spitz, W.J., Schumm, S.A., 1997. Tectonic geomorphology of the Mississippi Valley between Osceola, Arkansas and Friars Point, Mississippi. Engineering Geology 46, 259–280.

Stevens, G.R., 1974. Rugged Landscape, The Geology of Central New-Zealand. A.H. and A.W. Reed, Wellington, 286 pp.

Ten Brink, U.S., Schoenberg, N., Kovach, R.L., Ben-Avraham, Z., 1990. Uplift and possible Moho offset across the Dead Sea transform. In: Kovach, R.L., Ben-Avraham, Z. (Eds.), Geologic and Tectonic Processes of the Dead Sea Transform Zone. Tectonophysics 180, 71–85.

Twidale, C.R., 1971. Structural Landforms. Australian National Univ. Press, Canberra.

Wallace, R.E., 1967. Note on stream channels offset by the San Andreas Fault, southern Coast Range, California. Stanford Univ. Publ. (Geol. Sci.) 11, 6–20.

Wdowinski, S., Zilberman, E., 1996. Kinematic modeling of large scale structural asymmetry across the Dead Sea transform. Tectonophysics 266, 187–201.

Note to contributors

A detailed Guide for Authors is available upon request. Please pay special attention to the following notes:

Language

Manuscripts should be written in English. Authors whose native language is not English are recommended to seek the advice of a colleague who has English as his mother-tongue before submitting their manuscript. Occasional contributions in French will be considered for publication for the following journals: *ISPRS Journal of Photogrammetry & Remote Sensing* and *Review of Palaeobotany and Palynology*.

Authors in Japan please note: Upon request, Elsevier Science Japan will provide authors with a list of people who can check and improve the English of their paper (*before submission*). Please contact our Tokyo office: Elsevier Science K.K., 9-15 Higashi-Azabu 1-chome, Minato-ku, Tokyo 106-0044; phone: (+81) (3) 5561 5032; fax: (+81) (3) 5561 5045.

Preparation of the text

(a) The manuscript should preferably be prepared on a word processor and printed with double spacing and wide margins and include an abstract of not more than 500 words.
(b) Authors should use IUGS terminology. The use of S.I. units is also recommended.
(c) The title page should include the name(s) of the author(s), their affiliations, fax and e-mail numbers. In case of more than one author, please indicate to whom the correspondence should be addressed.

Keywords

Except for the journals *Coastal Engineering* and *Hydrometallurgy,* authors should provide 4 to 6 keywords. These must be taken from the most recent American Geological Institute GeoRef Thesaurus and should be placed beneath the abstract. Hydrometallurgy authors will be provided with a list of keywords by the editor upon submission of manuscripts.

References

(a) References in the text consist of the surname of the author(s), followed by the year of publication in parentheses. All references cited in the text should be given in the reference list and vice versa.
(b) The reference list should be in alphabetical order.

Tables

Tables should be compiled on separate sheets and should be numbered according to their sequence in the text. Tables can also be sent as glossy prints to avoid errors in typesetting.

Illustrations

(a) All illustrations should be numbered consecutively and referred to in the text.
(b) Drawings should be lettered throughout, the size of the lettering being appropriate to that of the drawings, but taking into account the possible need for reduction in size. The page format of the journal should be considered in designing the drawings.
(c) Photographs must be of good quality, printed on glossy paper.
(d) Figure captions should be supplied on a separate sheet.
(e) If contributors wish to have their original figures returned this should be requested in proof stage at the latest.
(f) Colour figures can be accepted providing the reproduction costs are met by the author. Please consult the publisher for information.

Page proofs

One set of page proofs will be sent to the corresponding author, to be checked for typesetting/editing. The author is not expected to make changes or corrections that constitute departures from the article in its accepted form. Proofs should be returned within 3 days.

Reprints

Fifty reprints of each article are supplied free of charge. Additional reprints can be ordered on a reprint order form which will be sent to the corresponding author upon receipt of the accepted article by the publisher.

Submission of manuscripts

Manuscripts originating from the Americas and Canada should be submitted in triplicate to:

R.A. Marston, Department of Geography and Recreation, University of Wyoming, P.O. Box 3371, Laramie, WY 82071-3371. USA. Phone: +1 307 766 6386. Fax: +1 307 766 3294. E-mail: marston@uwyo.edu.

Manuscripts originating from the rest of the world should be submitted in triplicate to:

A.M. Harvey, Department of Geography, University of Liverpool, Roxby Building, P.O. Box 147, Liverpool L69 3BX, U.K. Phone: +44 151 794 2878. Fax: +44 151 794 2866. E-mail: amharvey@liverpool.ac.uk.

Illustrations should also be submitted in triplicate. One set should be in a form ready for reproduction; the other two may be of lower quality.

Submission of an article is understood to imply that the article is original and unpublished and is not being considered for publication elsewhere.

Upon acceptance of an article by the journal, the author(s) will be asked to transfer the copyright of the article to the publisher. This transfer will ensure the widest possible dissemination of information under the U.S. Copyright Law.

For customers in the U.S. and Canada wishing additional bibliographic information on this and other Elsevier journals, please contact: Elsevier Science Company Inc., Journal Information Centre, 655 Avenue of the Americas, New York, NY 10010, Tel.: (212) 633-3750.

The indication of a fax and e-mail number on submission of the manuscript could assist in speeding communications. The fax number for the Amsterdam office is +31-20-4852459.

Submission of electronic text

Authors are requested to submit the final text on a 3.5" or 5.25" diskette. Both double density (DD) and high density (HD) diskettes are acceptable. As with the requirements for manuscript submission, the main text, list of references, tables and figure captions should be stored in separate text files with clearly identifiable file names. The format of these files depends on the word processor used. Texts written with Display Write, MultiMate, Microsoft Word, Samna Word, Sprint, T_EX, Volkswriter, Wang PC, WordMARC, WordPerfect and Wordstar or supplied in DCA/RFT, or DEC/DX format can be readily processed. In all other cases the preferred format is DOS text or ASCII. It is essential that the name and version of the word processing program, the type of computer on which the text was prepared, and format of the text files are clearly indicated.

Authors are requested to ensure that the contents of the diskette correspond exactly to the contents of the hard copy manuscript.

Discrepancies can lead to proofs of the wrong version being made. The word processed text should be in single column format. Keep the layout of the text as simple as possible; in particular, do not use the word processor's options to justify or to hyphenate the words.

If available, electronic files of the figures should also be included on a separate floppy disk.

Isr. J. Earth Sci.; 49: 143–158

Development of the Bet ha'Emeq structure and the tectonic activity of normal faults in the Galilee

Ari Matmon,[a,b,*] Ezra Zilberman,[b] and Yehouda Enzel[a,c]
[a]Department of Geology, Institute of Earth Sciences, The Hebrew University of Jerusalem, Jerusalem 91904, Israel
[b]Geological Survey of Israel, 30 Malkhe Yisrael Street, Jerusalem 95501, Israel
[c]Department of Geography, Hebrew University of Jerusalem, Jerusalem 91905, Israel

(Received 6 December 1999; accepted in revised form 31 May 2000)

ABSTRACT

Matmon, A., Zilberman, E., Enzel, Y. 2000. Development of the Bet ha'Emeq structure and the tectonic activity of normal faults in the Galilee. Isr. J. Earth Sci. 49: 143–158.

A morphometric study of the Bet ha'Emeq drainage system, Upper Galilee, combined with available geological and structural data, enables the detection of tectonic stages that took place in the region, as well as a better understanding of the influence of tectonic activity on surficial processes. The preservation of Senonian and younger rock units in the downfaulted blocks of the Bet ha'Emeq Valley implies that normal faulting at rates compatible to denudation initiated during the Miocene and lasted ~10 million years. During that time, ongoing truncation continued on the uplifted block, eliminating completely the Senonian units. The relation between the Bet ha'Emeq drainage system and adjacent structures implies that the relief of the Bet ha'Emeq Valley and the development of the drainage system in it preceded the development of the secondary uplifted blocks within the Bet ha'Emeq low structure, the neighboring Zurim Escarpment, and the formation of the regional tilt of the Upper Galilee. The present relation between the Zurim Escarpment and the Bet ha'Emeq drainage system suggests no observable retreat of the escarpment since its formation more than 4 Ma. Morphologic considerations and the existence of quartz geodes derived from the Cenomanian Deir Hana Formation on abandoned saddles along the present water divide of Nahal Bet ha'Emeq suggest that the headwaters of the Bet ha'Emeq drainage system used to be in the Beit Jann tectonic block. This block is currently disconnected from the Bet ha'Emeq drainage system due to normal displacement along the Sumi and Peqi'in faults. The present morphology of the Bet ha'Emeq Valley developed since the Pliocene. A fresh fault scarp in dolomite and knick points in Pleistocene travertine units in the western part of the Bet ha'Emeq Valley indicate late Pleistocene activity on the Bet ha'Emeq fault system. Incision of the Bet ha'Emeq drainage system as well as adjacent streams into alluvial terraces signals the response of the drainage system to the regional-scale uplift and is not associated with normal faulting of the Bet ha'Emeq system. The regional uplift is also expressed in the steep gradient of the Upper Galilee streams.

E-mail: amatmon@zoo.univ.ed
*Present address: Department of Geology, University of Vermont, Burlington, VT 05405, USA.

0021-2164/00 $4.00

The data collected in the Bet ha'Emeq and neighboring valleys indicate that faulting was active since the Miocene and until the late Pleistocene, and that the development of the landscape is mainly controlled by rates of faulting and regional uplift, and less by surficial processes.

INTRODUCTION

Active tectonics influence fluvial systems by either subsidence or uplift and by direct faulting on all temporal scales (e.g., Wallace, 1967; Stevens, 1974; Schumm, 1977, 1986). The change in slope causes changes in stream pattern and aggradation and/or incision of the stream. When stream incision occurs more slowly than uplift, a disruption of the drainage pattern will follow (Sparling, 1967; Twidale, 1971; Ollier, 1981; Harvey and Wells, 1987; Burbank et al., 1996; Gupta, 1997). The effect of direct displacement by faulting can be very dramatic (e.g., Keller, 1986; Rockwell et al., 1988; Spitz and Schumm, 1997). Slower deformation is more difficult to detect. However, long-term activity will result in the accumulation of both recognizable tectonic structures and deformation of the fluvial system (e.g., Gerson et al., 1984; Markewich, 1984; Ouchi, 1985; Merritts and Vincent, 1989; Chorowicz and Fabre, 1997; Spitz and Schumm, 1997).

In Israel, fluvial systems have been largely modified by recent tectonics (e.g., Bentor and Vroman, 1951; Garfunkel and Horovitz, 1966; Freund et al., 1968; Kafri and Heimann, 1994; Ginat et al., 1998; Kafri, 1997), and the drainage pattern has adjusted to the development of different morphotectonic features.

In this study, we reconstruct the development of a main drainage system in the Upper Galilee, northern Israel, and explain this development in relation to tectonic activity that took place in the region since the Miocene. The area is located at the margins of the Dead Sea Transform Valley (DSTV), so drainage development was affected both by the large-scale tectonics and by local inner Galilee faulting. Based on this reconstruction, we will evaluate the influence of the tectonic activity on the drainage system.

STUDY AREA

The Upper Galilee is located in northern Israel, between the Mediterranean Sea in the west and the DSTV in the east, and between the Bet Kerem Valley in the south and the Litani River, southern Lebanon, in the north (Fig. 1a). The surface of the Upper Galilee is a mountainous area that rises moderately from the coastal plain to an altitude of approximately 1000 m and is part of a regional erosional surface that developed during the Oligocene to Miocene (Garfunkel, 1988). The N–S-oriented main water divide is subparallel to the DSTV and the distance between them increases from 2 km in the northern Galilee, where the divide is located at the top of the rift's western rim, to 30 km in the southern part of the Galilee.

The Upper Galilee is crossed by two systems of faults trending NW and NE, which have sinistral and dextral displacements, respectively, accommodating N–S extension (Ron et al., 1984; Fig. 1a). Some of these faults curve to become E–W normal faults (Ron et al., 1984). Most of the folds that developed during the late Mesozoic as part of the Syrian Arc (Flexer et al., 1970) have no morphologic expression.

The tectonic development and erosional pattern that persisted in the Galilee since the Miocene did not leave a sedimentary record that can testify for stages of landscape formation. The absence of topographic expression on most of the Upper Galilee normal faults implies that they have not been active since the end of the Miocene when an extensive erosional surface was formed in this area (Picard, 1943; Yair, 1962; Garfunkel, 1988). Alternatively, it may imply that the rates of tectonic activity since the end of the Miocene did not exceed the regional denudation rates.

The stratigraphic sequence exposed in the Upper Galilee includes: (a) Lower Cretaceous sandstone and marls of the Kurnub Group (Eliezri, 1965), which are exposed only at the base of the Zurim and Ramim escarpments; (b) Upper Cretaceous limestone and dolomite of the Judea Group (Baida, 1961; Kafri, 1972), which cover most of the central hilly part of the Galilee. This sequence includes the quartz geodes horizon in the Cenomanian Deir Hana Formation, which is widely exposed in the Beit Jann area (Fig. 1b); (c) Senonian to Paleocene cherts, chalks, and marls of the Mt. Scopus Group (Flexer et al., 1970; Kafri, 1972); (d) Eocene limestones and chalks of the Avedat Group (Baida, 1961; Kafri, 1972), which are exposed at the eastern and western margins of the Galilee or in downfaulted blocks and small synclines in the center of the Galilee. In the eastern part of the Upper Galilee, there are late Pliocene to early Pleistocene volcanic fields. The valley floors in the Galilee are generally a

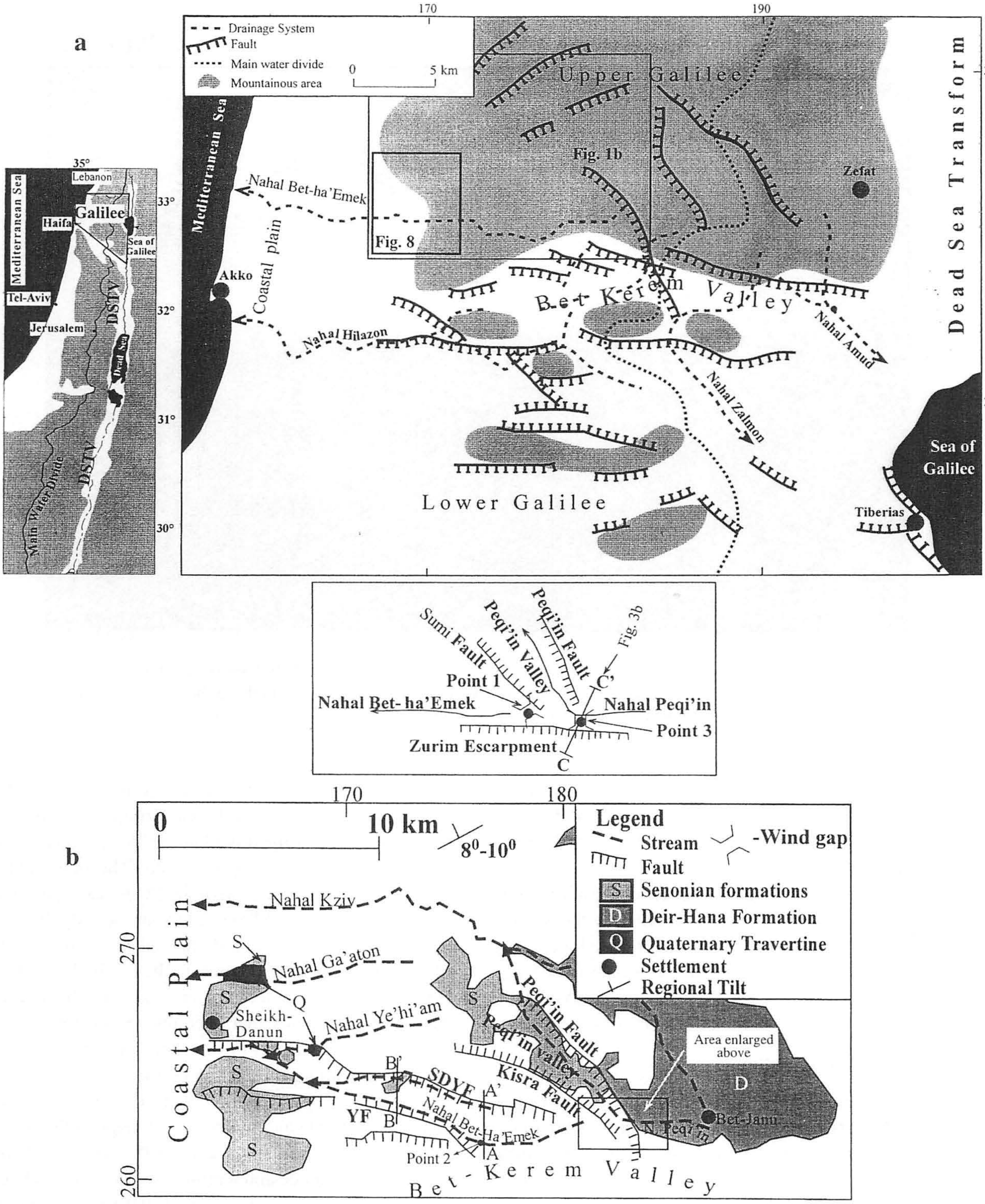

b

Fig. 1. (a) Generalized location map. DSTV—Dead Sea Transform Valley (geology after Picard and Golani, 1965); (b) detailed map of the Bet ha'Emeq area. The area of capture of the former headwaters of Nahal Bet ha'Emeq is schematically enlarged at the top of the figure. Only faults that are mentioned in the text appear in the figure. SDYF—Sheikh Danun–Yanuh Fault. YF—Yarka Fault. B-B'—cross section in Fig. 6. A-A'—cross section in Fig. 3a. C-C'—cross section in Fig. 3b. ⊢—regional dip direction. Geology after Eliezri, 1965; Kafri, 1972.

Fig. 2. Bet ha'Emeq structure. View to the east. The uplifted block on the left (north) is the Sheikh Danun–Yanuh block. The uplifted block on the right (south) is the Yarka block. Both blocks are bounded by normal faults at their base. The surface of the downfaulted block is incised in the north and south by the Yanuh and Bet ha'Emeq streams, respectively.

covered with Pleistocene to Holocene alluvial sediments with local silty clay deposits and soils. The climate of the area is semihumid Mediterranean (annual mean precipitation is 700–900 mm). Karst is the main erosion process in this carbonatic terrain, resulting in a low amount of coarse material delivery to the stream channels. The thin colluvial mantle on the slopes consists generally of silty soil with carbonate rock fragments, generally not larger than 10 cm. Alluvial fans are not common and mass wasting processes are rare.

The Bet ha'Emeq Valley

The Bet ha'Emeq faults (located in the western Upper Galilee; Fig. 1b) are unique in their prominent topographic expression (Fig. 2). The eastern part of the valley is a graben bounded in the north by the Sheikh Danun–Yanuh normal fault and in the south by the Yarka normal fault (Fig. 1b). The western part is a tilted block bounded in the north by the Sheikh Danun–Yanuh normal fault (Fig. 1b; Freund, 1959, 1970; Baida, 1961; Kafri, 1972). The vertical displacement along these faults ranges between 100 and 400 m (Freund, 1970; Kafri, 1972). In the uplifted blocks, limestones and dolomites of the Cenomanian to Turonian Judea Group are exposed, whereas the base of the downfaulted block is composed of chalks of the Mt. Scopus Group. The outstanding morphostructural expression of the Bet ha'Emeq normal faults indicates a post-Miocene tectonic activity that exceeded denudation rates and enabled the formation of substantial topography. Therefore the Bet ha'Emeq low structure serves as a sedimentary trap for Miocene to Quaternary sediments that accumulated on top of the Senonian units, whereas most of the Galilee was under erosional conditions during that period.

Several geological studies were carried out in the area. Baida (1961) and Kafri (1972) mapped the western part of the Galilee. Freund (1959) described the Cretaceous sequence and tectonics of the area and later calculated the extension of the normal fault system in the Galilee during the Neogene, including the Bet ha'Emeq system (Freund, 1970). Kafri (1997) proposed that the western part of the Bet ha'Emeq graben was part of an extensive Neogene drainage system that flowed from the eastern Galilee to the Mediterranean.

METHODS

A morphometric analysis of Nahal Bet ha'Emeq, which is the stream that drains the Bet ha'Emeq Valley (Fig. 1b) and its surroundings, was conducted. The analysis includes the construction of topographic cross sections perpendicular to Nahal Bet ha'Emeq at several points, longitudinal profiles of Nahal Bet ha'Emeq and other streams, and the calculation of the Vf parameter, which is indicative of the degree of incision. Vf values express the ratio between the width of the stream bed and the average depth of the stream bed below its interfluves on both sides. Vf values were calculated at 32 points, evenly spaced, along Nahal Bet ha'Emeq following the method described by Keller (1986). All topographic cross sections and profiles were constructed using GIS procedures and the Digital Terrain Model (DTM) (Hall, 1993) database.

Mapping of alluvial terraces at the western part of the Bet ha'Emeq Valley and adjacent drainage systems, and analysis of thin sections of calcrete horizons that formed on the alluvial material, help to determine the minimum age of the terraces using the calcrete stage index (Birkeland, 1984; Machette, 1985; Birkeland et al., 1991). Topographical maps were analyzed to detect remnants of the ancient course of the Nahal Bet ha'Emeq drainage system. Topographical features such as wide saddles were marked for later fieldwork based on the analyses of the maps. The sites, which appear to be remnants of ancient streams, were surveyed for direct evidence of fluvial deposits. At sites where these deposits were identified, we concentrated our efforts on exotic gravel that has no source in the present-day drainage basin. Possible sources for exotic gravel such as quartz geodes were marked. This enabled us to trace the gravels to their source, reconstruct the ancient drainage basin of Nahal Bet ha'Emeq, and evaluate the tectonic activity that took place in the area.

Combining available geological and structural data with the topographic and morphometric analysis enabled us to locate segments of the drainage system that were influenced by tectonic stages that took place between the early Miocene and the Pleistocene. Comparing longitudinal profiles of main stream channels in the Upper and Lower Galilee (including the Nahal Bet ha'Emeq stream channel and its tributaries) and correlating alluvial terraces in the western Upper Galilee streams helped to distinguish between deformation that was related to normal faulting of the Bet ha'Emeq fault system and regional uplift that was followed by a change in base level and regional incision of streams.

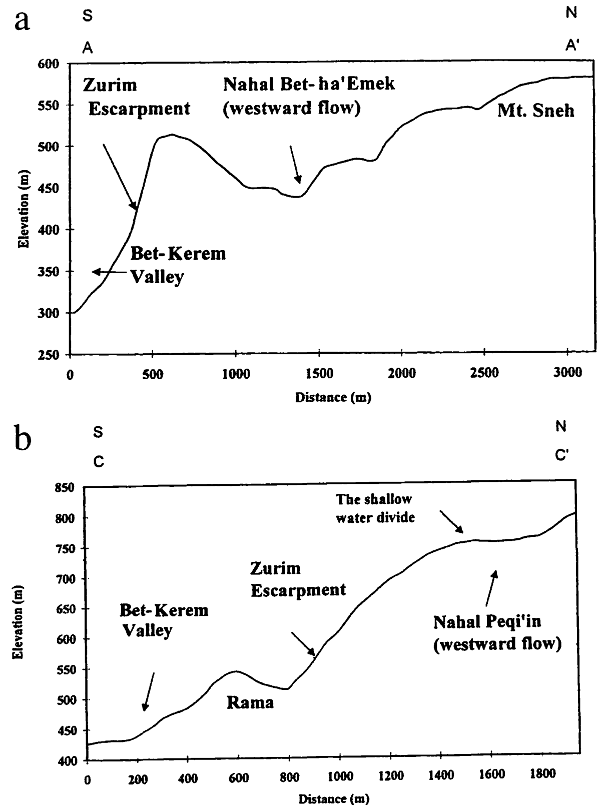

Fig. 3. (a) A topographic cross section of the area where Nahal Bet ha'Emeq reaches the closest to the Zurim Escarpment. For location of cross section, see Fig. 1b; (b) A topographic cross section of the area where Nahal Peqi'in reaches the closest to the Zurim Escarpment. For location of cross section, see Fig. 1b in enlarged area at top of figure.

FIELD OBSERVATIONS

The pattern of Nahal Bet ha'Emeq

The general flow direction of Nahal Bet ha'Emeq is westward from its eastern divide to the Mediterranean. At the eastern and central reaches of the drainage system, the divide between the Bet Kerem Valley and the Bet ha'Emeq Valley drainage basins lies right above the northern escarpment of the Bet Kerem Valley. Nahal Bet ha'Emeq meanders very close to the water divide between the two basins (point 2, Fig. 1b and Fig. 3a). Even though the deep valley of Bet Kerem is much closer to the upper reach of Nahal Bet ha'Emeq than the Mediterranean, Nahal Bet ha'Emeq flows to the further base level, the Mediterranean, along a gentler gradient. In addition, the course of Nahal Bet ha'Emeq does not follow the direction of the NW regional tilt of the Upper Galilee. Similar relations are observed at point 3 of Fig. 1b near the

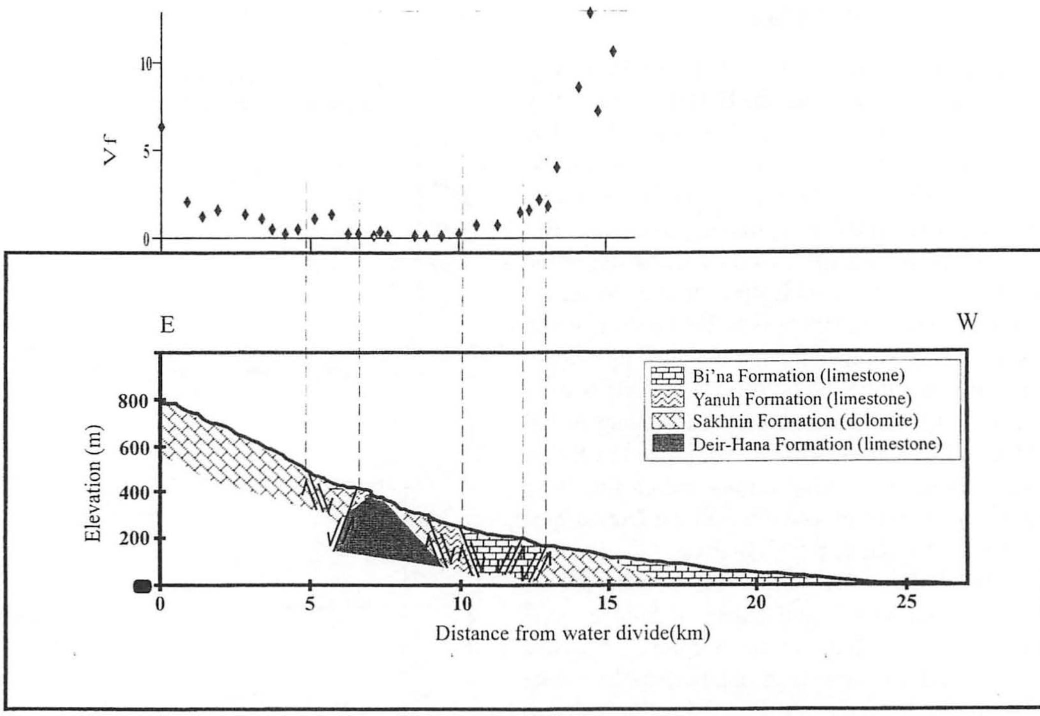

Fig. 4. Topographic profile of Nahal Bet ha'Emeq. Notice the correlation between the steep sections of the drainage system, the location of uplifted blocks it crosses, and the Vf low values. Lithology does not seem to influence the Vf value. All rock units are hard carbonate rocks (geology after Kafri, 1972).

village of Beit Jann. There, the divide between the Bet Kerem Valley and the former headwaters of Nahal Bet ha'Emeq rises only ~2 m above the channel bed (Fig. 3b).

Nahal Bet ha'Emeq crosses several uplifted structures (Fig. 4). The Nahal Bet ha'Emeq stream bed alternates from a wide and gentle gradient stream to a narrow, steep gradient stream as it crosses between uplifted to downfaulted blocks (Fig. 4). The correlation between Vf values and structure is good. Lithology does not seem to influence Vf values (Fig. 4). At the western reach of Nahal Bet ha'Emeq, Vf values increase as the stream enters the coastal plain. The local structure of uplifted blocks is buried under the coastal plain sediments.

Marine and alluvial sediments dating from the late Eocene to Pliocene, exposed at the western end of the Bet ha'Emeq Valley, indicate that the area subsided and trapped sediments since at least the early Oligocene (Matmon et al., in preparation). This is in contrast to the rest of the region that has been uplifted and under erosion since the middle Eocene.

These observations regarding Nahal Bet ha'Emeq imply that:

1. The stream valley of Nahal Bet ha'Emeq developed prior to both the development of the Zurim Escarpment and the tilting of the Upper Galilee to the NW, but later or contemporaneous with the Bet ha'Emeq graben.
2. The Zurim Escarpment did not retreat substantially since its formation and there is no process of river capturing.
3. The drainage system of Nahal Bet ha'Emeq is incised through the structures it crosses and it was not blocked and diverted by uplifted blocks. This implies that the drainage system developed before or at the same time the blocks were uplifted and that the rate of uplift did not exceed the rate of incision.

Longitudinal profile of Nahal Bet ha'Emeq

The headwaters of Nahal Bet ha'Emeq are located in a series of abandoned valleys on the Kisra Ridge which is uplifted by the Sumi Fault (point 1 in Fig. 1b; Fig. 5). Quartz geodes were found at the headwaters of Nahal Bet ha'Emeq. The only possible source for these geodes is the Deir Hana Formation (Eliezri, 1965), exposed on the Beit Jann uplifted block, east of the Peqi'in Valley (Fig. 1b). This block is currently

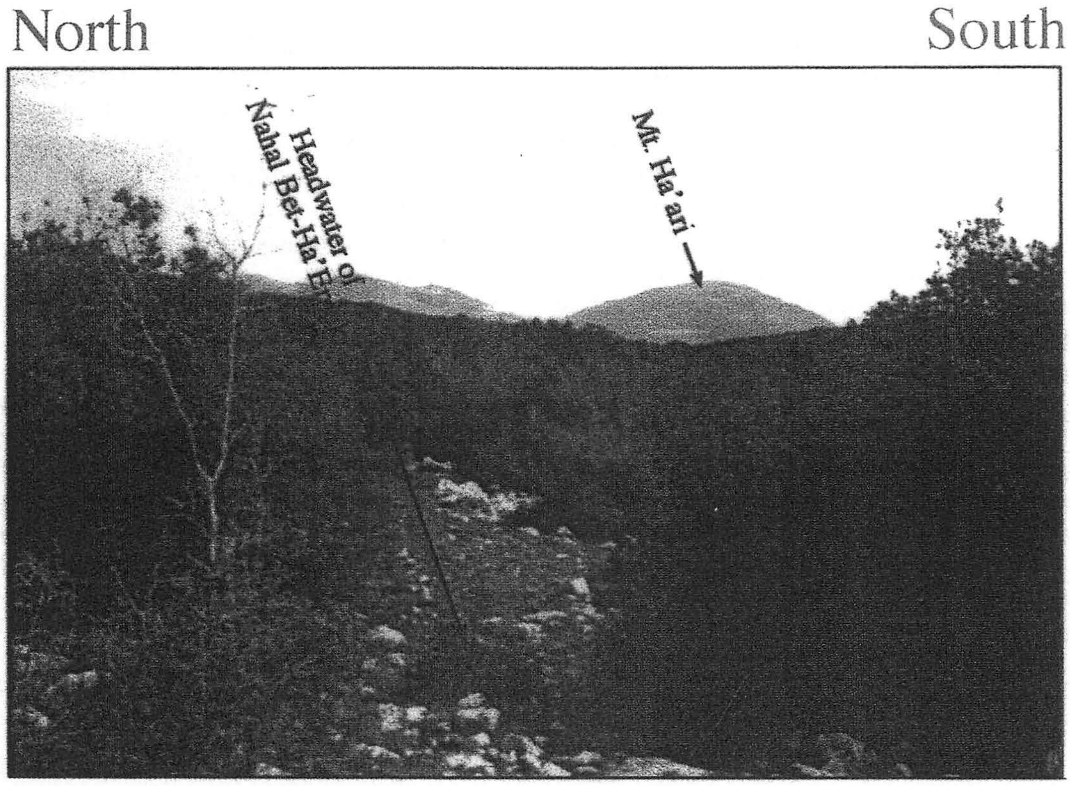

Fig. 5. The abandoned saddle at the present headwaters of Nahal Bet ha'Emeq. Quartz geodes were found on the saddle. The most likely source of the geodes is the Beit Jann block, which can be seen in the background. Presently, the Beit Jann block does not drain into the Bet ha'Emeq drainage system.

drained into the Peqi'in Valley and is disconnected from the Bet ha'Emeq drainage system by the uplifted block of the Sumi Fault.

Longitudinal profiles of the main westward-flowing streams in the Upper and Lower Galilee were constructed (Fig. 6). Two important observations are drawn from the comparison of the stream profiles: (i) the profiles of the Upper Galilee streams are steeper than the Lower Galilee streams and (ii) 3 Upper Galilee stream profiles are similar, with the upper reach of Nahal Bet ha'Emeq being anomalously steeper than the other Upper Galilee streams. These observations may reflect two tectonic phases that took place in the area:

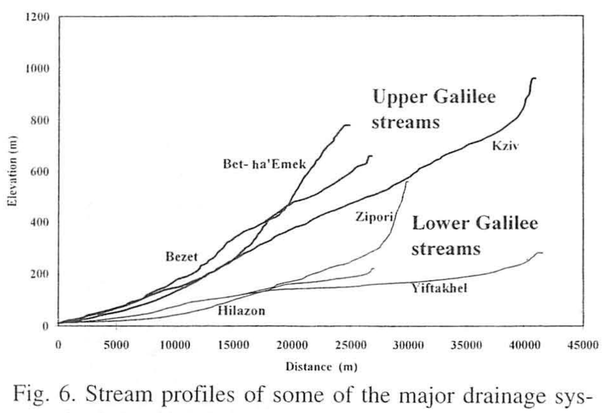

Fig. 6. Stream profiles of some of the major drainage systems in the Galilee. The Upper Galilee streams are significantly steeper than the Lower Galilee streams.

1. The Lower and Upper Galilee are uplifted due to arching of the west margins of the Dead Sea Transform Valley (Matmon et al., 1999). However, the Lower Galilee has been subsiding during the Late Cenozoic due to the extension process that formed the basin and range structure of the area (Freund, 1970; Ron et al., 1984). The steep profiles of the Upper Galilee reflect the arching, while the gentle profiles of the Lower Galilee reflect the subsidence of the Lower Galilee.
2. The relative steepness of the upper reach of Nahal Bet ha'Emeq reflects the uplift of the Kisra block

and points to the disequilibrium state of Nahal Bet ha'Emeq in relation to the relief formed by activity of the Kisra Fault. This observation and the existence of the quartz geodes at the headwaters of Nahal Bet ha'Emeq suggest that prior to the formation of the Kisra ridge by the activity of the Kisra fault, the headwaters of Nahal Bet ha'Emeq were located in the Beit Jann block. Vertical displacement along the Sumi and Peqi'in faults diverted the headwaters of Nahal Bet ha'Emeq into the subsiding Peqi'in Valley and steepened the current headwaters of Nahal Bet ha'Emeq.

The preservation of the Senonian sequence

A Senonian sequence of chalk and marl is preserved in the Bet ha'Emeq graben (Figs. 1b and 7; Kafri, 1972). The existence of the Senonian rocks in the graben helps put constraints on the relations between regional denudation and faulting in the area. To further the discussion on the implications of the occurrence of these Senonian rocks we provide a short review of the geological history of the region from the late Eocene to the middle Miocene. The Eocene sequence of limestone and chalk was deposited on the preexisting truncated folds of the Syrian Arc that began forming as early as the late Turonian (Flexer, 1964, 1968; Flexer et al., 1970). The regression of the Tethys Ocean at the end of the Eocene and the slow uplift of the land left behind a flat continental platform covered by Eocene carbonate units (Fig. 8A), which was drained westward by a regional drainage stystem (Picard, 1943, 1951; Garfunkel and Horowitz, 1966; Nir, 1970; Garfunkel, 1988; Avni, 1990, 1991; Zilberman, 1992; Garfunkel and Ben-Avraham, 1996; Begin and Zilberman, 1997). This drainage system eroded the uplifted terrain and exposed differentially rocks of the Judea Group, while the Senonian, and sometimes the Eocene, sequence was preserved in the synclines (Fig. 8C). The rate of uplift and erosion during the Oligocene and the Miocene are not well known. The abundant gravel of Eocene source in the Miocene conglomerates, even in areas where the Eocene sequence has been eroded, suggests that Eocene cover was still widespread during the early Miocene and that erosion was limited during the Oligocene (Garfunkel, 1970, 1978).

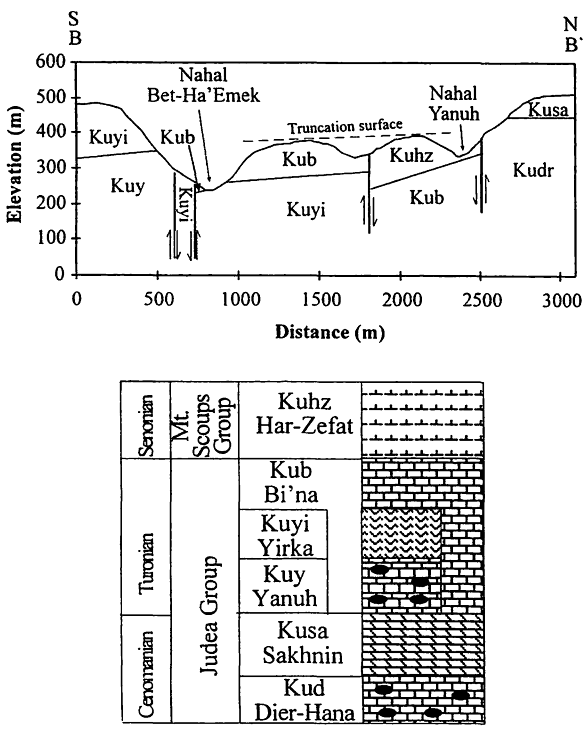

Fig. 7. Topographic and geologic cross section across Nahal Bet ha'Emeq in an area of preserved Senonian units in the downfaulted block. For location of cross section, see Fig. 1b. The downfaulted block has been incised by the Bet ha'Emeq stream and its tributaries. Notice the upper surface of the remnant hills in the downfaulted blocks. Modified after Kafri, 1972.

The preservation of the Senonian sequence in the Bet ha'Emeq graben, as well as along other fault-controlled structural lows in the Galilee, indicates that the structure already existed in the Miocene. This implies that vertical displacement of the Bet ha'Emeq fault system began early enough in the history of denudation, while Senonian rocks were still on the surface (Fig. 8B or 8D). This type of preserving mechanism of young stratigraphic units has been suggested as being responsible for (a) the existence of the Upper Mesozoic sequence in the grabens of Yotam and Netafim in the Elat area, (b) the preservation of the Hazeva Formation in the Karkom and Abu-Treifa grabens in the central Negev, and (c) the preservation of Maastrichtian-Neogene sequence along the boundary of the Dead Sea basin (e.g., Garfunkel, 1970; Agnon, 1982; Zilberman, 1993).

Ongoing erosion on the upper blocks and preservation of young sequences on the lower blocks requires that the rate of vertical displacement be lower than the rate of denudation. Fast vertical displacements will trigger rapid incision of the drainage network and, in turn, the abandonment of the top of the uplifted block and a significant decrease in erosion on the isolated high ridges (Matmon et al., 1998; Fig. 8B). In such a case, Senonian units are expected to be preserved on or near the summits of the uplifted isolated blocks. In places such as Mt. Zefat or Nazareth Mts., the summits, which are at the same elevation as neighboring summits, are built of Senonian and Eocene units. Nevertheless, this is not the case in the Galilee in general and in the Bet ha'Emeq area in particular. The complete erosion of the Senonian sequence from the uplifted block along with the preservation of the Senonian sequence on the downfaulted block could be achieved provided the Senonian sequence was removed from the uplifted block prior to the formation of the present topography (Fig. 8D). The present topography was formed only at a later stage (Fig. 8E).

Remnants of the low-relief terrain which predated the present topography are observed in the Bet ha'Emeq graben. The summits of the rounded hills which developed in the soft Senonian units form a flat level that does not correspond to the dip of the beds but truncates them (Fig. 7).

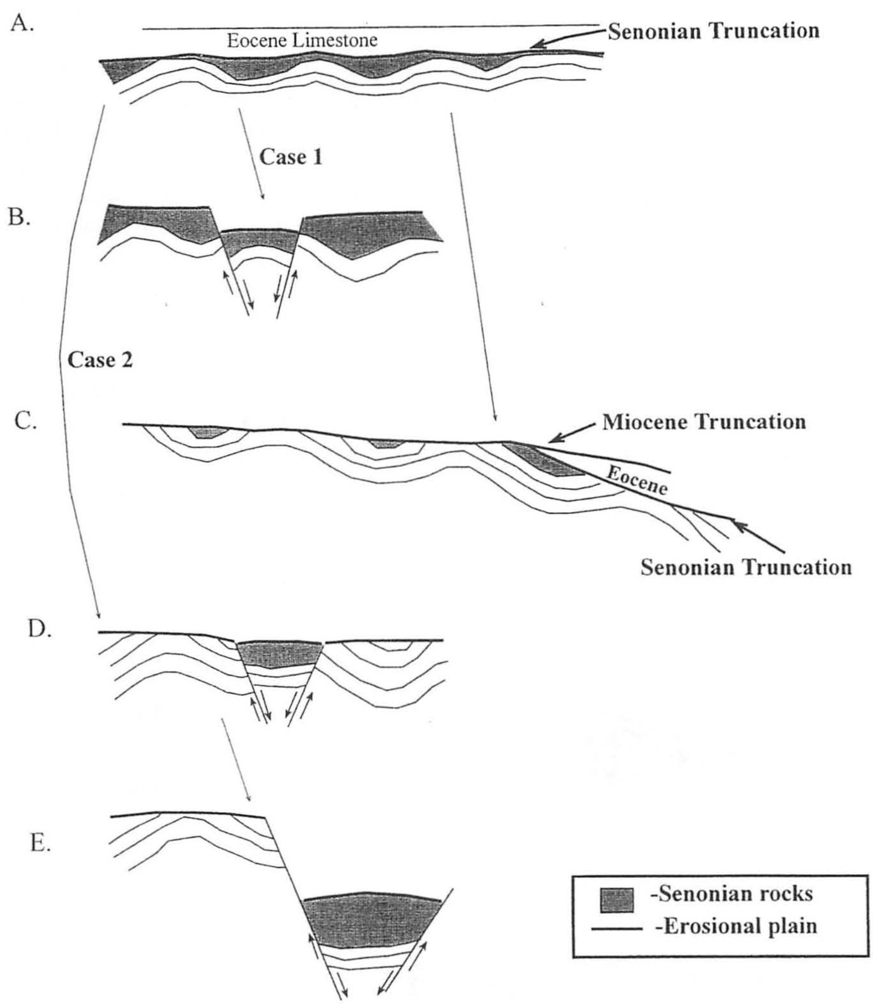

Fig. 8. A cartoon showing the mechanism for Senonian rock preservation. (A) Initial situation after the regression of the Tethys Ocean. Eocene carbonate sediments were deposited over an erosional surface that developed after the deposition of the Senonian sequence. (B) Case 1: Faulting and relief forming during early stages of Miocene truncation. In this case, the Senonian sequence is preserved both on the uplifted and downfaulted blocks. This situation does not occur in the Bet ha'Emeq graben, indicating that faulting was not accompanied by relief. (C) Ongoing truncation with no faulting. In this case, the Senonian sequence is preserved only in the synclines of the pre-Eocene structure. (D) Faulting during the early stages of truncation. The faulting is not associated with topography. This situation allows the ongoing truncation on the uplifted blocks while preserving the Senonian sequence on the downfaulted block. This situation occurs when the rate of vertical displacement is equal to the rate of truncation and it agrees with field observations in the Bet ha'Emeq area. (E) Final stage of uplifting forms the present topography.

Alluvial terraces

Alluvial terraces are rare along the slopes on both sides of the Bet ha'Emeq graben, which expose Upper Cretaceous rocks coated in places with calcrete. The scarcity of alluvial terraces might be because: (a) the flow level of the drainage system occupied the surface of the graben as it was downfaulted and there was no major incision phase, (b) incision phases were rapid and alluvial and rock-cut terraces were not formed, and (c) terraces that were formed were eroded from the slopes of the graben.

The terraces in the graben are confined to its western part (Fig. 9) and are situated 10 to 30 m above the present streambed. The terraces contain well-rounded limestone, dolomite, chalk and chert pebbles, and angular chert fragments. The pebbles are embedded in a highly developed calcrete coating that is currently eroding due to karst processes (Fig. 10). The thickness of the alluvium does not exceed several meters and it is deposited on benches incised into Senonian chalk at the margins of the valley (Fig. 11). The alluvial terraces probably experienced a long period of pedogenic process resulting in the development of Stage VI calcretes (Machette, 1985). In comparison to calcrete horizons in the southwestern United States, the age of these calcrete horizons, and therefore the terraces, is at least 400 Ka (Birkeland, 1984; Machette, 1985; Birkeland et al., 1991). At site (a) in Fig. 9 (coordinates 16540/26580 Israel Grid), the terrace leans on a relatively fresh fault scarp (Fig. 12), displacing the Upper Cretaceous Sakhnin Formation dolomite. The freshness of the fault scarp suggests displacement during the Late Pleistocene or Holocene (Gran et al., 1999), whereas the maturity of the calcrete suggests a much older age for the terrace. It should be emphasized that there is no direct field evidence on whether the conglomerate was deposited along the fault scarp or was displaced by it. Alluvial terraces similar in texture and composition to the alluvial terraces of Nahal Bet ha'Emeq, are found near Nahal Ga'aton about 10 km north of Nahal Bet ha'Emeq (Figs. 1b and 9), about 20 m above the Ga'aton stream bed and 10–20 m above the Itzhar channel bed, approximately 10 km south of Nahal Bet ha'Emeq.

A travertine unit, tens of meters thick, was deposited at the mouth of Nahal Yehi'am (Figs. 1b, 9; Baida, 1961; Kafri, 1972). At present, the channel is incising into the travertine, slowly eroding it away. The gradient of the Yehi'am channel in the area of the travertine beds is 5%. Similar relations between travertine units and incising channels can be seen at the mouth of Nahal Ga'aton (Fig. 9).

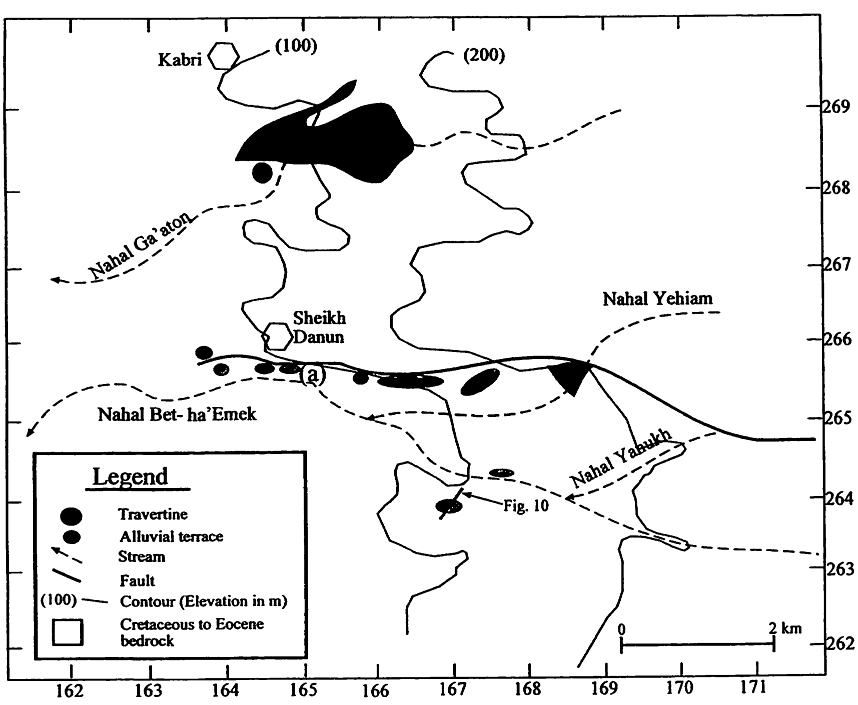

Fig. 9. A detailed map of travertine units and alluvial terraces in the western part of Nahal Bet ha'Emeq.

Fig. 10. Typical appearance of the alluvium in the terraces. The pebbles are cemented in a hard calcrete matrix. It can be seen that presently the calcrete is disintegrating and pebbles are being washed back to the active drainage system.

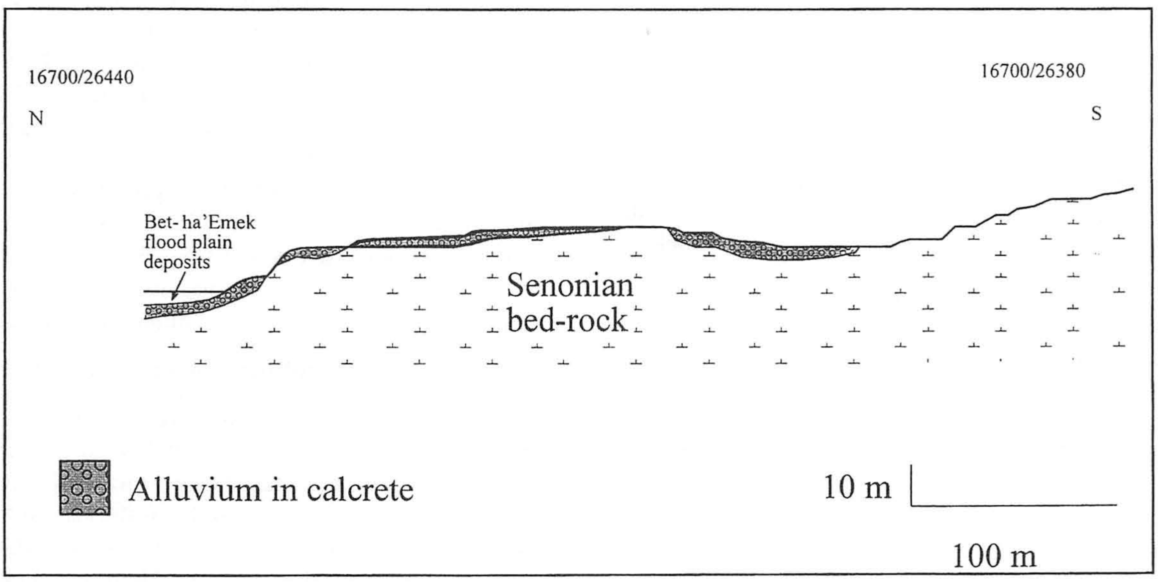

Fig. 11. A detailed cross section of an alluvial terrace on the southern margin of the Bet ha'Emeq Valley. The underlying chalk is exposed at different levels of the terrace, indicating that the thickness of the alluvium is only several meters and that it is deposited on benches in the Senonian chalk.

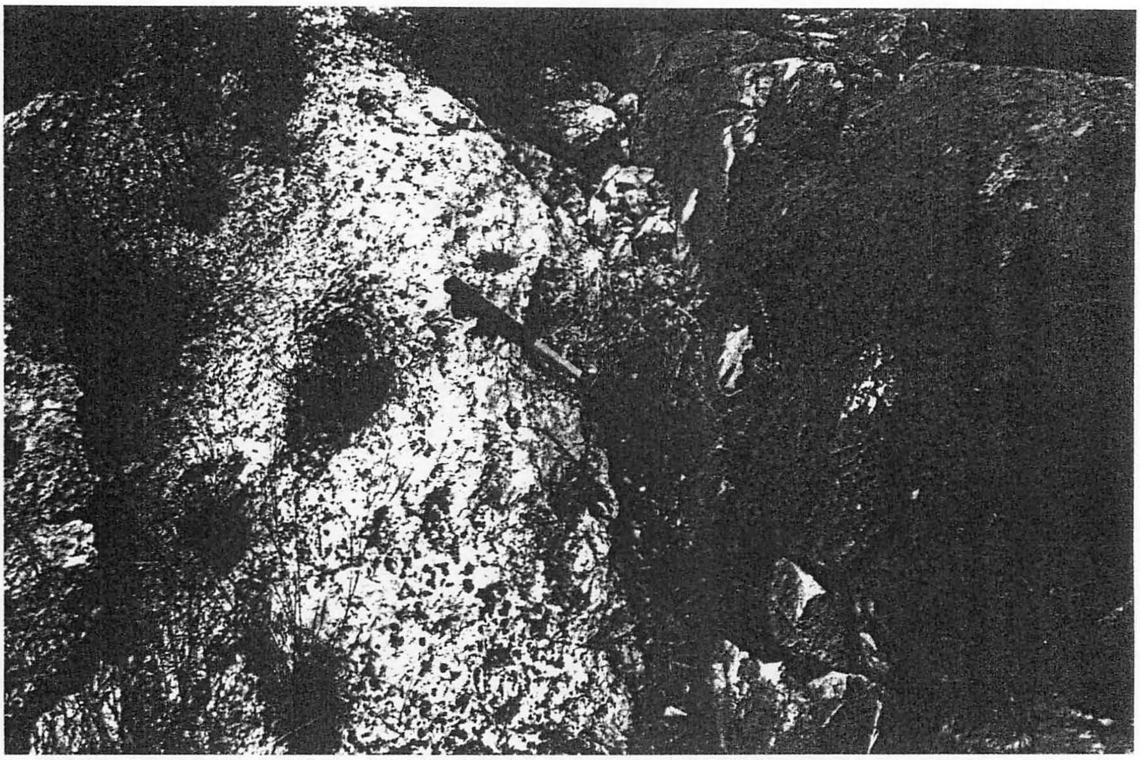

Fig. 12. Alluvial material against a fresh fault scarp built of dolomite of the Sakhnin Formation. For location, see point (a) in Fig. 7.

DISCUSSION AND CONCLUSIONS

The drainage pattern in the Bet ha'Emeq Valley and the preservation of a Senonian sequence on the downfaulted block indicate that the activity of the Bet ha'Emeq faults started early in the faulting history of the region and probably earlier than most of the other normal faults in the Galilee. The tectonic and erosional evolution of the Bet ha'Emeq structure and the development of the drainage system in the Bet ha'Emeq Valley can be divided into three stages, and the rates of tectonic and erosional phases are estimated below.

Stage 1—Beginning of denudation

The denudation of the region began sometime after the regression of the Tethys Ocean in the late Eocene. Begin and Zilberman (1997) estimated denudation rates of the mountainous backbone of Israel from the Oligocene to the Pleistocene. They calculated a typical denudation value of 20 m in a million years for an average relief of 100 m (which represents the landscape in the region during the Oligocene and Miocene). The Senonian to Eocene sequence in the Galilee is 150–250 m thick (Kafri 1972). Therefore, it would take no more than 7.5–12.5 million years to erode the Eocene to Senonian sequence. Regional denudation during the Oligocene was probably very limited. Evidence for initial relief and significant stripping of sediments is represented in continental sediments found along the margins of Samaria, Judea, and the Negev and dated to Upper Oligocene and Lower Miocene (~23 Ma) (Shaliv et al., 1991; Zilberman, 1992; Buchbinder and Zilberman, 1997). Therefore the lower part of the Senonian sequence could be exposed only in the middle Miocene, 7.5–12.5 million years after the beginning of significant denudation. We shall state that our time estimates for the activity of tectonic and erosional phases in the area are minimum estimates.

Stage 2—Normal faulting at denudation rates

As mentioned earlier, the preservation of the Senonian sequence in the Bet ha'Emeq graben required that faulting start before the Senonian sequence was totally eroded and that the rate of faulting was compatible with the rate of denudation, resulting in low-relief terrain. Therefore faulting must have started no later than Middle Miocene, probably 7.5–12.5 Myr after denudation began. The

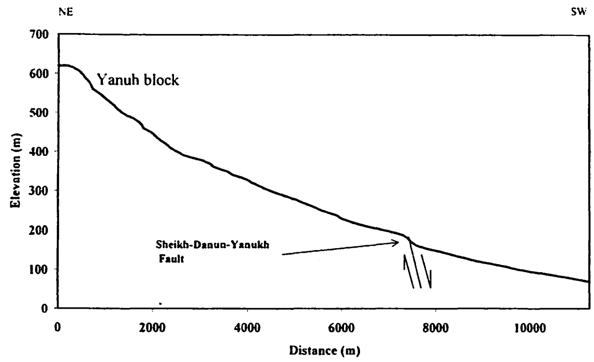

Fig. 13. Topographic cross section of the Yehi'am stream. A knick-point occurs where the northern normal Sheikh Danun– Yanuh fault crosses the stream.

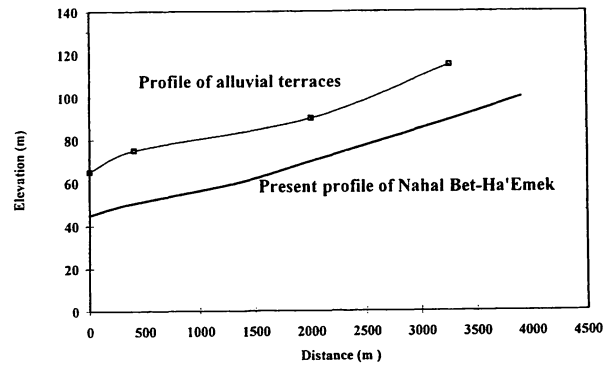

Fig. 14. A comparison of the gradient of the western part of the present Nahal Bet ha'Emeq with the reconstructed gradient of alluvial terraces above Nahal Bet ha'Emeq.

occurrence of late Eocene and early Oligocene units at the western end of the Bet ha'Emeq Valley indicate that it subsided and trapped sediments while the rest of the region was under erosion. The absence of Senonian units on the uplifted blocks indicates that denudation continued on the uplifted blocks south and north of the Bet ha'Emeq low structure after its initial subsidence. Matmon et al. (1998) demonstrated that the formation of tectonic relief in the Galilee caused a dramatic decline in the denudation rates along the interfluves that established on the uplifted blocks. If substantial relief were to develop, the reduced denudation rates that would follow it would allow the preservation of Senonian rocks on the uplifted blocks. Since this sequence is totally absent from the uplifted blocks, it must be concluded that the rate of normal faulting during this tectonic phase was equal to the rate of denudation of the uplifted blocks. The drainage system of Nahal Bet ha'Emeq, which occupied the shallow valley at this stage, incised through the uplifting secondary blocks that developed in the Bet ha'Emeq low structure.

The stratigraphic displacement between the Senonian preserved units in the valley and the Cenomanian rocks exposed at the top of the uplifted blocks reaches 400 m in some places (Kafri, 1972). Since only one-third of the stratigraphic displacement is expressed by topography, it appears that about two-thirds of the displacement occurred before the last tectonic phase that formed the present relief. Assuming vertical displacement rates that are compatible with denudation rates (20–25 m/Myr; Begin and Zilberman, 1997), the period dominated by low-rate displacement without forming topography lasted 10–11 Myr. This calculation is subjected to several uncertain parameters:

(1) The changes in rates of denudation. Begin and Zilberman (1997) estimate rates of denudation 10–60 m/Myr since the Miocene. This range can result in much shorter or longer periods of time needed to erode the sequence missing on top of the uplifted blocks. The rate of 20 m/Myr used above is the average rate calculated by Begin and Zilberman (1997) and it is a reasonable rate for an average relief of 100 m.
(2) Uncertainty of the thickness of sediments that were removed. The thickness of the eroded section ranges between 200 m and 400 m (Baida, 1961; Kafri, 1972). This range could shorten or extend the period of denudation by 20–25%. A thickness of 260 m of the eroded section was assumed based on structural data of the area (Kafri, 1972).

Stage 3—Development of the present topography

The present topographic expression of the Bet ha'Emeq graben was formed by a tectonic phase associated with high rates of vertical displacement. Considering that denudation started ~23 Ma and lasted 7.5–12.5 Myr in stable conditions and additional 10–11 Myr under slow rate displacement, topography was formed by a high rate of vertical displacement within the last 5.5 Ma. This estimate agrees with the results of topographic analysis by Matmon et al. (1998) that show that most of the morphotectonic features in the Galilee began forming about 4 Ma. It should be stated again that these estimates are minimum ones and that all three stages might have occurred earlier if substantial denudation began earlier than ~23 Ma.

The activity on the Bet ha'Emeq fault system continued through the Quaternary, as indicated by the fresh fault scarp in the Sakhnin dolomite (point (a) in

Fig. 9), evidence for shearing in the calcrete of the Sheikh Danun exposure (in preparation) and a knickpoint where the Ye'hiam channel crosses the Sheikh Danun–Yanuh fault (Fig. 13). These observations agree with the Quaternary displacement inferred by Sivan (1996).

The correlation between the different terraces observed in the lower Bet ha'Emeq Valley is not certain, although they are very similar in composition and texture. Whether these terraces are of the same age or not, the incision of approximately 20 m below the terraces by the recent drainage systems (Bet ha'Emeq, Ga'aton, Itzhar) indicates a response to a regional change in base level and is not directly related to local activity of the Bet ha'Emeq fault system. The incision into these terraces reflects a regional tectonic phase such as the ongoing arching of the Galilee (Matmon et al., 1999) or a fall in sea level.

The travertine at the intersection of the streams of Nahal Ye'hiam and Nahal Bet ha'Emeq (Baida, 1961; Kafri, 1972; Fig. 9) could not be deposited in a drainage configuration similar to the present one because of the steep gradient. At this gradient, the fast-flowing floodwaters of the ephemeral channel cannot precipitate $CaCO_3$ and accumulate the travertine (Heimann, 1985). A gentler gradient, which could be achieved by a higher base level, would result in a lower gradient of Nahal Yehi'am and allow slower flow and enable the deposition of the travertine unit. This higher base level could have existed before Nahal Bet ha'Emeq incised to its present level, possibly as a result of regional uplift. Similar relations between travertine units and incising channels are described in the northern Hula Valley (Heimann, 1985) and observed at the mouth of Nahal Ga'aton to the coastal plain and in the eastern Bet Kerem Valley.

The elevation of the alluvial terraces along the western part of the Bet ha'Emeq Valley increases from 65 m asl in the west to 115 m asl in the east, resulting in a gradient of 1.4%. This gradient is similar to the gradient of the active channel in this area (Fig. 14). The similarity in gradients indicates that the amount of uplift along the western part of the Bet ha'Emeq structure is uniform and that the axis of uplift is not located in or close to the part of Nahal Bet ha'Emeq where the alluvial terraces are, but farther to the east.

SUMMARY

The Bet ha'Emeq Valley is bounded by escarpments formed by normal faults and is a dominant topographic feature in the western Upper Galilee. The topographic relief of the Bet ha'Emeq normal faults is unique in the Upper Galilee, where most of the faults have no topographic expression. The geometry of Nahal Bet ha'Emeq is controlled by previous and recent tectonic structures related to the Bet ha'Emeq fault system. The primary subsidence along the Bet ha'Emeq fault system probably initiated prior to the formation of the Bet ha'Kerem Valley and the tilting of the Upper Galilee. The preservation of Senonian units on the downfaulted block in the central Bet ha'Emeq valley and late Eocene to early Oligocene sediments at the western end of the valley suggest that subsidence began in the middle Miocene (~15 Ma) and maybe even earlier, before these units were completely eroded from the area. The drainage system that occupied the Bet ha'Emeq Valley incised through the uplifted blocks that developed within the Bet ha'Emeq low structure. The ancient headwaters of the Nahal Bet ha'Emeq drainage system are located in the uplifted block of Beit Jann. They were disconnected from the rest of the drainage system due to the activity of the Peqi'in and Sumi faults and the formation of the Peqi'in Valley. The vertical displacement along the Sheikh Danun–Yanukh fault appears to have continued through the Quaternary. Even though this activity cannot be precisely dated, it is evident by a fresh fault scarp in the Sakhnin dolomite close to the western end of the Bet ha'Emeq Valley (Fig. 12) and by the knickpoint of Nahal Yehi'am in the Pleistocene travertine units (Fig. 13; Kafri, 1972).

Incision into alluvial terraces at the western reach of the Nahal Bet ha'Emeq, as well in other adjacent drainage systems, may indicate the response of the fluvial systems to the regional uplift of the Upper Galilee platform. The uplift is manifested in the steep gradient of the Upper Galilee streams.

In spite of the scarcity of Neogene and Quaternary sediments in the Bet ha'Emeq drainage system, morphometric analysis enables the detection of tectonic activity and increases the understanding of the relation between tectonic activity and surface processes.

ACKNOWLEDGMENTS

We thank R. Amit, Y. Nachmias, and D. Gluck for helping in the field and for fruitful discussions. The manuscript has benefited a great deal from reviews by A. Agnon and Y. Avni. This study was supported by the Atomic Energy Commission (Israel), the Geological Survey of Israel, and the Earth Sciences Administration, Israel.

REFERENCES

Agnon, A. 1982. Neogene development of the western margins of the Dead Sea Depression. Geol. Surv. Isr. Current Research 1981, pp. 27–29.

Avni, Y. 1990. The paleogeography and the evolution of the landscape in the western part of the central Negev, and the relationship to the evolution of Makhtesh-Ramon. In: Lavee, H., Schick, A., Yair, A., eds. Facets of the geomorphology of the Negev; the Ran Gerson Volume, Hebrew Univ., Jerusalem, pp. 67–84 (in Hebrew, English abstr.). Also published as Vol. 31 of Horizons in Geography (Ofaqim be-Geografia) by Dept. of Geography, Univ. of Haifa.

Avni, Y. 1991. The geology, paleogeography and landscape evolution of the Negev highlands and the western Ramon structure. Geol. Surv. Isr. Rep. GSI/6/91, 153 pp.

Baida, U. 1961. On the geology of the Ga'aton-Hilazon area, Western Galilee, Israel. Isr. J. Earth Sci. 13: 1–15.

Begin, Z.B., Zilberman, E. 1997. Main stages and rates of relief development in Israel. Geol. Surv. Isr. Rep. GSI/ 24/97, 63 pp.

Bentor, Y.K., Vroman, A.J. 1951. The geological map of the Negev, 1:100000, Sheet 18: (Abde) Avedat, with explanatory notes. 98 pp. (in Hebrew)

Birkeland, P.W. 1984. Soils and geomorphology. Oxford University Press, New York, 372 pp.

Birkeland, P.W., Machette, M.N., Haller, K.M. 1991. Soils as a tool for applied Quaternary geology. Miscellaneous publications 91-3, Utah Geological and Mineral Survey, Utah Department of Natural Resources.

Buchbinder, B., Zilberman, E. 1997. Sequence stratigraphy of Miocene–Pliocene carbonate-siliciclastic shelf deposits in the eastern Mediterranean margin (Israel): effects of eustasy and tectonics. Sediment. Geol. 112: 7–32.

Burbank, W.D., Leland, J., Fielding, E., Anderson, R.S., Brozovic, N., Reid, M.R., Duncan, C. 1996. Bedrock incision, rock uplift and threshold hillslopes in the northwestern Himalayas. Nature 379: 505–510.

Chorowicz, J., Fabre, J. 1997. Organization of drainage networks from space imagery in the Taneztouft Plateau (Western Sahara): implications for the recent intracratonic deformation. Geomorphology 21: 139–151.

Eliezri, I.Z. 1965. The geology of the Bet-Jann region (Galilee, Israel). Isr. J. Earth Sci. 14: 51–66.

Flexer, A. 1964. The paleogeography of the Senonian and Maastrichtian in northern Israel. Ph.D. thesis, Hebrew Univ., Jerusalem, 157 pp. (in Hebrew, English abstr.).

Flexer, A. 1968. Stratigraphy and facies development of Mount-Scopus Group (Senonian–Paleocene) in Israel and adjacent countries. Isr. J. Earth Sci. 17: 85–114.

Flexer, A., Freund, R., Reiss, Z., Buchbinder, B. 1970. Santonian paleostructure of the Galilee. Isr. J. Earth Sci. 19: 141–146.

Freund, R. 1959. On the stratigraphy and tectonics of the Upper Cretaceous in western Galilee. Bull. Res. Counc. Isr. 8G: 43–50.

Freund, R. 1970. The geometry of faulting in Galilee. Isr. J. Earth Sci. 19: 117–140.

Freund, R., Zak, I., Garfunkel, Z. 1968. Age and rate of seismal movement along the Dead Sea Transform. Nature 220: 253–255.

Garfunkel, Z. 1970. The tectonics of the western margins of the southern Arava. Ph.D. thesis, Hebrew Univ., Jerusalem, 204 pp. (in Hebrew, English abstr.).

Garfunkel, Z. 1978. The Negev—regional synthesis of sedimentary basins. 10th Int. Cong. Sedimentol., Jerusalem, Guidebook to excursions, Part 1, pp. 33–110.

Garfunkel, Z. 1988. The pre-Quaternary geology of Israel. In: Yom-Tov, Y., Tchernov, E., eds. The zoogeography of Israel. Dr W. Junk, The Hague, Netherlands, pp. 7–34.

Garfunkel, Z., Horowitz, A. 1966. The Upper Tertiary and Quaternary morphology of the Negev. Isr. J. Earth Sci. 15: 101–117.

Garfunkel, Z., Ben-Avraham, Z. 1996. The structure of the Dead Sea Basin. Tectonophysics 266: 155–176.

Gerson, R., Grossman, S., Bowman, D. 1984. Stages in the creation of a large rift valley—geomorphic evolution along the southern Dead Sea rift. In: Morisawa, M., Hack, J.T., eds. Tectonic geomorphology. Proc. 15th Annual Binghamton Geomorphology Symp., Sept. 1984, pp. 53–73.

Ginat, H., Enzel. Y., Avni, Y. 1998. Translocated Plio–Plestocene drainage systems along the Arava fault of the Dead Sea Transform. Tectonophysics 284: 151–160.

Gran, S.E., Matmon, A., Bierman, P.R., Enzel, Y., Caffee, M. 1999. Calculating fault displacement rates, in-situ cosmogenic chlorine-36 concentrations of a limestone normal fault scarp, northern Israel. Geol. Soc. Am. Abstracts with Programs. 30: A142–A143.

Gupta, S. 1997. Himalayan drainage patterns and the origin of fluvial megafans in the Ganges foreland basin. Geology 25: 11–14.

Hall, J. 1993. The GSI Digital Terrain Model (DTM) project completed. Geol. Surv. Isr. Current Research 8, pp. 47–50.

Harvey, A.M., Wells, S.G. 1987. Response of Quaternary fluvial systems to differential epeiorogenic uplift: Aguas and Feos river systems, southern Spain. Geology 15: 689–693

Heimann, A. 1985. The geology of the Banias Plateau and northern Hula Valley with an emphasis on travertine depositions. M.Sc. thesis, Hebrew Univ., Jerusalem, 155 pp. (in Hebrew, English abstr.).

Kafri, U. 1972. Geological map of Israel, 1:50,000, Sheet 1-IV, Nahariyya, Geol. Surv. Isr.

Kafri, U. 1997. Neogene to Quaternary drainage systems and their relationship to young tectonics: Lower Galilee, Israel. Geol. Surv. Isr. Rep. GSI/1/97.

Kafri, U., Heimann, A. 1994. Reversal of the paleodrainage system in the Sea of Galilee area as an indicator of the formation timing of the Dead Sea Rift valley base level in northern Israel. Palaeogeogr., Palaeoclimatol., Palaeoecol. 109: 101–109.

Keller, E.A. 1986. Investigation of active tectonics: use of surficial processes. In: Wallace, R.E., ed. Active tectonics: studies in geophysics. National Academy Press, Washington, DC, pp. 136–147.

Machette, M. 1985. Calcic soils of the Southwestern United States. Geol. Soc. Am., Spec. Pap. 203: 1–21.

Markewich, H.M. 1984. Geomorphic evidence for Pliocene–Pleistocene uplift in the area of the Cape-Fear Arch, North Carolina. In: Morisawa, M., Hack, J.T., eds. Tectonic geomorphology. Proc. 15th Annual Binghamton Geomorphology Symp., Sept. 1984, pp. 279–297.

Matmon, A., Zilberman, E., Enzel, Y. 1998. Morphometric analysis for determining the age of escarpments: an example from the Galilee, northern Israel, Geol. Surv. Isr. Rep. GSI/31/98.

Matmon, A., Enzel, Y., Zilberman, E., Heimann, A. 1999. Late Pliocene and Pleistocene reversal of drainage systems in northern Israel: tectonic implications. Geomorphology 28: 43–59.

Merritts, D., Vincent, K.R. 1989. Geomorphic response of coastal streams to low, intermediate, and high rates of uplift, Mendocino triple junction region, northern California. Geol. Soc. Am. Bull. 101: 1373–1388.

Nir, D. 1970. The geomorphology of Israel. Akademon Press, Hebrew Univ., Jerusalem, 404 pp. (in Hebrew).

Ollier, C.C. 1981. Tectonics and landforms. Longmans, New York, 324 pp.

Ouchi, S. 1985. Response of alluvial rivers to slow active tectonic movement. Geol. Soc. Am. Bull. 96: 504–515.

Picard, L. 1943. Structure and evolution of Palestine (with comparative notes on neighbouring countries). Bull. Geol. Dept., Hebrew Univ., Jerusalem 4 (2–4): 134 pp.

Picard, L. 1951. Geomorphogeny of Israel. Part I: the Negev. Bull. Res. Counc. Isr. 1: 5–32.

Picard, L., Golani, U. 1965. The geological map of Israel, northern sheet, 1:250000.

Rockwell, T.K., Keller, E.A., Dembroff, G.R. 1988. Quaternary rate of folding of the Ventura Avenue Anticline, western Transverse Ranges, Southern California, Geol. Soc. Am. Bull. 100: 850–858.

Ron, H., Freund, R., Garfunkel, Z., Nur, A. 1984. Block rotation by strike slip faulting: structural and paleomagnetic evidence. J. Geophys. Res. 89: 6256–6270.

Schumm, S.A. 1977. The fluvial system. Wiley, New York, 338 pp.

Schumm, S.A. 1986. Alluvial river response to active tectonics. In: Wallace R.E., ed. Active tectonics: studies in geophysics. National Academy Press, Washington, DC, pp. 80–94.

Shaliv, G., Mimran, Y., Hazor, Y. 1991. The sedimentary and structural history of the Bet Shean area and its regional implications. Isr. J. Earth Sci. 40: 161–179.

Sivan, D. 1996. Paleogeography of the Galilee coastal plain during the Quaternary. Geol. Surv. Isr. Rep. GSI/18/96.

Sparling, D.R. 1967. Anomalous drainage pattern and crustal tilting in Ottawa County, Ohio. Ohio J. Sci. 67: 378–381.

Spitz, W.J., Schumm, S.A. 1997. Tectonic geomorphology of the Mississippi Valley between Osceola, Arkansas and Friars Point, Mississippi. Eng. Geol. 46: 259–280.

Stevens, G.R. 1974. Rugged landscape, the geology of central New Zealand. A.H. and A.W. Reed, Wellington, 286 pp.

Twidale, C.R. 1971. Structural landforms. Australian National Univ. Press, Canberra.

Wallace, R.E. 1967. Note on stream channels offset by the San Andreas Fault, southern coast range. California, Stanford Univ. Publ. (Geol. Sci.) 11: 6–20.

Yair, A. 1962. The morphology of Nahal Dishon. M.Sc. thesis, Hebrew Univ., Jerusalem, 196 pp. (in Hebrew, English abstr.).

Zilberman, E. 1992. Remnants of Miocene landscape in the central and northern Negev and their paleogeographical implications. Geol. Surv. Isr. Bull. 83, 54 pp.

Zilberman, E. 1993. The Mahmal Graben and Nahal Hawwa: an introduction to the paleogeography of the central Negev in the Miocene. Isr. J. Earth Sci. 42: 197–209.

PUBLICATION DOCUMENTATION PAGE

1. **Publication No** Es-5-2001.	2.	3. Recipient Accession No.	
Title and Subtitle: **Pliocene-Pleistocene tectonics and landscape evolution in the Galilee**		**5. Publication Date 2/2001**	
Author(s): A. Matmonl		**6. Performing Organiz. Code:**	
9. Performing Organization Name and Address Geological survey of Israel, 30 Malkhei Yisrael St, Jerusalem		**10. Project/Task/Work Unit No.** **11. Contract No.**	
12. Sponsoring Organization(s) Name and Address (a) Ministry of National Infrastructures Earth Science Administration (b) Geological survey of Israel, 30 Malkhei Yisrael St, Jerusalem		**13. Type of Report and Period Covered: technical report (abstract of PhD thesis, 1995-2000).** --14. **Sponsoring Organiz. Code**	
Supplementary Note			
17. Identifiers/Key Words/Descriptors: Galilee, tectonic, geomorphology..			
18. Availability Statement **unpublished**		**19. Security Class (This Report)** ----------------------------- 20. Security Class (this Pages)	**21. No. of Pages 52** ----------------------------- -22. Price